Anna Ivanova Olsen

Time-variant reliability of dynamic systems by importance sampling and probabilistic analysis of ice loads

Doctoral thesis
for the degree of doktor ingeniør

Trondheim, August 2006

Norwegian University of
Science and Technology
Faculty of Engineering Science and Technology
Department of Structural Engineering

NTNU
Innovation and Creativity

NTNU
Norwegian University of Science and Technology

Doctoral thesis
for the degree of doktor ingeniør

Faculty of Engineering Science and Technology
Department of Structural Engineering

ISBN 82-471-8041-3 (printed ver.)
ISBN 82-471-8040-5 (electronic ver.)
ISSN 1503-8181

Doctoral Theses at NTNU, 1181

Printed by Tapir Uttrykk

Thesis for the dr.ing. degree

Time-variant reliability of dynamic systems by importance sampling and probabilistic analysis of ice loads

Anna Ivanova Olsen

August 2006

NTNU
Norwegian University of Science and Technology
Faculty of Engineering Science and Technology
Department of Structural Engineering

Abstract

This doctoral thesis is submitted to the Norwegian University of Science and Technology.

The main objective of this thesis is to develop an efficient simulation technique to estimate the failure probability of time-dependent systems, whose state is expressed as a solution of Itô stochastic differential equations.

The work is divided in two topics due to requirements of the scholarship.

The first part addresses to the problem of assessing the reliability of dynamic systems, where the first-passage probability is chosen as a performance measure of structures subjected to the irregular, stochastic environmental loads. This problem has received considerable attention recently but it still remains a challenge for a wide class of systems.

The improved importance sampling method is developed which allows the solution of the first-passage problem and its applicability for single degree of freedom linear and non-linear systems. Firstly, it is efficient for assessing small probabilities and it increases the convergence rate compared with the crude Monte Carlo method. Secondly, the procedure uses as much known analytical information about systems as possible.

The second part of the thesis features the probabilistic analysis of the ice loads on the Norströmsgrund lighthouse situated in the Baltic Sea. The objective is to verify the spatial correlation model of the ice forces on the structure and estimate the design values from the appropriately chosen extreme value distribution.

Acknowledgments

This work has been carried out under the supervision of Professor Arvid Næss at Department of Structural Engineering and Centre of Ships and Ocean Structures (CeSOS), Norwegian University of Science and Technology (NTNU), Trondheim, Norway.

The financial support from the Research Council of Norway is gratefully acknowledged.

I want to thank all people who helped me in my work on this thesis. Specially, the attendance and guidance of my supervisour Professor Arvid Næss is highly appreciated. The help and fruitful discussions with Professor Mikhail Dimentberg from Worcester Polytechnic Institute, MA, USA were most valuable. I acknowledge the assistance from Stewart Clark, English language advisor at NTNU and thank him for editing the thesis. The encouragement and guidance from Professor Torgeir Moan, the director of CeSOS is also acknowledged.

I appreciate the challenge that Professor Sveinung Løset from Department of Civil and Transport Engineering, NTNU, allowed me to work with. In addition, I am really thankful to him for the opportunity to visit and study at UNIS on Svalbard.

The support and encouragement from my family, friends who believed in me is appreciated. Many thanks go to my beloved husband Robert Olsen who was with me throughout all this tough time and gave me a lot of advice about programming. I am grateful to my fellow students and colleagues at the Department of Structural Engineering and then at the Department of Marine Technology and CeSOS for their support and allowing me to share the social activities.

Contents

Nomenclature

Latin letters

A	contact area
A, B	events
$c.o.v.$	coefficient of variation
D_{eff}	effective diameter
D_s	safety domain
$E[\cdot]$	mathematical expectation
$\mathcal{F}$	σ-algebra
$F^v(\cdot)$	utility function
$f_X(x)$	probability density function
$F_X(x)$	probability distribution function
$g(\cdot)$	limit state function
$G(\omega)$	one-sided density function
h_I	ice thickness
$h(t)$	impulse response function
$H(X, \dot{X})$	system total energy
$I[\cdot]$	indicator function
$J^v(\cdot)$	performance function
$K(\cdot)$	bequest function
L	correlation length
$L^v f$	differential operator

$m(X,t)$ drift function

N number of random experiments

N_{IS} number of samples in importance sampling procedure

$N(t)$ white process

$\widehat{P}$ probability estimator

$P(\cdot)$ probability measure

$\widetilde{P}(\cdot)$ transformed probability measure

P_e exceedance probability

p_{eff} effective pressure

p_f failure probability

$\hat{p}_f$ failure probability estimator

q normalization constant

$R(\zeta)$ return interval

$R_{XY}(t_1,t_2)$ cross-correlation function

s initial time point

SE standard error

$S(\omega)$ auto-spectral density function

t time

T_a air temperature

$\triangle t$ time increment

$t_{(1)}$ considered design time point

T_n natural period

$\{U_i\}_{i=1}^n$ set of normalized and uncorrelated Gaussian variables

u^* design point

$v(\cdot)$ control function

$Var[\cdot]$ variance

V_I ice drift velocity

$W(t)$ Wiener process

X random variable

x realization of random variable

x_c critical threshold

$X_h(t)$ homogenous solution for system displacement

$X(t)$, X_t stochastic process or stochastic vector process if mentioned

$\widetilde{X}(t)$ controlled stochastic process

$\dot{X}_h(t)$ homogenous solution for system velocity

Greek letters

β reliability index

β^* design point index

ε non-linearity parameter

$\Gamma_{XX}(t_1, t_2)$ auto-correlation function

γ intensity of white noise

γ_e equivalent noise intensity

λ nonlinearity parameter

μ mean value

μ_p mean effective pressure

$\nu_x^+(\cdot)$ mean upcrossing rate

Ω sample space

ω outcome of some random experiment

ω_0 system natural frequency

ω_e equivalent stiffness parameter

$\Phi(\cdot)$ Gaussian probability distribution function

$\phi(\cdot)$ Gaussian density function

σ standard deviation

σ_p standard deviation of effective pressure

$\sigma(X,t)$ diffusion function

$\tau(\zeta)$ exceeding duration

ξ system damping ratio

ζ threshold

Other symbols and labels

l.i.m. limit in mean square sense

$\mathbb{R}$ set of all real numbers

(a,b) scalar product of two vectors a and b

Abbreviations

AURL analytical upcrossing rate linearization

FORM first-order reliability method

GEV generalized extreme value distribution

GPD generalized Pareto distribution

LOLEIF Validation on **Lo**w **Le**vel **I**ce **F**orces on Coastal Structures

MCS crude Monte Carlo simulations

ML method of maximum likelihood

MSL mean square stochastic linearization method

NURL numerical upcrossing rate linearization

PWM method of probability weighted moments

SORM second-order reliability method

STRICE Measurements on **Str**uctures in **Ice**

Chapter 1

Introduction

The thesis consists of two separate parts. The first and the main body of the work is devoted to the improvement of Monte Carlo techniques to solve problems posed in the framework of time-dependent structural reliability. The second part describes the analysis of ice load measurements which were obtained during the LOLEIF and STRICE projects under the supervision of Professor Sveinung Løset from the Department of Civil and Transport Engineering, Marine Civil Engineering group, Norwegian University of Science and Technology (NTNU).

1.1 Background and motivation

The prediction of design parameters is an important issue in reliability assessment. Traditionally, structural design relies on deterministic analysis though the uncertainties in loads and material properties are not completely neglected. Safety factors may be introduced to separate strength and load variables (Melchers, 1999). However, due to the fast development of high technology, the increasing cost of equipment, the increasing threat to the environment and people's lives the probabilistic concept has become more and more in demand. Recent results show that it is not enough just to assume suitable dimensions, material properties and loads, it is crucial to take into account the fluctuations of the loads, the variability of the material properties and the uncertainties regarding analytical models. A comprehensive historical survey of structural reliability is given by Madsen et al. (1986) and Melchers (1999). Until now the theory has evolved from the safety factors concept through the probabilistic representation of models, loads, consequences as well as risk analysis.

In random vibration studies an important reliability measure is the first-passage probability density $p(T)$ which determines the probability $p(T)dT$ that the value of a random process surpasses a threshold for the first time during the interval from T to $T + dT$. For mechanical and structural engineer, a first-passage problem of considerable interest is that of the response of an oscillator subjected to random excitation. Moreover, the first-passage probability is closely related to the failure probability which is of main interest in this project. The exact solution of this problem has not been found even in the case of a stationary linear oscillator excited by white noise. The most widely spread asymptotic solution is based on the outcrossing approach (Rackwitz, 2001). In many applications the Poisson assumption for the outcrossings from the safe domain and the Rice formula for the upcrossing rate of the response can be used (Soong and Grigoriu, 1997). The determination of the outcrossing

rate is a computationally challenging problem, especially for non-stationary cases (Naess, 1990). Some examples exhibiting first-passage failure problems mentioned in Noori et al. (1995) are a breakdown of the resonant response to periodic excitation of limited power, a breakdown of the synchronous rotation of two unbalanced rotors with a common movable support, transitions between impact and non-impact motions of a vibroimpact system, and structural damage due to inelastic excursions during an earthquake. Generally, a highly seismic environment is an area where specific techniques are required to estimate the reliability (Bergman and Spencer Jr., 1985). An application of compliant offshore structures such as the dynamic response of tension leg platforms (TLP) is reviewed in Han and Benaroya (2002). Research on the reliability analysis of non-linear problems with implications for aerodynamic forces and other forces like ground motion is presented by Hampl (1985) in order to calculate the response of the structures when collapse limit states are of interest. Khan et al. (2003) estimated the failure probability of a cable stayed bridge under seismic excitation. Their parametric analyses were performed for important parameters such as critical tolerance level and soil condition. The conditional probability of failure was obtained using the moments of the spectral density from the frequency domain spectral analysis performed.

1.2 Survey of previous work

The methods of dynamic analysis of deterministic and stochastic models have evolved rapidly over the past century. Many well-written and comprehensive books on deterministic structural dynamics are available, e.g., Paz (1980), Bolotin et al. (1999). As an introduction to stochastic framework, the dynamical analysis of simple non-parametrical systems and non-linear structures under non-parametric excitations are reviewed by Lin et al. (1986). The authors have contributed a lot to the field of probabilistic structural dynamics (Lin, 1967; Lin and Cai, 1995). The stochastic structural dynamics is covered well in Lutes and Sarkani (1997) and Soong and Grigoriu (1997). More advanced mathematical formulations can be found in Adomian (1983).

The first-excursion probability is one of the important characteristics of the system excited by the random force. As it is mentioned before, no analytical solution exists and no general numerical procedure is available for this quantity. The only universal method is the Monte Carlo method. The disadvantages of this method are slow convergence and enormous computational expenses especially for small probability problems. In structural reliability, importance sampling is widely used to improve the efficiency of the crude Monte Carlo simulation method.

The Monte Carlo method was introduced by two scientists from Los Alamos Metropolis and Ulam (Metropolis and Ulam, 1949) shortly after the Second World War. However, similar experiments were also used to estimate the value of the constant π by George Buffon in the 18^{th} century. The history and various applications are given, for instance, in Bauer (1958) and Sobol' (1973). A general framework for using Monte Carlo methods in dynamical systems is given by Liu and Chen (1998).

For time-invariant problems a lot of research has been done and the simulation methods are proved to have many advantages compared with other approximated techniques

such as first-order reliability method (FORM) and second-order reliability method (SORM) (Madsen et al., 1986) and its extensions. Even if the direct or crude Monte Carlo method (Section 3.2.2) is shown to be ineffective for the evaluation of failure probability. Then it is possible to achieve a reduction in the variance and increase the rate of convergence of the failure probability estimate, using the variance reduction techniques and a combination of several techniques (Ayyub and Haldar, 1985; Grey and Melchers, 2003) as the conditional expectation, antithetic variates (Appendix B) together with ordinary importance sampling. Moreover, it was argued that the Monte Carlo method is inefficient for the sensitivity analysis. In this case Melchers and Ahammed (2002) showed the possibility to run the sensitivity analysis in the framework of the Monte Carlo method without extra simulations being required, even though there are a few restrictions on the form of the performance function.

If the reliability problem is referred to as time-variant, then two kinds of time dependency may be distinguished such as decaying material properties and stochastic dynamic loading. In this project, the systems under randomly varying loading are of interest, though the strength deterioration may be included as well.

Approximate analytical results on the first-passage problem can be obtained using the Rice formula for the upcrossing rate (Rackwitz, 2001), though the predictions based on these results are in general conservative or even wrong due to the restriction of independence of the outcrossings. The variety of the numerical approximation of the first-passage probability of the linear oscillator is given in Crandall (1970). These methods were based on the assumptions of the peak and envelope crossing independency, considering a two-state Markov process for the consequent outcrossings of the following thresholds. Roberts (1976) studied the envelope outcrossing problems using also the Markov character of the response of a linear oscillator. The discrete and continuous envelope cases were considered. The accuracy of the continuous approximation was poor whereas the discrete envelope method gave satisfactory results. Several applications where the analytical approximation of the outcrossing rates were used are reviewed.

In Aoki and Suzuki (1985), the performance of a mechanical appendage system under non-stationary earthquake excitation was evaluated. The theoretical method was used implying that the upcrossing rate is calculated from the assumption of normality of the system response. Results showed conservatism compared with the simulation results. Although the studies revealed that the failure probability of the appendage system with the perfectly elastic-plastic restoring force-deformation relation can be reduced by the energy absorbing effect. The application in aerospace framework is presented by Shiao (1991). Two methods are developed. The first one is based on the crossing rate and implemented for the systems with non-smooth random excitations with small uncertainties in the barrier. The second method is based on introducing the equivalent system, which is able to treat the large variations in the barrier and its large degradation. The use of the outcrossing rates and piecewise constant model of the resistance process is used in Gao et al. (2005) in the application of the estimation of the reliability of mooring lines taking into account the corrosion of the material.

Recently, more and more authors turn to the simulation methods as the most efficient and versatile (Naess, 1999). Dey and Mahadevan (1998) proposed an efficient method for

estimating time-variant failure probability of a redundant structural system, including the resistance degradation and information on periodic repairs. They incorporated the concepts of adaptive and conditional importance sampling, proposed by Karamchandani and Cornell (1991).

Several authors proposed to reduce the time-variant problem to a fixed time concept. For instance, Pradlwater and Schuëller (2004) introduced the idea of "averaged" excursion probability, which means taking into account the interaction between excursions at different time instances and define a static reliability problem. The random excitations are approximated by the Karhunen-Loeve expansion although their method is dependent on the successful choice of all important directions of the simulation corresponding to the boundary.

Tanaka (1997) proposed an importance sampling simulation scheme for estimating the reliability of a system, that can be described by a system of Itô type stochastic differential equations. This scheme uses the optimal measures based on the concept of design point in the first order second moment approach. A similar method is proposed in Takada (1998). The extension on non-Gaussian processes is proposed using the Karhunen-Loeve expansion and mapping between Gaussian and non-Gaussian random variables.

The possibility to perform effective simulations has been extensively studied. Bayer and Bucher (1998) considered the spectral representation of random processes which allows the implementation of the importance sampling on the random selection of the amplitudes of the response. The method was tested on the several non-linear systems using special computer software.

Bucher (2002) used the term "design point oscillations" for the oscillations which were defined by the FORM procedure and which led to the failure at a corresponding time instant. Furthermore, he suggested a multimodal importance sampling density which takes into account the interaction between the design points. The development of this method and implementation on non-linear problems is given in Macke and Bucher (2003).

Au and Beck (2001) proposed an importance sampling procedure for the evaluation of the first-passage probability of a multidimensional system subjected to a Gaussian excitation. They transformed the first-passage problem into a series-system reliability problem by discretizing the time interval in n even steps. Then the authors approximated the failure probability as the probability of the union of the failure events in all time-point components. They used a sampling density composed of a standard normal probability density function conditioned on the failure event in each time step. Koo and Der Kiureghian (2003) continued and extended this work for the non-linear systems. They compared their method with conventional importance sampling method with sampling density centred around design points, and the crude Monte Carlo and showed that the present method is more efficient in the sense of the reduced number of simulation samples. Vijalapura et al. (2000) considered a procedure for estimating the reliability of hysteretic systems using a similar method based on the FORM concept.

Moreover the attempt to extend this method efficiently to high-dimensional reliability problems with a large number of uncertain parameters is made by Au and Beck (2003). Remarks on the handling of the large number of random variables are offered by Schuëller et al. (2004). Besides, the thesis of Au (2001) gives very rigorous proofs here and continues this research topic. His results are used by Koutsourelakis et al. (2004) for a comparison study.

Koutsourelakis proposed a stepwise procedure which makes use of Markov chains.

The present procedure is based on the Girsanov transformation (Girsanov, 1960) of the Wiener process, which allows the definition of the control function added to the continuous Markov process in order to reduce the variance of the stochastic estimator (Newton, 1994). This optimization problem is a problem in stochastic optimal control. The optimal control function exists such as the variance diminishes to zero and the estimator becomes a deterministic quantity (Newton, 1994; Milstein, 1995). However this function is not achievable because the optimal control depends on this unknown estimator itself. Although if some approximation of the failure probability is obtainable then the suboptimal control function exists which will lead to variance reduction. Macke (2000) showed how the suboptimal control function can be designed using the approximated analytical solutions for a desired estimator. The number of samples was reduced, though the numerical effort to compute the control function was substantial. Macke (2000) pointed out that the correction term for the importance sampling procedure starts to deviate a lot for the levels where the behaviour of the original system differs substantially from the Gaussian assumption. In addition, the efficiency in variance reduction, i.e. the statistical error, is depending on the accuracy of the approximation. However, other approximations may be obtained using, for instance, the analytical expression for the control function obtained by Næss and Skaug (2000).

To conclude, many versatile and robust methods have been proposed and successfully used though many challenges for the first-passage problem are still open to be explored.

1.3 Objectives and scope

The objectives of the thesis are to improve the importance sampling procedure for the assessment of failure probability. A two-step procedure is proposed based on a design point oscillation concept, using a suboptimal Markov control function. The emphasis is on the possibility of using analytical expressions for all operations. The considered dynamical systems work in transition zone, i.e., they possess non-stationary properties.

The scope of this thesis is restricted to systems in which there are no parametric, or multiplicative, excitations present. This means that global or catastrophic failure is considered throughout present calculations. This is unlike systems with parametric excitation, where stochastic stability or bifurcation is often of principal concern. Moreover, in the present work the possibility of linearization of a system is assumed to be valid which is accepted to be unsuitable for studying the parametrical dynamic response (Roberts and Spanos, 1990).

Within the adopted methodology, the oscillatory systems with one degree of freedom are studied. The input excitations are white and non-white. The failure is considered in terms of a first passage of the considered limit state. The non-stationary processes, or processes of short duration, are of interest in this project. From all different variance reduction methods (cf. Appendix B), importance sampling in the framework of stochastic control theory is chosen as the most efficient.

1.4 Outline of the thesis

The major part of the thesis, i.e. Chapters 2 to 6 addresses the study of the reliability of dynamical systems by different Monte Carlo simulation methods.

This chapter gives the brief introduction, historical survey and state-of-art on the subject of dynamical structural analysis, reliability and Monte Carlo methodology.

A review of probability theory, the main aspects of stochastic processes and the stochastic differential equation framework are provided in Chapter 2.

Chapter 3 contains a thorough exposition of the various methods in reliability theory. The advantages and disadvantages of involving the randomness in the models and loads are discussed.

In Chapter 4, the concept of stochastic control is presented. The Hamilton-Jacobi-Bellman theorem is given. This is the main tool.

Chapter 5 contains the framework for the studied iterative importance sampling method. As the first example the motion of a linear oscillator is examined. Then the methodology is extended to non-linear systems such as the Duffing oscillator, oscillator with separable non-linear stiffness and damping and hysteretic oscillator. The oscillators excited by non-white external force are presented as well.

Finally, Chapter 6 concludes part one. Appendices A and B are intended to give a brief introduction in the basics of random number generation and various variance reduction methods.

The second part of the manuscript, Chapter 7 presents statistical and probabilistic analyses of ice load data carried out during my participation in the LOLEIF and STRICE projects.

Chapter 2

Stochastic process theory

2.1 Discussion about probability theory

The mathematical quantities and methodology used to describe a stochastic dynamics phenomenon are based on probability theory and stochastic process theory. These and related topics will be discussed in this chapter.

2.1.1 Random variables

The theory of probability in terms of how a random phenomenon can be described is not concerned with a physical nature and operational details of this phenomenon. Rather, it is only concerned with describing the statistical regularity pattern exhibited by the phenomenon. Probability theory therefore abstracts the random phenomenon by dealing only with that aspect which is common to all "random" phenomena, namely, the existence of a stable frequency pattern. Accordingly, the uncertain outcome of the observation of a random phenomenon is simply called a "random event", whatever the actual nature of the phenomenon may be (Bury, 1975).

This random event is an outcome, denoted ω, of some random experiment. The family of all possible distinct outcomes associated with the particular phenomenon is called the sample space $\Omega = \{\omega\}$. To achieve a useful characterization of the outcomes of the random experiment, one commonly introduces a family of subsets of the sample space Ω, namely a σ-algebra $\mathcal{F}$ of subsets with the following properties (Øksendal, 1998):

1. $\emptyset \in \mathcal{F}$;
2. $F \in \mathcal{F} \Rightarrow F^C \in \mathcal{F}$, where $F^C = \Omega \setminus F$ is the complement of F in Ω;
3. $A_1, A_2, \ldots \in \mathcal{F} \Rightarrow A = \bigcup_{i=1}^{\infty} A_i \in \mathcal{F}$.

The pair $(\Omega, \mathcal{F})$ is called a measurable space. The theory of sets with its basic concepts and algebraic operations may be implemented in the space $(\Omega, \mathcal{F})$ and its members (Soong and Grigoriu, 1997). The probability measure assigned to the measurable space is a function $P : \mathcal{F} \rightarrow [0, 1]$ such that

1. $P(\emptyset) = 0$, $P(\Omega) = 1$;

2. $0 \leq P(A) \leq 1$, $P(A^C) = 1 - P(A)$, where A^C is the complement;

3. if $\{A_i\}$ are mutually exclusive (i.e. $A_i \cap A_j = \emptyset$ if $i \neq j$) then

$$P\left(\bigcup_{i=1}^{\infty} A_i\right) = \sum_{i=1}^{\infty} P(A_i); \tag{2.1.1}$$

4. $P(A_1 \cup A_2) = P(A_1) + P(A_2) - P(A_1)P(A_2)$ and which may be reduced to

$$P(A \cup B) = P(A) + P(B) \quad \text{if} \quad A \cap B = \emptyset. \tag{2.1.2}$$

Then the triplet $(\Omega, \mathcal{F}, P)$ is called a probability space. It should be mentioned that if $\mathcal{F}$ is a σ-algebra in F, then F is a $\mathcal{F}$-measurable set. Thus the introduced measure may be interpreted as "the probability that the event F occurs". Besides, the conditional probability $P(A_1|A_2)$ of an event A_1 given that an event A_2 has occurred may be defined as

$$P(A_1|A_2) = \frac{P(A_1 \cap A_2)}{P(A_2)}, \tag{2.1.3}$$

where $P(A_2) > 0$.

It is possible that the occurrence or non-occurrence of A_1 is not affected by whether or not another event A_2 has occurred. Then its conditional probability $P(A_1|A_2)$ should be the same as $P(A_1)$, which implies that

$$P(A_1 \cap A_2) = P(A_1)P(A_2). \tag{2.1.4}$$

Then it may be said that events A and B are independent. This property can be generalized in the case of n events $A_1, A_2, \ldots, A_n$. If

$$P(A_{i_1} \cap A_{i_2} \cap \ldots \cap A_{i_k}) = P(A_{i_1})P(A_{i_2}) \cdots P(A_{i_k}) \tag{2.1.5}$$

for all non-empty sets $\{i_1, i_2, \ldots, i_k\}$ of the sets of indices $\{1, 2, \ldots, n\}$, then $A_1, A_2, \ldots, A_n$ are independent.

It should be mentioned, that if Ω is a topological space (Rudin, 1987) (e.g. $\Omega = \mathbb{R}^n$) and $\mathcal{B}$ is the smallest σ-algebra containing the open sets of Ω, then $\mathcal{B}$ is called the Borel σ-algebra and the elements $B \in \mathcal{B}$ are called Borel sets.

To go further, a random variable for a probability space $(\Omega, \mathcal{F}, P)$ may be defined as a function if it transfers the sample space into "the real world", i.e $X : \Omega \rightarrow \mathbb{R}^n$ and if the following statement holds

$$\{\omega \in \Omega : X(\omega) \leq a\} \in \mathcal{F} \quad \text{for each} \quad a \in \mathbb{R}^n \tag{2.1.6}$$

where $\{\omega \in \Omega : X(\omega) \leq a\}$ is an event for each $a \in \mathbb{R}^n$, where $\{X(\omega) \leq a\}$ is interpreted as componentwise inequalities. This implies that $\{\omega \in \Omega : X(\omega) \in B\}$ is an event for any Borel

subset B of $\mathbb{R}^n$. Moreover, every random variable induces a probability measure $P_X(B)$ on $\mathbb{R}^n$, defined by:

$$P_X(B) = P(X^{-1}(B)) = P(\{\omega \in \Omega : X(\omega) \in B\}) \tag{2.1.7}$$

for all $B \in \mathcal{B}$.

This measure is called the distribution of the random variable X and its probability space $(\mathbb{R}, \mathcal{B}, P_X)$ contains all of the essential information associated with it. Though inside this space the probability measure may be transformed in a certain way (Rudin, 1987).

A measure Q is said to be absolutely continuous with respect to another measure P, both being measures on $(\Omega, \mathcal{F})$, if $Q(A) = 0$ whenever $P(A) = 0$.

Theorem 1 (**The Theorem of Radon-Nikodym**). *Let P be a positive σ-finite measure on a σ-algebra $\mathcal{F}$ in a set Ω, and let $\widetilde{P}$ be another finite measure on $\mathcal{F}$ such as $\widetilde{P} \ll P$. There is a unique $h \in L^1(P)$ such that*

$$\widetilde{P}(E) = \int_E h dP \tag{2.1.8}$$

for every set $E \in \mathcal{F}$.

The function h which occurs in (2.1.8) is called the *Radon-Nikodym derivative* of $\widetilde{P}$ with respect to P. Also, if h is a member of $L^1(P)$, the integral in (2.1.8) defines a measure on $\mathcal{F}$ which is absolutely continuous with respect to P, see e.g. Rudin (1987). Equation (2.1.8) may be expressed in the form $d\widetilde{P} = hdP$ or $h = d\widetilde{P}/dP$. In following chapters this theorem will be of utmost importance because it allows us to define a transformation of probability measures in order to perform importance sampling procedure.

Returning to the distributions and using the terms of point functions in one dimension, the probability measure (2.1.7) may be rewritten as $F_X : \mathbb{R} \to \mathbb{R}$

$$F_X(x) = P_X((-\infty, x)) = P(\{\omega \in \Omega : X(\omega) \leq x\}). \tag{2.1.9}$$

what is called the cumulative distribution function of X. The distribution function $F_X(x)$ has the following properties:

1. $\lim_{x \to -\infty} F_X(x) = 0$
2. $\lim_{x \to +\infty} F_X(x) = 1$
3. $F_X(x)$ is nondecreasing function in x

The random variables may be discrete, continuous or combined (Kloeden and Platen, 1999). The main concern in this thesis is continuous variables. The continuous random variable is the variable which may take all possible values in $\mathbb{R}$ into account and satisfy the condition $P(\{\omega \in \Omega\} : X(\omega) = x) = 0$ for all $x \in \mathbb{R}$. Specifically, it is assumed that the associated distribution function $F_X(x)$ is absolutely continuous, which implies that it is differentiable almost everywhere with respect to Lebesgue measure. This means that there

exists a non-negative function $f_X(x)$, called *the probability density function*. The following relation is then true

$$F_X(x) = \int_{-\infty}^{x} f_X(\xi)d\xi \tag{2.1.10}$$

for all $x \in \mathbb{R}$.

Let $X : \Omega \to \mathbb{R}$ be a random vector variable. If $\int_\Omega |X(\omega)|dP(\omega) < \infty$ then the number

$$\int_\Omega X(\omega)dP(\omega) = \int_{\mathbb{R}^n} xdF_X(x) \tag{2.1.11}$$

is called *the expectation* of X with respect to P. Note that componentwise interpretation again applies.

More generally, if $g : \mathbb{R}^n \to \mathbb{R}$ is Borel measurable and $\int_\Omega |g(X(\omega))|dP(\omega) < \infty$

$$\int_\Omega g(X(\omega))dP(\omega) = \int_{\mathbb{R}^n} g(x)dF_X(x). \tag{2.1.12}$$

Again in the terms of one dimension and point function, the mathematical expectation of a random variable X is (Lutes and Sarkani, 1997)

$$E[X] = \mu = \int_{-\infty}^{\infty} xdF_X(x) = \int_{-\infty}^{\infty} xf_X(x)dx. \tag{2.1.13}$$

If a function $g(X) = X^n$ then Equation (2.1.12) becomes

$$E[X^n] = \alpha_n = \int_{-\infty}^{\infty} x^n dF_X(x) = \int_{-\infty}^{\infty} x^n f_X(x)dx. \tag{2.1.14}$$

Especially often the moments from second to fourth order are of interest.

The central moments are

$$E[(X-\mu)^n] = \mu_n = \int_{-\infty}^{\infty} (x-\mu)^n dF_X(x) = \int_{-\infty}^{\infty} (x-\mu)^n f_X(x)dx. \tag{2.1.15}$$

The second-order moment is of particular interest which is called the variance of the variable X. It defines spread of the variable from its expectation.

$$Var(X) = \mu_2 = E[(X-\mu)^2] = \int_{-\infty}^{\infty} (x-\mu)^2 dF_X(x) = \int_{-\infty}^{\infty} (x-\mu)^2 f_X(x)dx. \tag{2.1.16}$$

The above-mentioned notations and definitions are represented from a pure mathematical point of view. As for numerical estimations and statistical analysis, it may be deduced that the estimate of the probability of occurrence of an event A is (Wadsworth, 1997)

$$\widehat{P}(N) = \frac{N_A}{N} \tag{2.1.17}$$

where N_A is the number of experiments with outcome when the event A has occurred and N is the number of all experiments.

An estimate of the mathematical expectation (2.1.11) is

$$\widehat{\mu} = \frac{1}{N}\sum_{i=1}^{N} x_i \tag{2.1.18}$$

where x_i is the values of a random continuous variable X taken in each of experiments $i = 1, \ldots, N$. $\widehat{\mu}$ is called an average or a sample mean of the variable X.

An estimate of the second moment $E(X^2)$ commonly called the *mean squared value* of the random variable X, is given as

$$\widehat{\alpha}_2 = \frac{1}{N-1}\sum_{i=1}^{N} x_i^2 \tag{2.1.19}$$

$E(X^2)^{1/2}$ is called *the root-mean-square value* or *rms* of the variable X. Further, the estimate of the variance (2.1.16) is

$$\widehat{\sigma}^2 = \widehat{\mu}_2 = \frac{1}{N-1}\left(\sum_{i=1}^{N} x_i^2 - N \cdot \widehat{\mu}^2\right). \tag{2.1.20}$$

The standard deviation is defined as $\sigma = (E[(X-\mu)^2])^{1/2}$. Sometimes as a measure of the relative discrepancy in the data the coefficient of variation is used

$$c.o.v. = \frac{\sigma}{\mu} \tag{2.1.21}$$

or standard error

$$SE = \frac{\sigma}{\sqrt{N}\mu}. \tag{2.1.22}$$

To conclude this section, the most common and much used example of a random variable is a Gaussian random variable X. Its probability density function, f_X, is given as

$$f_X(x) = \frac{1}{\sqrt{2\pi}\sigma}\exp\left(-\frac{(x-\mu)^2}{2\sigma^2}\right) \tag{2.1.23}$$

and the probability distribution function denoted as F_X

$$F_X(x) = \int_{-\infty}^{x} f_X(u)du = \int_{-\infty}^{x} \frac{1}{\sqrt{2\pi}\sigma}\exp\left(-\frac{(u-\mu)^2}{2\sigma^2}\right)du \tag{2.1.24}$$

where μ is the mean value, σ is the standard deviation. Thus the Gaussian random variable is completely defined by its mean and standard deviation.

When $\mu = 0$ and $\sigma = 1$, then X is referred to as a standardized normal variable, and very often its probability density function is denoted by ϕ, while the corresponding distribution function is denoted by Φ.

The graph of $\phi(x)$ has the well-known bell-shaped curve, see Figure 2.1.

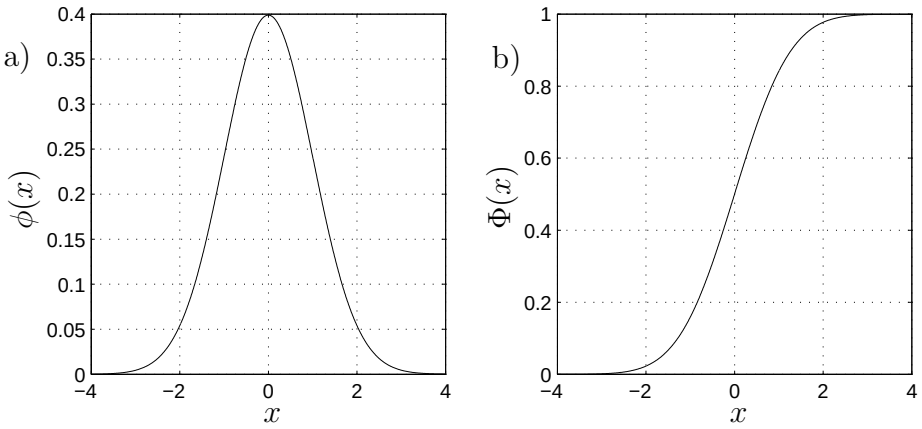

Figure 2.1: Probability density function $\phi(x)$ (a) and cumulative probability distribution function $\Phi(x)$ (b) of standard Gaussian random variable with mean zero and variance one.

2.2 Definition and major properties of the stochastic process

To continue the subject of the probability theory it is natural to define a stochastic process. There are several definitions of this concept. The one which is adapted here is from Øksendal (1998).

Definition 1. A stochastic process is a parameterized collection of random variables

$$\{X_t\}_{t \in T} \tag{2.2.1}$$

where T denotes a specified set of indices, defined on the probability space $(\Omega, \mathcal{F}, P)$ and assuming values in $\mathbb{R}^n$.

Another definition of *a stochastic process*, or *a random process*, is that it is a mathematical model of a dynamic process whose dependence on a parameter, t, is governed by probabilistic laws (Soong and Grigoriu, 1997). As it is defined there are many phenomena which may be described as a stochastic process, many environmental processes such as wind loads, ice loads. The latter will be attempted to be described in a probabilistic sense in the last chapter of this thesis.

As mentioned above, for each fixed $t \in T$, $X_t(\cdot) : \Omega \to \mathbb{R}^n$ is a random variable. On the other hand, for a fixed $\omega \in \Omega$ the function $t \to X_t(\omega)$ is a path or realization of X_t. Thus the process may be regarded as a function of two variables $(t, \omega) \to X(t, \omega) : T \times \Omega \to \mathbb{R}^n$. It is worth mentioning that it is often necessary to require that $X(t, \omega)$ is jointly measurable in (t, ω) (Øksendal, 1998).

Since $X(t)$ can be interpreted as a family of random variables indexed by t, it is obvious that the stochastic process is completely defined if the joint probability distribution functions are specified for whole family of random variables $X(t_1), X(t_2), \ldots$ for all finite sets $\{t_i\} \in T$ for discrete time case. This set of distributions constitutes the probability law of $X(t)$, $t \in T$. This can be also implemented for the continuous-parameter process if its samples are determined in some sense, with probability one, by their values at a countable set of points.

$$F_n(x_1, \ldots, x_n; t_1, \ldots, t_n) = P\{X_1 \leq x_1 \cap \ldots \cap X_n \leq x_n\} \tag{2.2.2}$$

is called the n^{th} distribution function of $X(t)$. This family of joint distribution functions satisfies the two Kolmogorov conditions:

1. The condition of consistency:

$$F_m(x_1, \ldots, x_n, +\infty, \ldots, +\infty; t_1, \ldots, t_n, \ldots, t_m) = F_n(x_1, \ldots, x_n; t_1, \ldots, t_n) \tag{2.2.3}$$

   for all $m > n$, which indicates that *marginal distributions* can be consistently generated from higher dimensional distributions.

2. The symmetry condition:

$$F_n(x_1, \ldots, x_n; t_1, \ldots, t_n) = F_n(x_{i_1}, \ldots, x_{i_n}; t_{i_1}, \ldots, t_{i_n}), \tag{2.2.4}$$

   where F_n is invariant under an arbitrary permutation $i_1, i_2, \ldots, i_n$ of indices $\{1, 2, \ldots\}$.

Correspondingly the n^{th} density function of $X(t)$, when it exists, is defined as

$$f_n(x_1, \ldots, x_n; t_1, \ldots, t_n) = \frac{\partial^n F_n(x_1, \ldots, x_n; t_1, \ldots, t_n)}{\partial x_1 \ldots \partial x_n}. \tag{2.2.5}$$

The second important issue about the stochastic process is moments. Those of a great importance are of the first and second order. The moments at a given $t \in T$ are defined as for a random variable (Eqs. 2.1.11, 2.1.12, 2.1.16, 2.1.15). The nm^{th} joint moment, $\alpha_{nm}(t_1, t_2)$ of $X(t)$ at t_1 and t_2 is defined by

$$\alpha_{nm}(t_1, t_2) = E[X^n(t_1)X^m(t_2)] = \int_{-\infty}^{\infty}\int_{-\infty}^{\infty} x_1^n x_2^m f_2(x_1, x_2; t_1, t_2) dx_1 dx_2. \tag{2.2.6}$$

Specifically the moment $\alpha_{11}(t_1, t_2)$, called the auto-correlation function and denoted $R_{XX}(t_1, t_2)$, plays an important role as a measure of linear interdependence between $X(t_1)$

and $X(t_2)$. A similar interdependence measure can be defined for two different stochastic processes

$$R_{XY}(t_1, t_2) = E[X(t_1), Y(t_2)], \tag{2.2.7}$$

which is called the cross-correlation function. Similarly, the auto-covariance function of $X(t)$ is given by

$$\begin{aligned} \Gamma_{XX}(t_1, t_2) &= E[(X(t_1) - \mu(t_1))(X(t_2) - \mu(t_2))] \\ &= \int_{-\infty}^{\infty} \int_{-\infty}^{\infty} (x_1 - \mu(t_1))(x_2 - \mu(t_2)) f_2(x_1, x_2; t_1, t_2) dx_1 dx_2. \end{aligned} \tag{2.2.8}$$

The next issue is based upon regularity. The stochastic processes can be divided in two classes: *non-stationary* and *stationary*. The probability distributions of non-stationary processes depend explicitly on time parameters. Most of real stochastic processes are obviously non-stationary (Soong and Grigoriu, 1997). But many of these processes can be modelled, approximated or they converge to the stationary processes. So the class of the stationary processes is very important since they represent a form of probabilistic equilibrium in the sense that the time instants at which they are examined are not important. It is said that the stochastic process $X(t)$ is strictly stationary if its probability distributions are invariant under an arbitrary translation of the time parameter, i.e.

$$\begin{aligned} &F_n(x_1, \ldots, x_n; t_1, \ldots, t_n) = F_n(x_1, \ldots, x_n; t_1 + \tau, \ldots, t_n + \tau), \\ &t_j \in T \quad \text{and} \quad (t_j + \tau) \in T,\ j = 1, 2, \ldots, n. \end{aligned} \tag{2.2.9}$$

This implies the following important properties for moments of the stationary process:

- $E[X^k(t)] = const$ for any $k = 1, 2, \ldots$.
- The correlation function depends only upon the difference of the time instance for $X(t_1)$ and $X(t_2)$, where $t_1 = t$ and $t_2 = t - \tau$ and since

$$F_2(x_1, x_2; t_1, t_2) = F_2(x_1, x_2; t_2 - t_1) \tag{2.2.10}$$

then

$$E[X(t)X(t + \tau)] = R(t + \tau - t) = R(\tau) \tag{2.2.11}$$

where the correlation function $R(\tau)$ is symmetrical.

But usually it is rather difficult to detect the pure stationarity since property (2.2.9) must hold for all n. Hence a weakly stationary process can be defined as a wide-sense stationary process.

Definition 2. A stochastic process $X(t)$ is *weakly stationary* if $E[X^2(t)] < \infty$ for every t, and

$$|E[X(t)]| = const \tag{2.2.12}$$

and

$$E[X(t_1)X(t_2)] = R(t_2 - t_1). \tag{2.2.13}$$

For experimental time series the issue of ergodicity is important. This property shows the possibility of a long, single observation to represent certain statistical averages of the whole stochastic process. The time averaging of a given function $g(x(t))$, where $x(t)$ is a realization of a stochastic process $X(t)$, is defined by

$$\overline{g(x(t))} = \lim_{T\to\infty} \frac{1}{2T} \int_{-T}^{T} g(x(t))dt \tag{2.2.14}$$

if the limit exists. Then the following definition of ergodicity may be given (Soong and Grigoriu, 1997):

Definition 3. A stationary process $X(t)$, $t \in T$, is said to be *ergodic relative to* G if, for every $g(\cdot) \in G$, G being the appropriate domain of functions,

$$\overline{g(X(t))} = E[g(X(t))] \tag{2.2.15}$$

with probability one, that is, with a possible exception of a subset of sample functions $g(X(t))$ with zero probability of occurrence.

Moreover a power spectral density function $S(\omega)$ can be defined for the weakly stationary process $X(t)$. This quantity and the correlation function (2.2.11) form a Fourier transform pair and defined by *the Wiener-Khintchine formulas*

$$S(\omega) = \frac{1}{2\pi} \int_{-\infty}^{\infty} e^{-\mathrm{i}\omega\tau} R(\tau)d\tau, \tag{2.2.16}$$

$$R(\tau) = \int_{-\infty}^{\infty} e^{\mathrm{i}\omega\tau} S(\omega)d\omega \tag{2.2.17}$$

Since $S(-\omega) = S(\omega)$, and negative values of ω lack physical content, it is customary in the applications to use the one-sided power spectral density function given by

$$\begin{aligned} G(\omega) &= 2S(\omega), \quad \omega > 0 \\ &= 0, \quad \text{otherwise} \end{aligned}$$

Also when $\tau = 0$, Eq. (2.2.17) becomes

$$R(0) = E[X^2(t)] = 2\int_0^\infty S(\omega)d\omega = \int_0^\infty G(\omega)d\omega. \tag{2.2.18}$$

Returning to the subject of continuous valued and continuous parametered stochastic process $X(t)$ with given autocorrelation function

$$R_{XX}(t_1, t_2) = E[X(t_1)X(t_2)] \tag{2.2.19}$$

the following properties can be defined (Lin and Cai, 1995):

- *Continuity:* $X(t)$ is continuous at t in the L_2 sense, that is $\lim_{h\to 0} E[|X(t+h)-X(t)|^2] = 0$, which is denoted by
$$\underset{h\to 0}{\text{l.i.m.}} X(t+h) = X(t), \tag{2.2.20}$$
if and only if $R_{XX}(t_1, t_2)$ is continuous along the diagonal $t_1 = t_2 = t$.

- *Differentiability:* $X(t)$ is differentiable in the L_2 sense; that is,
$$\dot{X}(t) = \frac{d}{dt}X(t) = \underset{h\to 0}{\text{l.i.m.}} \frac{X(t+h) - X(t)}{h} \tag{2.2.21}$$
exists, if and only if $\frac{\partial^2}{\partial t_1 \partial t_2} R_{XX}(t_1, t_2)$ exists along diagonal $t_1 = t_2 = t$.

- *Integrability:* $X(t)$ is Reimann-integrable in the L_2 sense; that is
$$Y(t) = \int_a^b h(t,\tau)X(\tau)d\tau = \underset{\substack{h\to 0\\ \Delta_n\to 0}}{\text{l.i.m.}} \sum_{j=1}^{n} h(t,\tau_j')X(\tau_j')(\tau_{j+1} - \tau_j) \tag{2.2.22}$$
exists, where $h(t,\tau)$ is a deterministic weighting function, $a = \tau_0 < \tau_1 < \ldots < \tau_{n+1} = b$, $\tau_j \le \tau_j' \le \tau_{j+1}$, and $\Delta_n = \max_{0\le j\le n}(\tau_{j+1} - \tau_j)$, if and only if
$$J(t) = \int_a^b \int_a^b h(t,\tau)h(t,u)R(\tau,u)d\tau du < \infty \tag{2.2.23}$$

The next sections present some examples of stochastic processes which will be extensively used throughout the thesis.

2.2.1 The Gaussian process

As a first example a Gaussian process can be defined.

Definition 4. The stochastic process $X(t)$ is called Gaussian if all its n^{th} probability distributions are jointly Gaussian for all n.

The standard Gaussian process has the mean value zero and the variance of one, it is also called sometimes the normal process, denoted $N(0,1)$. Based upon the Central Limit Theorem (Soong and Grigoriu, 1997), a Gaussian stochastic process can be expected to occur whenever it represents the sum of a very large number of independent random effects of similar order of magnitude at each time instant.

2.2.2 The Markov process

For most stochastic dynamics applications, a Markov process $X(t)$ is usually used. The process we are concerned with is assumed to be continuously valued, and its time parameter t is defined in a continuous space (Karlin and Taylor, 1975). Roughly speaking, *a Markov process* is a process with the property that, given the value of X_t, the value of X_s, $s > t$, do not depend on the values of X_u, $u < t$; that is the probability of any particular future behaviour of the process, when its present state is known exactly, is not altered by additional knowledge concerning its past behavior. Though a continuously valued and continuously parametered Markov process is a mathematical idealization, it can also serve as a good approximation for the real physical processes. The definition of a Markov process is given (Lin and Cai, 1995):

Definition 5. A stochastic process $X(t)$ is said to be a scalar Markov process if it has the property

$$\begin{aligned} P[X(t_n) &\leq x_n | X(t_{n-1}) = x_{n-1}, \ldots, X(t_1) = x_1] \\ &= P[X(t_n) \leq x_n | X(t_{n-1}) = x_{n-1}] \qquad t_n > t_{n-1} > \cdots > t_1, \end{aligned} \tag{2.2.24}$$

where $P[\cdot]$ denotes the probability of an event, and where the statement following a vertical bar specifies certain conditions under which such a probability is defined. In the present case, the conditions are known values of $X(t)$ at earlier time instants $t_1, \ldots, t_{n-1}$. A sufficient condition for $X(t)$ to be a Markov process is that its increments in any two non-overlapping intervals are independent; that is, $X(t_2) - X(t_1)$ and $X(t_4) - X(t_3)$ are independent as long as $t_1 < t_2 \leq t_3 < t_4$. Thus, such a Markov process is a process with *independent increments*.

A Markov process is defined completely by the transitional probability function given by

$$F(s, x; t, B) = P(X(t) \in B | X(s) = x) \tag{2.2.25}$$

for all Borel subsets B of $\mathbb{R}$, and an initial condition.

A rich and useful class of such Markov processes are diffusion processes. The definition of a diffusion process is given (Karlin and Taylor, 1981):

Definition 6. A continuous time parameter stochastic process which possesses the (strong) Markov property and for which the sample paths $X(t)$ are (almost always) continuous functions of t is called a *diffusion process*.

2.2.3 The Wiener process

The simplest example of a Markov process is perhaps the *Wiener process*, also known as the *Brownian motion*, process, denoted by $W(t)$ or $B(t)$ (Soong and Grigoriu, 1997; Karlin and Taylor, 1975). Here the notation $W(t)$ is used to distinguish between the mathematical and physical processes.

Definition 7. The Wiener process is a stochastic process $\{W(t); t \geq 0\}$ with the following properties:

- For every pair of disjoint time intervals $[t_1, t_2]$ and $[t_3, t_4]$, $t_1 < t_2 \leq t_3 < t_4$, the increments $W(t_4) - W(t_3)$ and $W(t_2) - W(t_1)$ are independent random variables normally distributed with mean 0 and variance $\sigma^2(t_2 - t_1)$, $0 \leq t_1 < t_2$, and σ is a positive constant.

- $W(0) = 0$, $E[W(t)] = 0$ and $W(t)$ is continuous at time $t = 0$.

- Correlation function $E[W(t_1), W(t_2)] = \sigma^2 \min\{t_1, t_2\}$; namely,

$$E[W(t_1), W(t_2)] = \begin{cases} \sigma^2 t_1, & t_1 < t_2 \\ \sigma^2 t_2, & t_1 > t_2 \end{cases} \tag{2.2.26}$$

The probability law governing the transition is stationary in time and therefore the transition probability density of $W(t)$ does not depend on initial time, namely

$$p(t, x) = \frac{1}{\sqrt{2\pi t}\sigma} \exp\left(-\frac{x^2}{2t\sigma^2}\right). \tag{2.2.27}$$

The Wiener process having a unit variance parameter σ is called the *standard Wiener process*. A realization of a standard Wiener process is shown in Fig. (2.2).

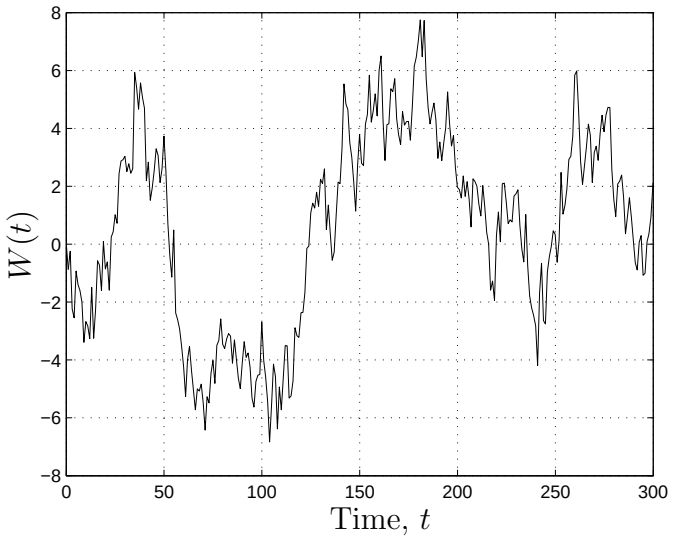

Figure 2.2: The standard Wiener process.

Also it can be shown that the Wiener process has continuous sample path with probability one since, for any $\varepsilon > 0$

$$P[|W(t + h) - W(t)| < \varepsilon] = 1 - 2\Phi\left(-\frac{\varepsilon}{\sigma\sqrt{h}}\right) \to 1 \tag{2.2.28}$$

as $h \to 0$. On the other hand, since

$$P\left[\left|\frac{W(t+h)-W(t)}{h}\right| > \varepsilon\right] = 2\Phi\left(-\frac{\varepsilon h}{\sigma\sqrt{h}}\right) \to 1 \tag{2.2.29}$$

as $h \to 0$, the Wiener process has non-differentiable samples with probability one. Nonetheless, the Wiener process has a formal derivative. This will be performed below.

2.2.4 The white noise process

The white noise process, denoted $N(t)$, is widely used in applications. The process is called "white" due to the "white light" which has the property that its power spectral density is flat over the visible portion of electromagnetic spectrum. Hence the definition of this random process is following:

Definition 8. The stochastic process $\{N(t); 0 \leq t\}$ is a white noise if it has the following properties:

- $N(t)$ is a stationary Gaussian process with mean value $E[N(t)] = 0$.
- One-sided spectral density $G(\omega) = G_0$.
- Autocorrelation function

$$E[N(t_1), N(t_2)] = \pi G_0 \delta(t_1 - t_2) \tag{2.2.30}$$

The process $N(t)$ itself can never be realized, only a discretized approximation can be sampled. A realization of a discretized white noise process is shown in Fig. (2.3).

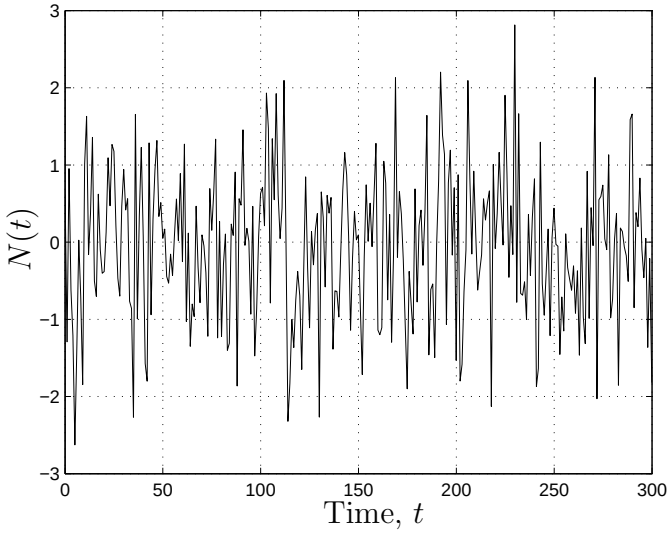

Figure 2.3: The discretized white noise realization with mean zero and variance one.

To show that the white noise can be a formal derivative of a Wiener process, let $W(t)$ be a standard Wiener process. For fixed $h > 0$ define a new process X^h by

$$X^h(t) = \frac{W(t+h) - W(t)}{h} \tag{2.2.31}$$

for all $t \geq 0$. This is a weakly stationary Gaussian process with zero mean values and covariances

$$\Gamma_{X^h X^h}(\tau) = \frac{1}{h} \max\left\{0, 1 - \frac{|\tau|}{h}\right\} \tag{2.2.32}$$

and it thus has spectral density

$$S_h(\omega) = \frac{1}{\pi h} \int_0^h \left(1 - \frac{|s|}{h}\right) \cos(\omega s) ds = \frac{1}{\pi} \frac{1 - \cos(\omega h)}{(\omega h)^2.} \tag{2.2.33}$$

This density is very broad for small h and indeed, converges to $1/\pi$ for all $\omega \neq 0$ as $h \to 0$, which suggests that the process X^h converges in some sense to a Gaussian white noise process $N(t)$ as h converges to 0 and hence a Gaussian white noise process is a derivative of a Wiener process.

Thus in a usual sense, the white noise cannot be a physical process, but its physical realization can be approximated to any desired degree of accuracy by some conventional stochastic process with broad banded spectra, such as Eq. (2.2.31).

2.3 Itô stochastic differential equations

The structural dynamics problems can be usually defined by a certain differential equation or by a system of several differential equations. The inclusion of random effects in these differential equations leads to two distinct classes of equations, for which the solution processes have differentiable and non-differentiable sample paths, respectively. They require fundamentally different methods of analysis. The first class of equations is when an ordinary differential equation is excited by a fairly regular stochastic process or it has random coefficients, or a random initial value, or combination of these. The equation is called a *random differential equation* and can be solved as ordinary differential equations. Sample paths are at least differentiable functions.

The second class occurs when the forcing is an irregular stochastic process such as Gaussian white noise. Then the integration must be done in the Itô or Stratonovich sense. They are called *stochastic differential equations* or *SDEs*, and in general their solutions inherit the non-differentiability of sample paths from the Wiener process. Further on, the Itô SDE will be used. The existence and uniqueness theorems for SDE are given in the books on the subject Øksendal (1998), Kloeden and Platen (1999), Lin and Cai (1995).

As it was mentioned above, Markov, Wiener and white noise processes are hardly physical and represent idealized models, but, on the other hand, they possess very convenient properties. The replacement of the real broad-banded process is fair enough unless it is input for the differential operator, which is known to be an operator with a finite bandwidth.

Even if the input happens to be also a narrow-band process, it is possible in many cases to approximate it by the filtered white noise, where the filter is usually also of differential type. Furthermore, the measurements of the real processes are done with some time gaps and not continuously. Thus, the time interval between the consecutive observations can be chosen so that the load values at these points would be uncorrelated. Obviously this specific time interval should be less than so-called relaxation time which defines the memory of the process (Lin and Cai, 1995).

The Wiener process can thus be used as a building block to construct other processes generated as a solution of corresponding SDE

$$dX(t) = m(X,t)dt + \sigma(X,t)dW(t), \tag{2.3.1}$$

where $m(X,t)$ and $\sigma(X,t)$ are called the *drift* and *diffusion coefficients*, respectively, and where $W(t)$ is a standard Wiener process, see properties (Def. 7). The drift function states that the large changes in the value of $X(t)$ are unlikely because $P[|X(t)-X(s)| > \varepsilon \,|\, X(s) = x]$ is of order $o(t-s)$, $s < t$, and the process has the continuous samples with probability one.

$$E[X(t) - X(s) \,|\, X(s) = x] = m(x,s)(t-s) + o(t-s). \tag{2.3.2}$$

The diffusion function defines the second-order characteristics or the variance of the corresponding diffusion process

$$E[(X(t) - X(s))^2 \,|\, X(s) = x] = \sigma^2(x,s)(t-s) + o(t-s). \tag{2.3.3}$$

The interpretation of these functions is given in Soong and Grigoriu (1997). Now, Eq. (2.3.1) is equivalent to

$$X(t) = X(0) + \int_0^t m(X(u),u)du + \int_0^t \sigma(X(u),u)dW(u). \tag{2.3.4}$$

The first integral is the ordinary Riemann-Stieltjes integral. This is unlike the second integral, which cannot be defined in an ordinary sense because of unbounded variation of the Wiener process samples. Though Itô proposed that it can be interpreted as a forward L_2 integral, it can be calculated as an Itô integral.

$$\int_0^t \sigma(X(u),u)dW(u) = \operatorname*{l.i.m.}_{\substack{n\to\infty \\ \max \triangle u \to 0}} \sum_{j=1}^{n} \sigma(X(u_j),u_j)(W(u_{j+1}) - W(u_j)). \tag{2.3.5}$$

If the second integral in Eq. (2.3.4) is interpreted in the Itô sense then it can be shown that if a constant k exists and the Lipschitz's condition

$$|m(x,\tau) - m(y,\tau)| + |\sigma(x,\tau) - \sigma(y,\tau)| \le k|x-y| \tag{2.3.6}$$

for any x, y, $s \le \tau \le t$ and the growth condition

$$|m(x,\tau)|^2 + |\sigma(x,\tau)|^2 \le k^2|1 + |x|^2|, \quad \forall x, \tag{2.3.7}$$

are satisfied then the solution $X(t)$ of the Itô equation (Eq. 2.3.1) is a unique non-anticipating process in $[s,t]$ and it is a Markov process.

It is also worth mentioning that the usual chain rule of differentiation is not applicable for the Itô stochastic differential equation because the drift and diffusion parts of the right-hand side are not of the same order of magnitude. The Itô's special differential rule for an arbitrary scalar function $g(X,t)$ for a Markov process $X(t)$ is developed as following

$$dg = \left(\frac{\partial g}{\partial t} + \mathcal{L}_X g\right) dt + \sigma(X,t)\frac{\partial g}{\partial X} dW(t), \tag{2.3.8}$$

where $g = g(X(t),t)$, $\mathcal{L}_X$ is known as the generating differential operator of the Markov process $X(t)$, given by

$$\mathcal{L}_X = m(X,t)\frac{\partial}{\partial X} + \frac{1}{2}\sigma^2(X,t)\frac{\partial^2}{\partial X^2}. \tag{2.3.9}$$

The next important result for SDEs is the *the Fokker-Plank equation* given by

$$\frac{\partial f}{\partial t} = -\frac{\partial}{\partial x}[m(x,t)f] + \frac{1}{2}\frac{\partial^2}{\partial x^2}[\sigma^2(x,t)f], \tag{2.3.10}$$

where $f(x,t|x_0,t_0)$ denotes the conditional probability density of $X(t)$ given that $X(t_0) = x_0$. Thus the initial condition for the partial differential equation (2.3.10) is $f(x,t_0|x_0,t_0) = \delta(x - x_0)$.

For the vector diffusion process $X(t) = (X_1(t),\ldots,X_n(t))^T$ (T denotes transposition) and m-dimensional $W(t) = (W_1(t),\ldots,W_m(t))^T$, the equations (2.3.8-2.3.10) take the form

$$dg = \left(\frac{\partial g}{\partial t} + \sum_{i=1}^{n} m_i \frac{\partial g}{\partial x_i} + \frac{1}{2}\sum_{i=1}^{n}\sum_{j=1}^{m} b_{ij}\frac{\partial^2 g}{\partial x_i \partial x_j}\right) dt + \sum_{i=1}^{n}\sum_{j=1}^{m} b_{ij}\frac{\partial g}{\partial x_i} dW(t) \tag{2.3.11}$$

where $b_{ij} = [\sigma(X,t)\sigma(X,t)^T]_{ij}$, now $m(X,t) = (m_1,\ldots,m_n)^T$ and $\sigma(X,t) = \{\sigma_{ij}\}$, $i = 1,\ldots,n$, $j = 1,\ldots,m$. So then the Fokker-Plank equation takes the form

$$\frac{\partial f}{\partial t} = -\sum_{i=1}^{n}\frac{\partial}{\partial x_i}(m_i f) + \frac{1}{2}\sum_{i=1}^{n}\sum_{j=1}^{m}\frac{\partial^2}{\partial x_i \partial x_j}(b_{ij} f). \tag{2.3.12}$$

2.4 Numerical integration of SDE

As for deterministic differential equations, there is a class of SDEs for which the solution is known analytically. For the one-dimensional case the solutions of explicitly solvable SDEs are given, for instance, in Kloeden and Platen (1999). The general solution and its properties of random vibration problems for linear and some non-linear systems are presented in Soong and Grigoriu (1997). Though certainly the numerical implementation of these assumes the use of approximation methods. The general Euler and Runge-Kutta schemes are presented in this section and the particular expressions and further explanations will be given in Chapter 5.

2.4.1 The Euler approximation

One of the simplest time discrete approximations of an Itô process is the *Euler approximation*, or the *Euler-Maruyama approximation*. It represents the simplest strong Taylor approximation (Kloeden and Platen, 1999). Let $X(t)$, $t_0 \leq t \leq T$, be a solution of an SDE given by (2.3.1) with initial value $X(t_0) = x_0$, in general X is a vector process. For a given discretization $t_0 < t_1 < \cdots < t_i < \cdots < t_M = T$ of the time interval $[t_0, T]$, an Euler approximation is a continuous time stochastic process $Y = \{Y(t), t_0 \leq t \leq T\}$ satisfying the iterative scheme

$$Y_{i+1} = Y_i + m(Y_i, t_i)\Delta t_i + \sigma(Y_i, t_i)\Delta W_i \tag{2.4.1}$$

for $i = 0, 1, 2, \ldots, M-1$ where $Y_i = Y(t_i)$, $\Delta t_i = t_{i+1} - t_i$, $\Delta W_i = W_{i+1} - W_i$ and with initial value $Y_0 = x_0$. In order to simulate the increments of the Wiener process the independent Gaussian random numbers are used. In the numerical experiments the random number generator for normal distribution from the standard NAGC library (http://www.nag.co.uk/) is used. The algorithms and ideas about random number generators are given in Appendix A. The same procedure is available for higher dimension systems.

The absolute error average $E[|X(T) - Y^{\delta}(T)|]$ between the approximation and Itô process at the time T defines the order of strong convergency if there is constant $C > 0$, which does not depend on δ, and a $\delta_0 > 0$ such that

$$E[|X(T) - Y^{\delta}(T)|] \leq C\delta^{\gamma} \tag{2.4.2}$$

for each $\delta \in (0, \delta_0)$, where δ is a maximum step size of discrete scheme. Thus the Euler scheme attains the strong order of convergency $\gamma = 0.5$ (Kloeden and Platen, 1999). For the case when $\sigma(X, t)$ does not depend on X, the Euler scheme has the order of convergence, also called the mean-square order of accuracy, $\gamma = 1$. Nevertheless the Euler scheme is not a robust tool in the case of the non-linear drift and diffusion coefficients. Other more sophisticated and robust schemes are considered in Milstein (1995), Kloeden and Platen (1999).

2.4.2 The Runge-Kutta approximation

The classical 4th order Runge-Kutta (RK) method is concerned with the numerical solution of the deterministic initial value problem given

$$\dot{Y} = f(t, Y(t)), \quad Y(t_0) = Y_0. \tag{2.4.3}$$

Assume that the discrete approximation is made with an M-stage explicit RK scheme (Carpenter and Kennedy, 1994). The implementation over a time step Δt is accomplished

by

$$k_1 = f(t_0, Y_0), \tag{2.4.4}$$

$$k_i = f\left(t_0 + c_i\Delta t, Y_0 + \Delta t \sum_{j=1}^{i-1} a_{i,j}k_j\right) \quad i = 2, \ldots, M \tag{2.4.5}$$

$$Y_1 = Y_0 + \Delta t \sum_{j=1}^{M} b_j k_j, \tag{2.4.6}$$

where $Y_1 = Y(t_0 + \Delta t)$ and fixed scalars $a_{i,j}$, b_j, c_i are the coefficients of the RK formula.

Consequently, Kloeden and Platen (1999) and Skaug (2000) refer to the standard 4-stage RK procedure, where

$$\begin{aligned} c_2 = c_3 = \frac{1}{2},\ c_4 = 0, \\ a_{2,1} = a_{3,2} = \frac{1}{2},\ a_{4,3} = 1, \\ b_1 = b_4 = \frac{1}{6},\ b_2 = b_3 = \frac{1}{3}. \end{aligned} \tag{2.4.7}$$

For the numerical integration of the stochastic differential equation

$$dX(t) = m(X,t)dt + \sigma(X,t)dW(t), \tag{2.4.8}$$

for cases where $\sigma(X(t), t) = \sigma(t)$, that is, σ does not depend on X, it is assumed appropriate to use the RK approximation for the drift part and keep the Euler approximation for the diffusion part. Then the so-called Runge-Kutta-Maruyama method is given

$$X_{i+1} = X_i + \Delta t \sum_{j=1}^{M} b_j k_j + \sigma(X_i, t_i)\Delta W_i \tag{2.4.9}$$

where b_j, k_j are the coefficients (Eqs. 2.4.4-2.4.6), $\Delta W_i = W_{i+1} - W_i$ are the increments of the Wiener process, which are independent Gaussian variables with expectation zero and variance Δt. Hereafter, the diffusion function is assumed independent of the state space variable X though the general notations are preserved.

For the purposes of this thesis, the accuracy of the above-mentioned scheme is fair enough, though the more complicated and accurate procedures are available if needed (Milstein, 1995; Kloeden and Platen, 1999). The 5-stage RK method of Carpenter and Kennedy (1994) is used for the numerical simulations due to the lower storage requirements compared with the standard 4-stage method.

Chapter 3

Reliability

3.1 Introduction

Traditionally, structural design has relied on deterministic analyses. Nevertheless the uncertainties in loads and material properties were not completely neglected. The safety factors were introduced to separate strengths and loads. The subject of structural reliability started to evolve from the beginning of the 1920s. The detailed history of the subject is given, for instance, in Madsen et al. (1986).

The study of structural reliability is concerned with the calculation and prediction of the probability of limit state violation for engineered structures at any stage during their life. Here it is implied that the limit state is the requirements of the safety of the structure against collapse, limitations for damage or deflections etc. The probability of the occurrence of an event such as limit state violation is a numerical measure of the chance of its occurrence. This measure may either be obtained from the experimental measurements of the long-term frequency of the occurrence of the event for a similar structure, which is rarely available for a sufficient long period, or by subjective estimation of the numerical value. Usually both methodologies are used to get an estimate. Thus the efficiency of a reliability method depends on how much information about a given problem has been utilized; additional information can often be exploited to accelerate the convergence of the failure probability estimate. In essence, the efficiency of a reliability method is often gained at the expense of generality (Au and Beck, 2001).

In probabilistic assessments any uncertainty about a variable given in terms of a probability density function, is explicitly taken into account, unlike the deterministic way of measuring safety by *factor of safety*, or *load factor*. The factor of safety defines a gap between the applied stress, moment or displacement and the corresponding capacity to resist these load effects. The alternative and useful measure of safety is the *safety margin*, which in its simplest form can be expressed as

$$M = R - S, \tag{3.1.1}$$

where R is the resistance and S is the resultant load effect. By this formulation, $M = 0$ is the limit state. This measure is extensively used in the probabilistic analysis as well. As one might see, this formulation is much alike the cost-benefit principle.

Further in the probabilistic analysis it is possible to classify the reliability methods by their order of uncertainty

- First level: deterministic - like methods that employ only one characteristic value of each uncertain parameter;
- Second level: the methods that employ two values of each uncertain parameter (commonly mean and variance) and measure of correlation between the parameters, for instance, reliability index methods, which will be described later;
- Third level: methods that require a knowledge of joint distribution of all uncertain parameters
- Fourth level: methods that combine the structural analysis and economical aspects of structural design.

The reliability assessment is not a rule for the structural safety but it is the recommendation and is in addition to the existing methods. The calibration methods exist to supply the different estimations from the techniques of the different levels. It allows taking into account parameters and factors such as structure reliability itself and the cost of the construction as well as the comfort exploitation.

3.2 Time-invariant case

In structural reliability the basic variables are assumed to be uncertain and can be represented by their density functions. Load, resistance, geometry or workmanship can be defined as these basic variables and described in probabilistic terms. The basic random variables are collected in the a random vector $Z = (Z_1, Z_2, \ldots, Z_n)$ which has the joint probability density function $f_Z(z)$. Assume Z, that is a random point in n-dimensional vector space, to be time independent. Then different failure modes can be defined in a *failure function* or *limit state function* $g(Z)$. The boundary between the safe states and the failed states in Z-space is the set of limit states which corresponds to $g(Z) = 0$ (Fig. 3.1).

The *reliability* of the systems is defined as a probability that the vector Z lays inside a safe domain

$$p_S = P\{g(Z) > 0\} = \int_{D_S} f_Z(z)dz. \tag{3.2.1}$$

It follows that the *failure probability* is defined as the complement to the reliability

$$p_f = 1 - p_S = P\{g(Z) \leq 0\} = \int_{D_f} f_Z(z)dz. \tag{3.2.2}$$

For instance, if a system can be described by two basic variables such as the stress S and resistance R with joint density function $f_{RS}(r, s)$ and marginal density functions $f_S(s)$ and $f_R(r)$ and by the safety margin $M = g(Z) = R - S$,

$$p_f = P\{R - S \leq 0\} = \int\int_{D_F} f_{RS}(r, s)drds. \tag{3.2.3}$$

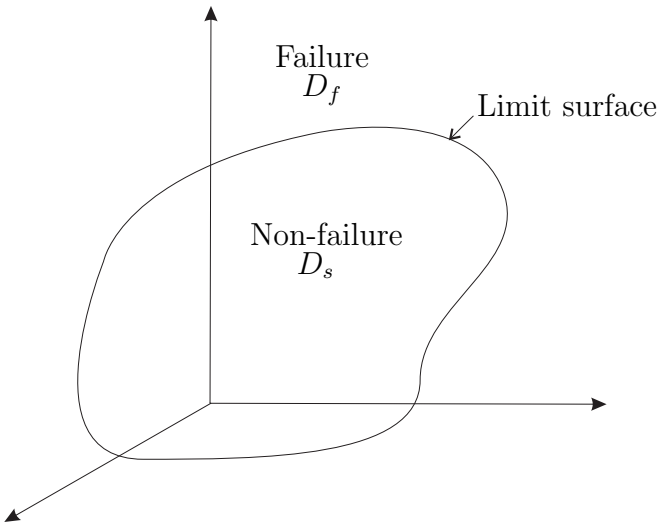

Figure 3.1: Limiting surface in the state space.

Assume that R and S are independent, then

$$p_f = P\{R - S \leq 0\} = \int_{-\infty}^{\infty} \int_{-\infty}^{s \geq r} f_R(r) f_S(s) dr ds \tag{3.2.4}$$

which is reduced to a convolution integral. Moreover if R and S are normally distributed, then the probability of failure

$$p_f = P\{R - S \leq 0\} = P\{M \leq 0\} = \Phi\left(\frac{0 - \mu_M}{\sigma_M}\right) = \Phi(-\beta), \tag{3.2.5}$$

where $\Phi(\cdot)$ is the standard Gaussian distribution (Eq. 2.1.24), $\mu_M = \mu_R - \mu_S$ and $\sigma_M^2 = \sigma_R^2 + \sigma_S^2$ are the mean value and the variance of a random variable, $M = g(Z) = R - S$, given by well-known rules for addition (subtraction) of normal random variables. β is called the *safety index* or *reliability index* which is extensively used in reliability theory (Fig. 3.2).

In general, the integration of Eq. (3.2.2) cannot be performed analytically. There are basically two methods to deal with this integral:

- multidimensional integration of the original program using numerical approximation such as simulation and by
- transforming the basic variables of the original problem into the space of independent standard Gaussian variables and perform the integration of the standard Gaussian distributions.

To conclude, it is worth mentioning that for convenience the indicator function may be introduced, defined by

$$I(x) = \begin{cases} 0 & \text{if} \quad x > 0 \\ 1 & \text{if} \quad x \leq 0 \end{cases} \tag{3.2.6}$$

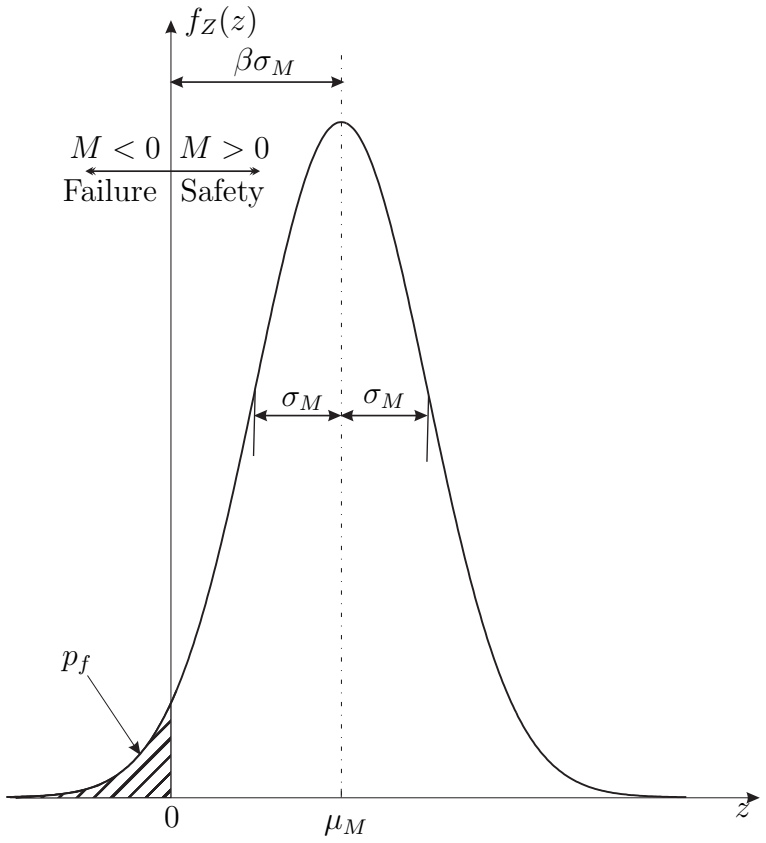

Figure 3.2: Distribution of safety margin.

There are some other types of indicator function but they are of no interest in this thesis. Thus the failure probability becomes:

$$p_f = E\{I[g(Z)]\} = \int_z \cdots \int I[g(z)] f_Z(z) dz. \tag{3.2.7}$$

3.2.1 FORM

To continue on the subject of reliability, the methodology developed throughout the thesis is based on using the first-order reliability method *FORM*. This technique can be implemented for the second and third level reliability methods after the classification given in the introduction, depending on the distributions of the basic variables. For implementation of FORM the number of the basic variables must be finite. Indeed if FORM is the technique for second and third level methods then all basic variables are given by the mean and covariances, and by their joint density function correspondingly.

The FORM method is based on the idea of a *reliability index* (or *safety index*) β. Assume a safety margin is defined as above, i.e. $M = g(Z)$, then Cornell (1969) defined reliability

index as

$$\beta_C = \frac{\mu_M}{\sigma_M}. \tag{3.2.8}$$

An illustration of this is given in Fig. (3.2).

For a general non-linear failure function, linearization of the safety margin around the point z gives a linear safety margin

$$M = g(z) + \sum_{i=1}^{n} \frac{\partial g}{\partial z_i}(z)(Z_i - z_i) \tag{3.2.9}$$

with the corresponding reliability index β:

$$\beta = \frac{g(z) + \sum_{i=1}^{n} \frac{\partial g}{\partial z_i}(z)(E[Z_i] - z_i)}{\left(\sum_{i=1}^{n} \sum_{j=1}^{n} \frac{\partial g}{\partial z_i} \frac{\partial g}{\partial z_j} Cov(Z_i, Z_j) \right)^{1/2}} \tag{3.2.10}$$

where $Cov(Z_i, Z_j) = E[(Z_i - E[Z_i])(Z_j - E[Z_j])]$.

This reliability index is called a *first-order second-moment reliability index*. However, the so-called invariance problem arises because it can be shown that the failure function can be written in many different but equivalent ways, for instance, for the stress-resistance formulation here: $g(Z) = R - S$ or $g(Z) = R/S - 1$.

To avoid this problem, a third interpretation of the reliability index was given by Hasofer and Lind (1974) which is invariant with respect to the mathematical formulation of the safety margin. It is proposed that there is a mapping of the set of basic variables into a set of normalized and uncorrelated Gaussian variables $\{U_i\}$, $i = 1, \ldots, n$ with expected value zero and unit standard deviation. By this transformation the failure surface in the new U space is given as

$$g(z) = g_u(u) = 0. \tag{3.2.11}$$

The point closest to the origin is called the *β-point* or the *design point*. Thus the Hasofer and Lind reliability index defined in the U-space is invariant to different equivalent formulations of the failure function because it is related directly to the failure surface and not directly to the failure function. First of all, it is important to find the design point in this space. The design point u^* is the solution for the constrained optimization problem

$$\min_{g_u(u)=0} \sqrt{\sum_{i=1}^{n} u_i^2}. \tag{3.2.12}$$

Then the unit normal vector $\vec{\alpha}$ to the failure surface at the design point directed toward the failure set is constructed (see Fig. 3.3)

$$\vec{\alpha} = -\frac{\nabla g(u^*)}{|\nabla g(u^*)|}. \tag{3.2.13}$$

At last, the reliability index is given as

$$\beta = \vec{\alpha} \cdot u^*. \tag{3.2.14}$$

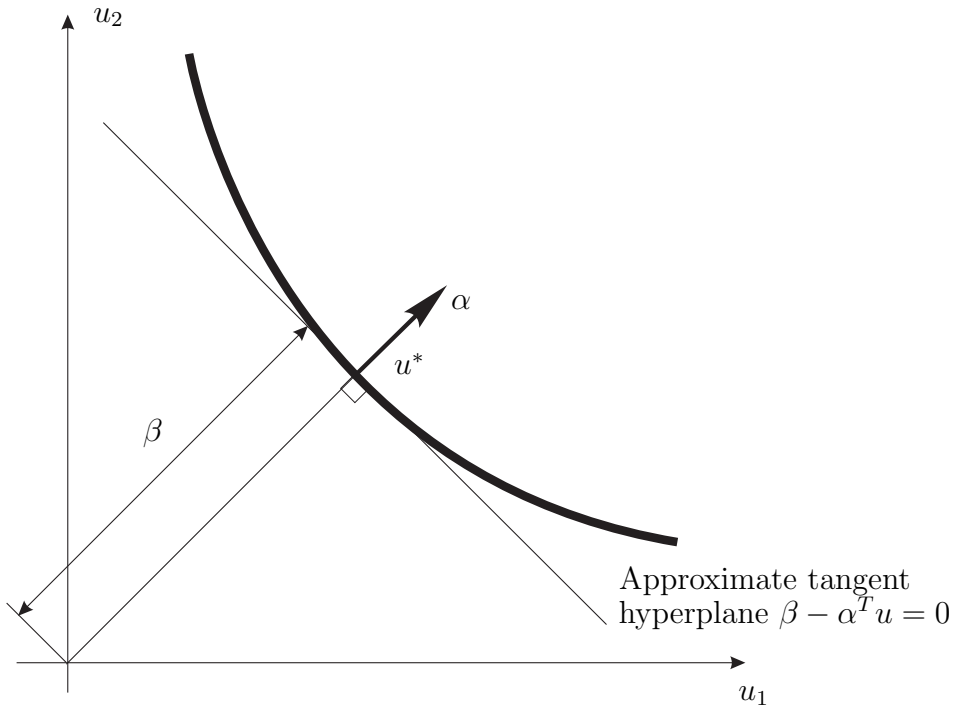

Figure 3.3: Design point on the failure surface.

Thus the calculation of the reliability index has become an optimization problem. Consequently problems arise about whether the failure surface has several local minima and how to combine the reliability indices of several members of the structure (der Kiureghian and Dakessian, 1998). Moreover, the concept reliability index can be generalized further, but only the Hasofer and Lind definition is used throughout the thesis because it best serves our purposes.

3.2.2 Simulation techniques and Monte Carlo method

The concept of the simulation methods is to generate the realizations of the basic variables, to find in which domain, safe or failure, these realizations are situated and estimate their contributions to reliability or failure probability depending on their position. The universal and simplest method is a *direct* or *crude Monte Carlo method*. Besides, other methods such as importance sampling, adaptive sampling, directional simulation (Rubenstein, 1981; Ditlevsen and Madsen, 2003) that have been developed in recent years. In this thesis, the focus is on the importance sampling techniques, used for improving of the Monte Carlo method results.

The underlying idea of the Monte Carlo method is to compose a stochastic process which produces a random variable whose expected value is the solution to a certain problem. The general implementation and applications are described in detail by Bauer (1958). Let us assume that the basic variables Z can be mapped by some regular transformation to the normalized U-space of Gaussian variables. Thus, the failure surface $g(Z) = 0$ transforms correspondingly (Eq. 3.2.11). Further, the u-subscript will be omitted for convenience. Thus the estimate of the mean value in the game of chances for Eq. (3.2.7) in the normalized U-space is given as

$$\hat{p}_f = \frac{1}{N} \sum_{j=1}^{N} I[g(u_j)], \tag{3.2.15}$$

where N is the number of stochastic experiments and u_j is a vector of the j^{th} realization of the standard Gaussian vector U. The standard deviation of $\hat{p}_f$ is estimated as

$$\sigma = \sqrt{\frac{\hat{p}_f(1-\hat{p}_f)}{N}}. \tag{3.2.16}$$

It is obvious that the error and convergence rate is proportional to $1/\sqrt{N\hat{p}_f}$.

For the direct Monte Carlo method, the realizations of the normal vector U will be distributed mostly around the origin. This is unlike the importance sampling techniques, where the samples are concentrated in the domain which gives the largest contribution to the failure probability.

$$p_f = \int \cdots \int I[g(u)] f_U(u) du = \int \cdots \int I[g(y)] \frac{f_U(y)}{f_S(y)} f_S(y) dy \tag{3.2.17}$$

where the importance sampling density $f_S(y)$ has been suitably chosen. The estimate of failure probability by importance sampling is defined by

$$\hat{p}_f = \frac{1}{N} \sum_{j=1}^{N} I[g(y_j)] \frac{f_U(y_j)}{f_S(y_j)} \tag{3.2.18}$$

and the standard deviation in this case is

$$\sigma = \sqrt{\frac{1}{N(N-1)} \left\{ \sum_{j=1}^{N} \left(I[g(y_j)] \frac{f_U(y_j)}{f_S(y_j)} \right)^2 - \frac{1}{N} \left(\sum_{j=1}^{N} I[g(y_j)] \frac{f_U(y_j)}{f_S(y_j)} \right)^2 \right\}}. \tag{3.2.19}$$

This methodology is also called *variance reduction*. The aim of these techniques is to reduce the error of the estimators and to increase the rate of convergency. The other variance reduction techniques are briefly discussed in Appendix B.

3.3 Time-variant case

The actions on the structure, as well as material properties and exploitation conditions very often explicitly depend on time. Thus in general, the basic variables change in time. In this thesis dynamical loads are assumed. The response of the structure $X(t)$ is governed by the SDE (2.3.1). Then the failure probability (Eq. 3.2.2) is defined in the probability space $(\Omega, \mathcal{F}, \mathcal{F}_\tau, P)$, where $\mathcal{F}_\tau$, $t_0 \leq \tau \leq T$ is a non-decreasing family of σ-sub-algebras,

$$p_f(T; t_0) = 1 - \int_{E_S} dP(\omega) = \int_{\Omega} I[g(X(\cdot, \omega))]\, dP(\omega) = E(I[g(X)]), \tag{3.3.1}$$

where $E_s = \{\omega : X(t, \omega) \in D_s, \forall\, t : t_0 \leq t \leq T\}$ is the safe subspace, $I[g(X)]$ is an indicator function defined as follows: $I[g(X)] = 0$ for $\omega \in E_S$, $I[g(X)] = 1$ otherwise, see (Eq. 3.2.6).

The exact value of this integral is difficult to obtain. No analytical solution is known today. It can be estimated by simulation techniques or by suitable approximations.

One such approximation is obtained by assuming that the excursion events outside of the safe domain constitutes a Poisson process $N_{D_s}(t)$, where $N_{D_s}(t)$ denotes the number of excursions during the time interval (t_0, T). The reliability coincides with the probability that the initial response $X(t_0)$ belongs to the safe domain and the response does not leave the safe domain during $(t_0, T]$, which is given as (Soong and Grigoriu, 1997)

$$p_s(T; t_0) = P\{(X(t_0) \in D_s) \cap (N_{D_s}(\tau) = 0)\}, \tag{3.3.2}$$

where $\tau = T - t_0$. It can be approximated by

$$p_s(T; t_0) \approx P\{X(t_0) \in D_s\} P\{N_{D_s}(\tau) = 0\} \tag{3.3.3}$$

under the assumption that the events $\{X(t_0) \in D_s\}$ and $\{N_{D_S}(\tau) = 0\}$ are independent. Another simplification is that the D_s-outcrossings of $X(t)$ follow an inhomogeneous Poisson process of intensity $\nu_{D_s}(t)$ at time t. Moreover also if $P\{X(t_0) \in D_s\} = 1$ then the result is obtained as

$$p_s(T; t_0) \simeq \exp\left(-\int_{t_0}^{T} \nu_{D_S}(s) ds\right) \tag{3.3.4}$$

or if $X(t)$ is a stationary process in addition, then

$$p_s(T; t_0) \simeq \exp\left(-\nu_{D_s}(T - t_0)\right) \tag{3.3.5}$$

and the approximation of the failure probability is given

$$p_f(T; t_0) = 1 - p_s(T; t_0) \approx 1 - \exp\left(-\int_{t_0}^{T} \nu_{D_s}(s) ds\right). \tag{3.3.6}$$

The mean rate of D_s-outcrossings is given

$$\nu_{D_s}(t) = \frac{d}{dt} E[N_{D_s}(t)] \tag{3.3.7}$$

where $E[N_{D_s}(t)]$ is a mean number of excursions of $X(\tau)$ outside D_s during $(0,t)$. Moreover the definition of the outcrossing rate requires that the process is regular, that is to say the probability of having more than one crossing in small interval of time must be negligible.

The mean crossing rate of a univariate stochastic process $X(t)$ from a safe domain $D_s = (-\infty, x)$ can be defined from the famous Rice formula (Rice, 1954; Soong and Grigoriu, 1997)

$$\nu_x^+(t) = \int_0^\infty \zeta f(x,\zeta;t)d\zeta, \tag{3.3.8}$$

where $f(x,\dot{x};t)$ denotes the joint probability density function of $\{X(t), \dot{X}(t)\}$.

The crossing rate of the stationary Gaussian process $X(t)$ (Def. 4, Chapter 2) with mean value μ and variance σ^2 is given

$$\nu_x^+(t) = \nu_x^+ = \frac{\dot{\sigma}}{\sqrt{2\pi}}\phi\left(\frac{x-\mu}{\sigma}\right) \tag{3.3.9}$$

where $\dot{\sigma}$ is the standard deviation of $\dot{X}(t) = dX(t)/dt$ and $\phi(\cdot)$ is the Gaussian density function (Eq. 2.1.23).

Nevertheless, the Poisson approximation assumes a lot of restrictions which rarely hold for the wide class of real processes (Soong and Grigoriu, 1997). Despite all advantages of this method, the Monte Carlo simulation techniques are still the best in the competition. The only drawback of the crude or direct method is the slow convergence (Section 3.2.2). However as it will be shown in Chapter 5, the variance reduction methods such as importance sampling are applicable for improving the Monte Carlo procedure based on the measure transformation method proposed by Girsanov (1960).

3.3.1 Simulation technique and Monte Carlo method

Let $f(X(t_0+T))$ be a function or a functional of the stochastic vector process $X(t)$ which is a solution of a certain SDE (2.3.1). Then two errors arise during the computation of $E[f(X(t_0+T))]$ by the direct Monte Carlo method. First of all, there is a corresponding numerical error during the discrete integration of the SDE. Let $\hat{X}(t_0+T)$ denote an approximate solution of this equation. Secondly, there is an error in the Monte Carlo method. Since $Var(f(\hat{X}(t_0+T)))$ is close to $Var(f(X(t_0+T)))$, we may assume that the error in the Monte Carlo method can be bounded by $(Var(f(X(t_0+T)))/N)^{1/2}$ (Milstein, 1995). If $Var(f(X(t_0+T)))$ is large, then, in order to achieve satisfactory precision, we have to take into account a very large number of trajectories. The improvement may be achieved by implementing the variance reduction methods such as for instance by the importance sampling technique.

To define a measure analogous to the sampling density in Section 3.2.2 it is necessary to define a certain transformation. Moreover the stochastic processes must be consistent with their probability measures. Define the Wiener process $W(t)$ with respect to measure P on σ-algebras $\mathcal{F}_s$, $\mathcal{F}_s \subset \mathcal{F}_t$, $t > s$ then the Girsanov transformation of measure (Girsanov, 1960) can be applied. This changing of measures is absolute continuous (Chung and Williams,

1990) because samples of the Wiener process are absolutely continuous as it was discussed in Section 2.2.3.

Let $X(t)$ be a solution of

$$dX(t) = m(X,t)dt + \sigma(X,t)dW(t). \tag{3.3.10}$$

Let $v(t,\omega) = (v_1, \ldots, v_n)$ be a non-anticipative bounded process such as it depends only on the behaviour of a system before time t; and define a diffusion

$$d\rho_s^t(v) = -\frac{1}{2}v(t,\omega)^2 dt + v(t,\omega)dW(t). \tag{3.3.11}$$

Then the following theorem can be stated (Øksendal, 1998; Fleming and Rishel, 1975).

Theorem 2 (The Girsanov theorem)**.** *Let $W(t) = \{w(t,\omega), P, \mathcal{F}_t\}$ be a Wiener process in $\mathbb{R}_n$. Define an Itô process $\widetilde{W}(t)$ of the form*

$$d\widetilde{W}(t) = -v(t,\omega)dt + dW(t), \quad t \le T < \infty, \ \widetilde{W}(0) = 0. \tag{3.3.12}$$

Assume that $v(t,\omega)$ satisfies Novikov's condition

$$E\left[\exp\left(\frac{1}{2}\int_0^T v^2(s,\omega)ds\right)\right] < \infty. \tag{3.3.13}$$

Introduce the new measure $\widetilde{P}$ as

$$d\widetilde{P}(\omega) = \exp\rho_s^T(v)dP(\omega), \tag{3.3.14}$$

where $\rho_s^T(v)$ is the solution of (3.3.11). $\widetilde{P}$ will be absolutely continuous with respect to P. Moreover assume that $\widetilde{P}(\Omega) = 1$.

Then

$$d\widetilde{X}(t) = m(\widetilde{X},t)dt + \sigma(\widetilde{X},t)v(t,\omega)dt + \sigma(\widetilde{X},t)d\widetilde{W}(t)), \tag{3.3.15}$$

where $\widetilde{W}(t) = \{\widetilde{w}(t,\omega), \widetilde{P}, \mathcal{F}_t\}$ is a Wiener process with respect to a probability measure $\widetilde{P}(\omega)$.

The rigorous proof is given in Girsanov (1960). Other variations of this theorem and applications are considered in Øksendal (1998), Fleming and Rishel (1975). The $\exp\rho_s^T(v)$ is called the *Radon-Nikodym* derivative (Rudin, 1987).

Thus the transformation of measures gives the desired importance sampling measure. In particular when $v(t,\omega) = v(t,X)$, the new SDE with changed Wiener process is given

$$\begin{aligned} d\widetilde{X}(t) &= m(t,\widetilde{X})dt + \sigma(t,\widetilde{X})v(t,\widetilde{X})dt + \sigma(t,\widetilde{X})d\widetilde{W}(t), \\ \widetilde{X}(s) &= x, \end{aligned} \tag{3.3.16}$$

where $\widetilde{X}(t)$ is a new improved response considered on the time interval $(s,T]$ with given initial condition. The associated failure probability integral now takes the form

$$p_f(T;s,x) = \int_{\Omega} I[g(\widetilde{X})] \left(\frac{dP}{d\widetilde{P}}\right) d\widetilde{P}, \tag{3.3.17}$$

where the Random-Nikodym derivative under the transformed Wiener process $\widetilde{W}(t)$ is given by Naess (1999)

$$\left(\frac{dP}{d\widetilde{P}}\right) = \exp\left(-\int_s^T v(\tau,\widetilde{X}(\tau))d\widetilde{W}(\tau) - \frac{1}{2}\int_s^T v^2(\tau,\widetilde{X}(\tau))d\tau\right). \tag{3.3.18}$$

The problem of how to choose the function $v(t,\omega)$ will be discussed in the next chapter. Further, this function is called a control function because it allows us to control the dynamics of the system in a desirable way. However, choosing an arbitrary change of probability measure aiming at the more frequent excursion from the safe domain may lead to the estimate with greater or even infinite variance. To avoid this, the control is obtained by the requirement of minimum variance of the failure probability estimate (Section 4.3).

3.3.2 FORM and design point excitations

In the proposed method of improving the convergence rate and reducing the systematic error, which will be given further in Chapter 5, the so-called design point excitation method is utilized. First this technique was considered in Li and Der Kiureghian (1995), then continued and expanded in Tanaka (1997), Macke (1999) and Næss and Skaug (2000). Thus the introduction and basic notation will given here, though the examples will be presented in Chapter 5.

The design point excitation procedure is based on FORM interpretation of the reliability problem. As was mentioned in the Section 3.2.1 in order to implement FORM the number of the basic variables must be finite. In the time dependent case, this condition is violated when the stochastic process has a continuous time parameter. However, due to numerical integration, time discretization allows us to reduce the quantity of basic variables to a finite number. In Chapter 5, this concept will be used to create the first approximation of the failure probability on the sets of the initial values in the state space and initial times.

Assume that $X(t) = \{X_1(t),\ldots,X_n(t)\}$ is a solution of SDE (2.3.1) on the interval $(s,T]$. To find the path of this solution the equidistant time discretization is used with step size $\Delta t = (T-s)/M$

$$s = t_0 \le t_1 \le \ldots \le t_i \le \ldots \le t_M = T \quad t_i = s + i\Delta t \tag{3.3.19}$$

Using the Euler approximation (Section 2.4.1) the SDE (2.3.1) can be approximated by the difference scheme

$$\begin{aligned} X_k(t_{i+1}) &= X_k(t_i) + m_k(t_i,X)\Delta t + \sum_{j=1}^{q}\sigma_{kj}(t_i,X)\Delta W_j(t_i) \\ X_k(s) &= x_k, \end{aligned} \tag{3.3.20}$$

with $W(t) = (W_1(t), \ldots, W_q(t))$ is a q-dimensional unit Wiener process. The dimensions of the state space and the Wiener process are determined by the dynamics of the system in general formulation. The increments of this vector process can be written as

$$\Delta W_j(t_i) = U_{ji}\sqrt{\Delta t} \quad (j = 1, \ldots, q;\ i = 0, \ldots, M-1) \tag{3.3.21}$$

with U_{ji} being mutually independent normal variables.

Failure is now approximated by checking the discretized process $X(t_i)$, for $i = 0, \ldots, M$, that is, $E_s \approx \{g(X(t_i)) > 0 : i = 0, \ldots, M\}$. Thus the failure surface may be expressed relative to the normalized variables U_{ji}, $i = 0, \ldots, M-1$ and $j = 1, \ldots, q$ by introducing a suitable failure function g_U:

$$g_U(u_{10}, \ldots, u_{q(M-1)}) = 0. \tag{3.3.22}$$

In this formulation it is clear that $E_s \approx \bigcap_{i=0}^{M-1} E_i$, where $E_i = \{g(X(t_i) > 0\}$. That is, a series system approximation has been adopted. The reliability of a series system can be simply approximated by the reliability of the subsystem with the lowest reliability considering failure functions g_{Ui}, $E_i = \{g_{Ui}(U_{10}, \ldots, U_{q(i-1)}) > 0\}$. The reliability index $\beta(t_i)$ of each subsystem is obtained by finding the coordinates of the point on the failure surface $g_{Ui}(u_{10}, \ldots, u_{q(i-1)}) = 0$ that minimize the distance to the origin. The simple series system reliability estimate is then given by

$$\beta^*(t^*) = \min_{s \le t_i \le T} \beta(t_i) \tag{3.3.23}$$

with corresponding most likely excitations leading to an out-crossing of this boundary at the exit time $t^* \in (s, T]$ defined as $u^* = (u^*_{10}, \ldots, u^*_{q(M-1)})$.

This kind of approximation fits systems which are dominated by a single passage time, as for instance, crack growth problems (Tanaka, 2000). In the case of oscillatory systems when excursions from the safe domain show some periodicity, the contribution to the failure probability is made by several time points. Not taking this into account will follow to the essential underestimation (Næss and Skaug, 2000).

If we consider the controlled system (Eq. 3.3.16) on (s, T) in the discrete form

$$\begin{aligned}\widetilde{X}_k(t_{i+1}) = \widetilde{X}_k(t_i) + m_k(t_i, \widetilde{X})\Delta t + \sum_{j=1}^{q} \sigma_{kj}(t_i, \widetilde{X}) v_j^*(t_i)\Delta t \\ + \sum_{j=1}^{q} \sigma_{kj}(t_i, \widetilde{X})\Delta W_j(t_i),\end{aligned} \tag{3.3.24}$$

with given above most likely excitations u^*. Then the controls $v_j^*(t_i, \widetilde{X})$ are given as

$$v_j^*(t_i, \widetilde{X}) = v_j^*(t_i) = \frac{1}{\sqrt{\Delta t}} u^*_{ji}, \quad (0 \le i \le M-1, j = 1, \ldots, q). \tag{3.3.25}$$

Macke and Bucher (2003) showed that the action of the controls corresponded to the other exit times, not only for the time t^*, can be equally important for the resultant failure probability. Then they proposed a weighting procedure based on a probability density function of the exit times. The importance sampling probability at each time point is proportional to the importance factor

$$\frac{\Phi(-\beta(t_i))}{\sum_{j=1}^{M} \Phi(-\beta(t_j))}, \tag{3.3.26}$$

which takes the interaction between controls explicitly into account. We shall return to this question in Chapter 5.

Chapter 4

Stochastic control theory

In order to reduce the variance of the estimate for the failure probability functional (Eq. 3.3.1), it would be desirable to speed up the first-passage event, i.e. to control the stochastic process in such way that failure would occur almost surely during the considered time interval. Definitely, the changing of a sample path will affect the probability measure of the response process. However, the Girsanov transformation (Theorem 2) takes this effect into account. Thus the objective of this chapter is to present a special optimal control function which minimizes the estimating error of the failure probability and which satisfies the conditions of the measure transformation.

4.1 Preliminaries about stochastic control

The general stochastic control theory assumes that the state of a system a time t can be described by an Ito process X_t given by an SDE of the form

$$\begin{aligned} dX_t = dX_t^v &= m(t, X_t, v_t)dt + \sigma(t, X_t, v_t)dW_t\,, \quad s \le t \le T \\ X_s &= x, \end{aligned} \tag{4.1.1}$$

where $x = (x_1, \ldots, x_n)$ are deterministic initial conditions, $X_t \in \mathbb{R}^n$, W_t is a q-dimensional Wiener process. Here $v_t \in V \subset \mathbb{R}^k$ is a parameter whose value we can choose in the given Borel set V at any instant t in order to control the process X_t (Øksendal, 1998). Thus $v_t = v(t, \omega)$ is a stochastic process. Here it is essential that the function $\omega \to v(t, \omega)$ is $\mathcal{F}_t$-measurable, or at least $\mathcal{F}_t^{(q)}$-measurable, where $\mathcal{F}_t^{(q)}$ denotes the σ-algebra generated by W_r for $r \le t$. Assume given two continuous functions, the *utility rate* function $F : \mathbb{R} \times \mathbb{R}^n \times V \to \mathbb{R}$ and the *bequest function* function $K : \mathbb{R} \times \mathbb{R}^n \to \mathbb{R}$, let $G = (0, T) \times D_s$, and let $\hat{T} = \hat{T}^{s,x}$ be the first exit time after s from G for the process (r, X_r), that is,

$$\hat{T} = \hat{T}^{s,x}(\omega) = \inf\{r > s; (r, X_r) \notin G\} \le T, \tag{4.1.2}$$

These functions define the performance function

$$J^v(s, x) = E\left[\int_s^{\hat{T}} F(t, X_t, v_t)dt + K(\hat{T}, X_{\hat{T}})\right]. \tag{4.1.3}$$

This defines a challenging optimization problem: To find for each $x \in D_s$ the number $\Phi(s,x)$ and a control $v^* = v^*(t,\omega)$ such that

$$\Phi(s,x) = \sup_{v(t,\omega)} J^v(s,x) = J^{v^*}(s,x), \tag{4.1.4}$$

where the supremum is taken over all $\mathcal{F}_t^{(q)}$-adapted processes $\{v_t\}$ with values in V. If such control v^* exists then it is called an *optimal control* and Φ is called the *optimal performance*.

The control can be classified by the type of function set V which allows us to choose numerical methods properly. First of all, the function $v(t,\omega) = v(t)$ may be deterministic, independent of the state of the system. Such control is called an *open loop* control. The example is the "design point" excitation shown in Section 3.3.2. Then processes $\{v(t)\}$ may be adaptive with regard to σ-algebra $\mathcal{M}_t$ generated by the $\{X_s^v; s \le t\}$. These controls are called *closed loop* or *feedback* controls. The third type of controllers is then the controller has just partial knowledge about the state of a system through some adjacent noise process $R(t)$. Hence the control $\{v(t)\}$ must be adapted w.r.t. σ-algebra $\mathcal{N}_t$ generated by $\{R_s; s \le t\}$. The special feature of this type is that it splits into the linear filtering problem and corresponding deterministic control problem (Øksendal, 1998) (Separation Principle). The fourth and the last type is Markov controllers $v(T,\omega) = v(t, X_t(\omega))$. Thus the value v at a time instant t depends only on the state (x,t) assuming that process v does not depend on initial conditions. Therefore, by choosing these controls v, the output X_t becomes an Itô diffusion, in particular a Markov process.

Consider first the Markov control $v(t,\omega) = v(t, X_t(\omega))$. Let us define the following operator for $v \in V$ and $f \in C_0^2(\mathbb{R} \times \mathbb{R}^n)$ is defined

$$(L^v f)(s,x) = \frac{\partial f(s,x)}{\partial s} + \sum_{i=1}^{n} m_i(s,x,v)\frac{\partial f(s,x)}{\partial x_i} + \frac{1}{2}\sum_{i,j=1}^{n} a_{ij}(s,x,v)\frac{\partial^2 f(s,x)}{\partial x_i \partial x_j}, \tag{4.1.5}$$

where $a_{ij} = \frac{1}{2}(\sigma\sigma^T)_{ij}$ and $x = (x_1, \ldots, x_n)$. Therefore the first fundamental result on stochastic control theory is the following (adapted from Øksendal (1998)):

Theorem 3 (The Hamilton-Jacobi-Bellman (HJB) equation)**.** *Define*

$$\Phi(s,x) = \sup\{J^v(s,x);\ v = v(s,X_s)\ \textit{Markov control}\}. \tag{4.1.6}$$

Suppose that $\Phi \in C^2(G) \cap C(\overline{G})$ is bounded. The probability law of X_t, $s \le t \le T$, with $X(s) = x \in D_s$ is denoted by $Q^{s,x}$. Suppose that an optimal Markov control v^* exists, and that ∂G is regular for $t, X_t(v^*)$ (regularity means that $Q^{(s,x)}(\hat{T} = 0) = 1$ for all $(s,x) \in \partial G$, or $x \in \partial D_s$). Then

$$\sup_{v \in V}\{F(s,x,v) + (L^v\Phi)(s,x)\} = 0 \quad \textit{for all} \quad (s,x) \in G \tag{4.1.7}$$

and

$$\Phi(s,x) = K(s,x) \quad \textit{for all} \quad (s,x) \in \partial G. \tag{4.1.8}$$

The supremum in (4.1.7) is obtained if $v = v^*(s,x)$ where $v^*(s,x)$ is optimal, i.e.

$$F(s,x,v^*(s,x)) + (L^{v^*}(s,x)\Phi)(s,x) = 0 \quad \textit{for all} \quad (s,x) \in G. \tag{4.1.9}$$

A rigorous proof of this theorem is given in Øksendal (1998), as well as a converse theorem and an application to an arbitrary $\mathcal{F}_t^{(q)}$-adapted control. Eq. (4.1.9) is also called equation of Dynamic Programming method introduced by Bellman (1957), Bellman and Dreyfus (1962).

The HJB theorem can also be applied for the corresponding minimization problem

$$\Psi(s,x) = \inf_{v \in V} J^v(s,x) = J^{v^*}(s,x). \tag{4.1.10}$$

Correspondingly, the performance function becomes

$$\Psi(s,x) = -\sup_v\{-J^v(s,x)\} = -\sup_v \left\{ E^{s,x}\left[-\int_s^T F^v(\tau, X_\tau)d\tau - K(T,X_T)\right]\right\} \tag{4.1.11}$$

so $-\Psi$ coincides with the solution Φ of the problem (4.1.4), but with F replaced by $-F$ and K replaced by $-K$. Following these changes the HJB equation is applicable to Ψ, but with reverse signs.

4.2 Optimal control

To reduce the computational error after implementation of the Monte Carlo method (3.3.1), as it was mentioned above, the Girsanov transformation allows us to improve our original equation (Eq. 2.3.1)

$$dX = m(t,X)dt + \sigma(t,X)dW(t) \tag{4.2.1}$$

by the external drift function $v(t,X)$ from Theorem (2)

$$d\widetilde{X} = m(t,\widetilde{X})dt + \sigma(t,\widetilde{X})v(t,\widetilde{X})dt + \sigma(t,\widetilde{X})d\widetilde{W}(t). \tag{4.2.2}$$

Let the Radon-Nikodym derivative (Eq. 3.3.18) denote $dP/d\widetilde{P} = \zeta_s^T$, where ζ_s^t is a scalar Markov process

$$d\zeta_s^t = -\zeta_s^t v(t,\widetilde{X}_t)d\widetilde{W}(t), \tag{4.2.3}$$

$$\zeta_T^T = 1. \tag{4.2.4}$$

Note that both processes are given with respect to the importance sampling measure $\widetilde{P}$. The extended system considered now is a set of Eqs. (4.2.2) and (4.2.3). By the Theorem 2 for any v:

$$E[f(X_{s,x}(T))]|_{4.2.1} = E\left[f(\widetilde{X}_{s,x}(T))\zeta_s^T\right]|_{4.2.2}. \tag{4.2.5}$$

Denote $Z = f(\widetilde{X}_{s,x}^T)\zeta_s^T$, it is clear that $E[Z]$ does not depend on the choice of the control v, while its variance $Var(Z) = E[Z^2] - (E[Z])^2$ does depend on v.

Let $\Psi = E[f(X^T_{s,x})]$, where $X^T_{s,x}$ is a solution of the original equation (Eq. 4.2.1). Then by Theorem 6.1 (p.129) in Fleming and Rishel (1975) the following boundary problem is true

$$(L^0\Psi)(s,x) = \frac{\partial\Psi}{\partial s} + \sum_{i=1}^{n} m_i \frac{\partial\Psi}{\partial x_i} + \frac{1}{2}\sum_{i=1}^{n}\sum_{j,k=1}^{n} \sigma_{ij}\sigma_{ik}\frac{\partial^2\Psi}{\partial x_j \partial x_k} = 0, \tag{4.2.6}$$

$$\Psi(T,x) = f(x). \tag{4.2.7}$$

Therefore, the natural condition for choosing control v is the minimization of the quantity $Var(Z)$. Besides, since $E[Z]$ is independent on v, the performance function (Eq. 4.1.3) takes the form

$$J^v(s,x) = E[(f(\widetilde{X}^T_{s,x})\zeta^T_s)^2], \tag{4.2.8}$$

where the utility rate function $F^v(t,\widetilde{X}(t)) = 0$ and the bequest function $K(T,\widetilde{X}_T)) = (f(\widetilde{X}^T_{s,x})\zeta^T_s)^2$ in terms of stochastic control theory. The optimal performance is defined

$$\Phi(s,x) = \inf_{v\in V} J^v(s,x) = J^{v^*}(s,x). \tag{4.2.9}$$

Applying Theorem 3, assume that v^* is the optimal control then Equation (4.1.9) takes the form

$$(L^{v^*}\Phi)(s,x) = 0 \tag{4.2.10}$$

with the boundary condition (Eq. 4.1.8)

$$\Phi(T,x) = (f(X^T_{T,x})\zeta^T_T)^2 = f^2(x), \tag{4.2.11}$$

where $L^{v^*}(s,x)$ is an operator given by (Eq. 4.1.5)

$$(L^{v^*}\Phi)(s,x) = \frac{\partial\Phi}{\partial s} + \sum_{i=1}^{n} m_i\frac{\partial\Phi}{\partial x_i} + \sum_{i=1}^{q} v_i\left(\sigma_i, \frac{\partial\Phi}{\partial x}\right) + \tag{4.2.12}$$
$$\frac{1}{2}\sum_{i=1}^{q}\sum_{j,k=1}^{n}\sigma_{ij}\sigma_{ik}\frac{\partial^2\Phi}{\partial x_j\partial x_k} - 2\sum_{i=1}^{q} v_i\left(\sigma_i,\frac{\partial\Phi}{\partial x}\right) + \Phi\sum_{i=1}^{q} v_i^2.$$

Here and further, the notation $\left(\sigma_i, \frac{\partial\Phi}{\partial x}\right)$ means a scalar product of these two vectors $\sigma_i = (\sigma_{i1}, \sigma_{i2}\ldots, \sigma_{in})$ and $\frac{\partial\Phi}{\partial x}$.

After minimization ($v \neq 0$) the control function equals

$$v_i = \frac{1}{2\Phi}\left(\sigma_i, \frac{\partial\Phi}{\partial x}\right). \tag{4.2.13}$$

Therefore, the performance function $\Phi(s,t)$ satisfies the following boundary problem (using the theorem from Fleming and Rishel (1975))

$$(L^0\Phi)(s,x) - \frac{1}{4\Phi(s,x)}\sum_{i=1}^{q}\left(\sigma_i,\frac{\partial\Phi}{\partial x}\right)^2 = 0 \tag{4.2.14}$$

$$\Phi(T,x) = f(x)^2, \tag{4.2.15}$$

taking into account that $\zeta_T^T = 1$.

The goal now is to link this representation of the optimal control function to the original failure probability. Let $\Phi = (\Psi)^2$, indeed $\Phi \geq 0$. Then $\Psi(s,x)$ is also the solution to Eq. (4.2.14)

$$2\Psi\left(\frac{\partial\Psi}{\partial s} + \sum_{i=1}^{n} m_i \frac{\partial\Psi}{\partial x_i} + \frac{1}{2}\sum_{i=1}^{q}\sum_{j,k=1}^{n} \sigma_{ij}\sigma_{ik}\frac{\partial^2\Psi}{\partial x_j \partial x_k}\right) + \tag{4.2.16}$$

$$\sum_{i=1}^{q}\sum_{j,k=1}^{n} \sigma_{ij}\sigma_{ik}\frac{\partial\Psi}{\partial x_j}\frac{\partial\Psi}{\partial x_k} - \frac{1}{4\Psi^2}\cdot 4\Psi^2 \sum_{i=1}^{q}\left(\sigma_i, \frac{\partial\Psi}{\partial x}\right)^2 = 0 \tag{4.2.17}$$

$$\Psi(T,x) = f(x). \tag{4.2.18}$$

Moreover, the optimal control will take the form

$$v_i = \frac{1}{\Psi}\left(\sigma_i, \frac{\partial\Psi}{\partial x}\right). \tag{4.2.19}$$

In Milstein (1995) it is proved that if $v = v^*$ is the optimal control, then $f(X)$ becomes a deterministic quantity.

There are some requirements about the function $f(x)$ but they can easily be overcome as it is shown in Milstein (1995), Macke (1999), Macke and Bucher (2003). In the case, when $f(x) = I[x]$ is the indicator function, and the aim is to assess the failure probability when those requirements are fulfilled.

4.3 Suboptimal control

The expression for the optimal control $v(x,s)$ (Eq. 4.2.19) includes the value of the failure probability $p_f(T;x,s)$ which has to be known in advance and in addition as a function in state space and time. Nevertheless, the form of this solution for the problem can be exploited whether the approximation for $p_f(T;x,s)$ is available. Then the suboptimal control $\widehat{v}(x,s)$ can be constructed and it will still lead to substantial variance reduction.

Let $\widehat{v}(s,x)$ be a suboptimal control. Again the quantity $E[f(X_{s,x}^T)] = E[f^v(\widetilde{X}_{s,x}^T)\zeta_s^T(\widehat{v})]$, where $\widetilde{X}_{s,x}^T$ is solution of Eq. (4.2.2), will be unaffected by the choice of control function. On the contrary, the variance of this estimate depends on the choice of control. It was proved above in the case of the optimal control that the variance of the estimate equals zero. In the case of suboptimal control, the variance is non-zero although it will still remain small.

The reliability problem is now considered in the time interval $(s,T]$ with deterministic initial condition $X(s) = x$, and $p_f(T;s,x)$ denotes the associated failure probability. The Monte Carlo estimate of the failure probability based on measure $\widetilde{P}$ is given in Naess (1999)

$$\widehat{p}_f(T;s,x) \;=\; \frac{1}{N}\sum_{i=1}^{N} I[g(\widetilde{x}^i)]\left(\frac{dP}{d\widetilde{P}}\right)^i. \tag{4.3.1}$$

Analysing Eqs. (3.3.1) and (3.3.17), it is obvious that the failure probability is independent of the choice of controller, whereas the variance does depend on v. Invoking the theory of stochastic control again it can be shown that there is an optimal control function (Milstein, 1995) for minimizing the functional

$$J = \widetilde{E}\left[I^2[g(\widetilde{X})]\left(\frac{dP}{d\widetilde{P}}\right)^2\right] \to \min, \tag{4.3.2}$$

viz.,

$$v^*(s,x) = \frac{1}{p_f(T;s,x)}\left(\sigma(s,x)\cdot\frac{\partial p_f(T;s,x)}{\partial x}\right). \tag{4.3.3}$$

It can be proved (Milstein, 1995) that if $v^*(s,x)$ is the optimal control function, then the variance of the failure probability estimator is zero, thus the estimator is a deterministic quantity. However, from (4.3.3) it follows that the optimal control function depends on the failure probability $p_f(T;s,x)$, which has to be known for all values of the arguments $(s,x) \in (0,T]\times\mathbb{R}^n$. But, of course, if the answer is known there is no need to control the system. On the other hand, if the failure probability can be calculated approximately on a suitable finite grid in $(0,T]\times\mathbb{R}^n$, i.e. $\widehat{p}_f(T;s,x)$, then it is possible to construct a suboptimal control function $v(s,x)$ such as:

$$v(s,x) = \frac{1}{\widehat{p}_f(T;s,x)}\left(\sigma(s,x)\cdot\frac{\partial \widehat{p}_f(T;s,x)}{\partial x}\right) \tag{4.3.4}$$

which obviously gives non-zero variance of the estimator, but still it reduces it substantially while $\widehat{p}_f(T;s,x) \approx p_f(T;s,x)$. Thus, the goal is to provide such approximation.

Chapter 5

Importance sampling

In this chapter the proposed two-step importance sampling procedure for time-variant reliability problem is presented.

5.1 Methodology

Although the optimal control as shown in Milstein (1995) is not achievable, different types of a suboptimal control have been developed (Au and Beck, 2001; Macke and Bucher, 2003). The deterministic control based on the design point oscillations was mainly used. The aim of this chapter is to illustrate that both types of control functions (open loop control and Markov control) can be used together in an iterative procedure to obtain an accurate failure probability estimate. As was mentioned in the introduction, the scope of the project is single degree of freedom oscillators given as

$$\ddot{X} + f(\dot{X}, X) = F(t), \tag{5.1.1}$$

where the external excitation $F(t)$ is white or coloured noise. Let $Y_1(t) = X(t)$ and $Y_2(t) = \dot{X}(t)$ then Eq. (5.1.1) may be expressed in the state space form

$$\dot{Y}(t) = A(Y(t), t) + gF(t) \tag{5.1.2}$$

where

$$Y(t) = \begin{bmatrix} Y_1(t) \\ Y_2(t) \end{bmatrix}, \quad g = \begin{bmatrix} 0 \\ 1 \end{bmatrix}. \tag{5.1.3}$$

The variance reduction procedure consists of two iterations. First, a rough estimate of the failure probability as a function of the state space and time variables, $\widehat{p}_f(T; y_1, y_2, t)$, is obtained by using the design point oscillations for an auxiliary linear system.

Secondly, using the analytical expression for the optimal control function (Eq. 4.2.19) the suboptimal controller is obtained

$$v(x, \dot{x}, s) = \frac{\sigma}{\widehat{p}_f(T; x, \dot{x}, t)} \frac{\partial \widehat{p}_f(T; x, \dot{x}, t)}{\partial \dot{x}} \tag{5.1.4}$$

where σ is the intensity parameter of an equivalent white noise

$$F(t) \approx \sigma N(t), \tag{5.1.5}$$

where process $N(t)$ is white noise (Section 2.2.4).

Thus, using the importance sampling procedure once more, the reliability of the dynamic system, or its complement, the failure probability, is calculated.

As was mentioned, the auxiliary linear equation is used for the evaluation of the failure probability approximation in the non-linear case for the first iteration. The reason is that the analytic expression for the design point oscillations is available in this case. However, the linearization should be handled with care because the mean square stochastic linearization can give the wrong results for the first-passage probabilities for a quite large class of non-linear problems (Naess, 1995). The concept of linearization which will suit the estimation of the failure probability is thought to be the equivalence of the mean upcrossing rates of non-linear oscillator and its linearized version. Furthermore, other heuristic approaches are proposed for the construction of the appropriate auxiliary linear single degree of freedom system.

5.2 Linear oscillator

A wide class of engineering systems can be modelled, to a first approximation, in terms of linear differential equations of motion, if the amplitude of motion is relatively small. Thus, the first considered numerical example is linear oscillations of a light damped spring-mass model. Motion of the linear oscillator (Fig. 5.1) excited by the external force $F(t)$ follows the second-order differential equation:

$$\begin{aligned} &\ddot{X} + 2\xi\omega_0\dot{X} + \omega_0^2 X = F(t), \\ &X(s) = x, \qquad \dot{X}(s) = \dot{x}, \end{aligned} \tag{5.2.1}$$

where ξ is the viscous damping ratio and ω_0 is the system natural frequency.

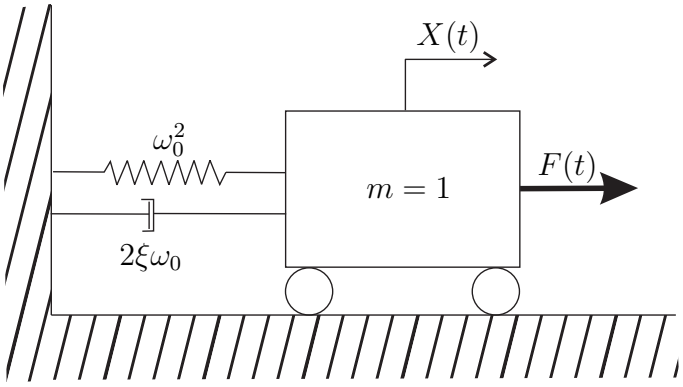

Figure 5.1: Model of a damped linear oscillator.

Equation (5.2.1) can be written in a standard form, i.e., as a system of first-order differential equations. Let $Y_1(t) = X(t)$ and $Y_2(t) = \dot{X}(t)$ then

$$\dot{Y}(t) = A \cdot Y(t) + gF(t) \tag{5.2.2}$$

where

$$Y(t) = \begin{bmatrix} Y_1(t) \\ Y_2(t) \end{bmatrix}, \quad A = \begin{bmatrix} 0 & 1 \\ -\omega_0^2 & -2\xi\omega_0 \end{bmatrix}, \quad g = \begin{bmatrix} 0 \\ 1 \end{bmatrix}. \tag{5.2.3}$$

Equation (5.2.2) has a general explicit analytical solution known from the deterministic dynamic analysis (Soong and Grigoriu, 1997)

$$Y(t) = \Phi(t-s)y + \int_s^t \Phi(t-\tau)gF(\tau)d\tau, \tag{5.2.4}$$

where the fundamental matrix is given as

$$\Phi(\tau) = \exp^{-\xi\omega_0\tau} \begin{bmatrix} \cos\omega_d\tau + \frac{\xi\omega_0}{\omega_d}\sin\omega_d\tau & \frac{\omega_0}{\omega_d}\sin\omega_d\tau \\ -\frac{\omega_0}{\omega_d}\sin\omega_d\tau & \cos\omega_d\tau - \frac{\xi\omega_0}{\omega_d}\sin\omega_d\tau \end{bmatrix} \tag{5.2.5}$$

where $\omega_d = \omega_0\sqrt{1-\xi^2}$.

Homogenous solutions for displacement $X(t)$ and velocity $\dot{X}(t)$ are given correspondingly

$$X_h(t) = \frac{\mathrm{e}^{-\xi\omega_0 t}}{\omega_d}((\xi\omega_0 x + \dot{x})\sin\omega_d t + \omega_d x\cos\omega_d t), \tag{5.2.6}$$

$$\dot{X}_h(t) = \frac{\mathrm{e}^{-\xi\omega_0 t}}{\omega_d}(-(\omega_0^2 x + \xi\omega_0\dot{x})\sin\omega_d t + \omega_d\dot{x}\cos\omega_d t). \tag{5.2.7}$$

Thus, the general solution for the displacement $X(t)$ is

$$X(t) = X_h(t-s) + \int_s^t h(t-\tau)F(\tau)d\tau, \tag{5.2.8}$$

where $h(t)$ is impulse response function given

$$h(t) = \frac{e^{-\xi\omega_0 t}}{\omega_d}\sin\omega_d t. \tag{5.2.9}$$

Assume that external excitations may be represented as a standard Gaussian white noise $N(t)$ with zero mean and unit standard deviation multiplied by a suitable constant. Then

$$\ddot{X} + 2\xi\omega_0\dot{X} + \omega_0^2 X = \sqrt{\gamma}N(t). \tag{5.2.10}$$

The following probabilistic properties of a linear oscillator can be obtained (Crandall, 1970):

- Mean value for steady state $E[X(t)] = 0$, $E[\dot{X}(t)] = 0$.

- The approximate transition variance of the response $X(t)$

$$\sigma_X^2(t) \cong \frac{\pi G_0}{4\xi\omega_0^3}\left(1 - \frac{1}{\omega_d^2}e^{-2\xi\omega_0 t}(\omega_d^2 + 2\xi^2\omega_0^2\sin^2\omega_d t + \xi\omega_0\omega_d \sin 2\omega_d t)\right). \tag{5.2.11}$$

- Standard deviations for the stationary solution, when $t \to \infty$, for $X(t)$ and $\dot{X}(t)$ is correspondingly

$$\sigma_0^2 = \frac{\pi G_0}{4\xi\omega_0^3}, \quad \dot{\sigma}_0^2 = \frac{\pi G_0}{4\xi\omega_0}, \tag{5.2.12}$$

  where G_0 is one-sided spectral density, $\pi G_0 = \gamma$ is the intensity of the external force.

- The autocorrelation function of the response $X(t)$ (Naess, 1990) is given as

$$R_X(\tau) = \sigma_0^2 e^{-\xi\omega_0|\tau|}\left(\cos\omega_d\tau + \frac{\xi\omega_0}{\omega_d}\sin\omega_d|\tau|\right). \tag{5.2.13}$$

- The power spectral density (Eq. 2.2.16) is defined (Lutes and Sarkani, 1997)

$$S_X(\omega) = \frac{G_0/2}{(\omega_0^2 - \omega^2)^2 + (2\xi\omega_0\omega)^2}. \tag{5.2.14}$$

Actually the linear oscillator can be seen as a filter. Depending on the value of damping ratio ξ, it can be a narrow-banded or broad-banded filter. Examples are illustrated in Fig. (5.2).

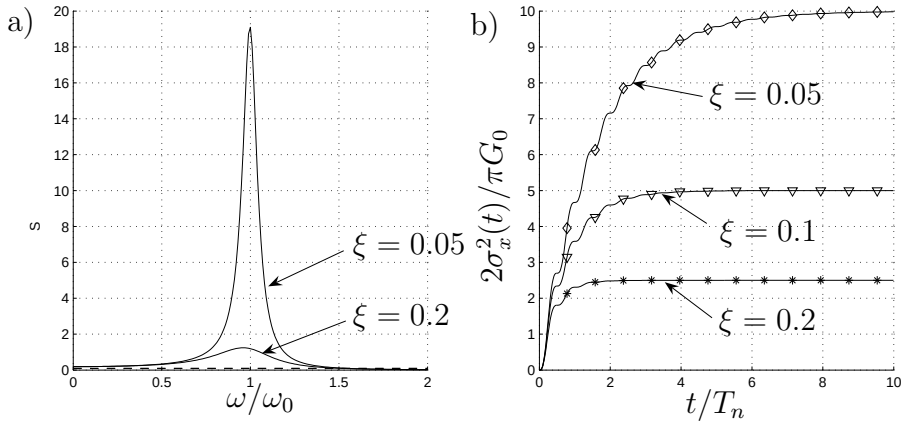

Figure 5.2: a) Power spectral density and b) variance of the displacement $X(t)$ for different values of damping ratio ξ.

Equation (5.2.10) can be written as an Itô SDE:

$$\begin{aligned} dY_1(t) &= Y_2(t)dt \\ dY_2(t) &= -2\xi\omega_0 Y_2(t)dt - \omega_0^2 Y_1(t)dt + \sqrt{\gamma}dW(t) \end{aligned} \tag{5.2.15}$$

where, as previously, $Y_1(t) = X(t)$ and $Y_2(t) = \dot{X}(t)$, $W(t)$ is a standard scalar Wiener process (Section 2.2.3). Since the analytical solution is known

$$X(t) = X_h(t-s) + \gamma \int_s^t h(t-\tau) dW(\tau)\,, \quad s \le t \le T, \tag{5.2.16}$$

where the second term on the rhs is a stochastic integral (Kloeden and Platen, 1999).

As it was discussed earlier in Chapter 3, one of the important reliability problems is the first-passage time. Thus assume that the considered safe domain is given by

$$D_S = \{(x, \dot{x}) : x < x_c, \dot{x} \in \mathbb{R}\}, \tag{5.2.17}$$

where x_c is a prescribed critical threshold for any $0 \le s \le t \le T$. Hence the limit state function is linear and can be written as follows

$$g(Y) = x_c - X(t). \tag{5.2.18}$$

Integrating numerically Eq. (5.2.16) by using the Euler scheme (Eq. 3.3.20), assuming an equidistant time step $\Delta t = (T-s)/m$, it is obtained that

$$X(t_j) = X_h(t_j - s) + \sqrt{\gamma} \sum_{i=1}^{j} h_{ji} U_i \sqrt{\Delta t}, \tag{5.2.19}$$

where $X_h(t)$ is the homogeneous solution given (5.2.8), $s < t_j \le T$, $t_j = s + j \cdot \triangle t$, $h_{ji} = h((j-i)\cdot\Delta t)$, $U_i\sqrt{\Delta t} = W(i\cdot\Delta t) - W((i-1)\cdot\Delta t)$ is the increments of the Wiener process. U_i are the independent standard Gaussian variables with zero mean and unit standard deviation. Then the limit state function (Eq. 5.2.18) takes the form

$$g(Y(t_j)) = x_c - X(t_j) = x_c - X_h(t_j - s) - \sqrt{\gamma} \sum_{i=1}^{j} h_{ji} U_i \sqrt{\Delta t} = g_j(U_1, \ldots, U_j). \tag{5.2.20}$$

The limit state surface $g_j(u_1, \ldots, u_j) = 0$, gives the expression for the design point index (Eq. 3.2.12) at a time point t_j

$$\beta(t_j) = \sqrt{\sum_{i=1}^{j} u_i^2}, \tag{5.2.21}$$

where

$$u_i = \frac{x_c - X_h(t_j - s)}{\sqrt{\gamma} \sum\limits_{i=1}^{j} h_{ji}^2 \sqrt{\Delta t}} \cdot h_{ji}. \tag{5.2.22}$$

In order to achieve the variance reduction the Girsanov transformation (Theorem 2) is used. Thus, Equation (5.2.15) takes the form

$$\begin{aligned} d\widetilde{Y}_1(t) &= \widetilde{Y}_2(t)dt \\ d\widetilde{Y}_2(t) &= -2\xi\omega_0\widetilde{Y}_2(t)dt - \omega_0^2\widetilde{Y}_1(t)dt + \sqrt{\gamma}v(t,\widetilde{Y})dt + \sqrt{\gamma}d\widetilde{W}(t) \end{aligned} \tag{5.2.23}$$

where $\widetilde{W}(t)$ is a new Wiener process generated with respect to an importance sampling measure $\widetilde{P}$.

The control function is assumed to be deterministic, i.e. $v(t,\widetilde{Y}) = v(t)$ is an open-loop control in order to obtain a first approximation of the failure probability functional. Then the following control function (Eq. 3.3.25) is used

$$v_i = \frac{x_c - X_h(t_j - s)}{\sqrt{\gamma}\sum\limits_{i=1}^{j} h_{ji}^2 \Delta t} \cdot h_{ji}, \tag{5.2.24}$$

where if $\Delta t \to 0$ then Eq. (5.2.24) can be written in the integral form (Skaug, 2000)

$$v(t) = \frac{x_c - X_h(t_j - s)}{\sqrt{\gamma}\int\limits_{s}^{t_j} h^2(t_j - \tau)d\tau} \cdot h(t_j - t)\,, \quad s \le t \le t_j. \tag{5.2.25}$$

Using this control function (Eq. 5.2.25), the failure is assumed to happen at a single time point t_j. It was mentioned in Section 3.3.2 that this is not suited to the oscillatory systems, but the simplicity of this expression and the possibility to define the control function analytically makes it tempting to use it.

It is proposed to apply design point oscillations which cause failure at the end of the considered time interval T in order to obtain the first approximation of the failure probability. That is natural because most of the samples will approach the critical threshold at the end of response duration, especially samples started at zero initial conditions. The design point index in this case has a minimum at the end point T, that is

$$\beta^* = \beta(T) = \min_{s \le t \le T} \beta(t). \tag{5.2.26}$$

However, considering non-zero initial conditions the system may obviously tend to fail at the beginning of the time interval because of the system's initial energy. To compensate for this effect it was proposed to use design point oscillations which lead to a failure event at the time of the first maximum of the homogeneous solution $X_h(t-s)$. In Fig. (5.3), the design point index is illustrated for the system with zero and non-zero initial values. The curve corresponding to the non-zero initial values and marked with asterisks $(*)$ also has the global minimum at the end point T. Nevertheless, the first local minimum near the origin has a magnitude comparable with the global minimum value. Hence, the failure near this point will give a significant contribution to the failure probability. Taking into account these features two design times $t_{(1)} = T$ and $t_{(2)} = t^{max}$ are used and weighted according to their importance (Eq. 3.3.26).

In the following two sections the proposed procedure, results and discussion are presented.

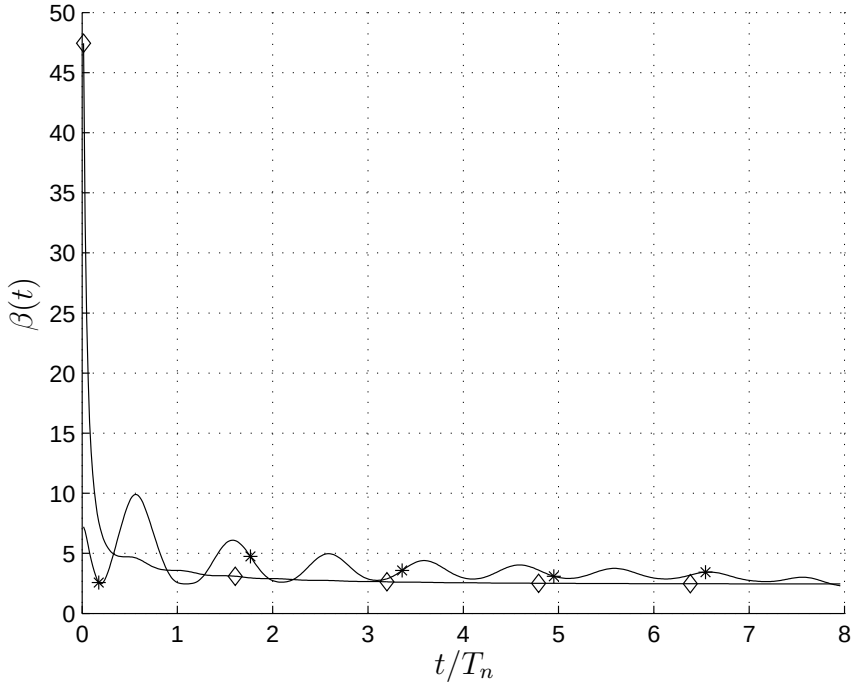

Figure 5.3: The design point index vs time; ($\diamond$) - zero initial values, ($*$) - non-zero initial values.

Procedure

On the first iteration the simulations using the open loop control (Eq. 5.2.25) are performed on a grid of initial values $(x, \dot{x})$ and for different values of a starting time point s. The number of samples used in the first iteration is $n_x \times n_{\dot{x}} \times n_t \times N_1$, where n_x, $n_{\dot{x}}$ are number of grid points in the state-space, n_t is number of the starting points, N_1 is number of samples for each fixed $(x, \dot{x}, s)$.

The low accuracy in the approximate calculation of the failure probability allows us to use a crude grid in the physical space and time. The smoothing of the failure probability data are required afterwards in order to obtain values for the second iteration. The data are represented as a family of 2D surfaces in $\mathbb{R}^2 = [X \times \dot{X}]$. In Fig. (5.4) one of these surfaces is plotted corresponded to a starting time $s = 0$. The consequent surfaces are deeper at the origin and shallow at the borders.

A control which leads to a failure at the end of the observation time $t_{(1)} = T = 10 \cdot T_n$, where $T_n = 2\pi$ [sec], was investigated by Næss and Skaug (2000) and results showed substantial underestimation compared with the direct Monte Carlo method (Fig. 5.5). Moreover, for particular values of the initial values $(x, \dot{x})$ the oscillator fails almost surely at the beginning of the time interval due to the large amount of initial energy in the system. Therefore, forcing the system to leave the safe domain at the end gives unrealistically low values of the Radon-Nikodym derivative (Eq. 3.3.18). To recap, such estimates show the degree of

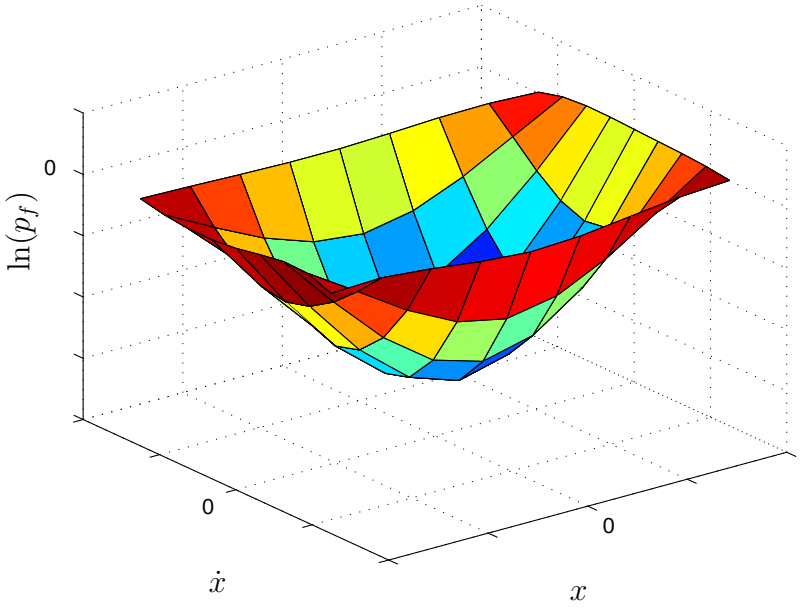

Figure 5.4: Results of the first iteration - approximated failure probability in $\mathbb{R}^2 = [X \times \dot{X}]$ smoothed by B-spline.

impossibility of the changes that the control is required to make. Illustrations of samples of the uncontrolled process and the controlled process with zero and nonzero initial values are shown in Fig. (5.6). The design point oscillations at the second time point are initiated to compensate for these low values. Namely, at the point of the maximum of the homogeneous solution $X_h(t)$ which can be obtained analytically. Both contributions are weighted by their importance factors (Eq. 3.3.26).

On the second iteration the obtained data are numerically differentiated in the $\dot{X}$-direction. Then on the second iteration the importance sampling procedure is implemented using the Markov control $v(t, X(t), \dot{X}(t))$.

Discussion and results

The following cases were considered during the study of the method: case 1 is a narrow-band oscillatory system, where the damping ratio is $\xi = 0.05$, and case 2 is a broad-band one with $\xi = 0.2$ (Olsen and Naess, 2005b, 2006). The first model might correspond to the oscillations of an aircraft structure and the second one might represent the vibration of some rubber elements in a machine. For both cases the free oscillation frequency $\omega_0 = 1\,[1/\text{sec}]$ and the intensity of external excitations $\gamma = 0.3$ are the same.

For the narrow-band case the transient period is about $8 \cdot T_n$, whereas for the broad-band case the transient period is about $1.5 \cdot T_n$, where $T_n = 2\pi\,[\text{sec}]$. The sample paths for both cases are shown in Figs. (5.7-5.8) correspondingly. The ordinate on all figures is normalized by σ_0 (Eq. 5.2.12). The a)-plots on both figures present the samples of the displacement $X(t)$

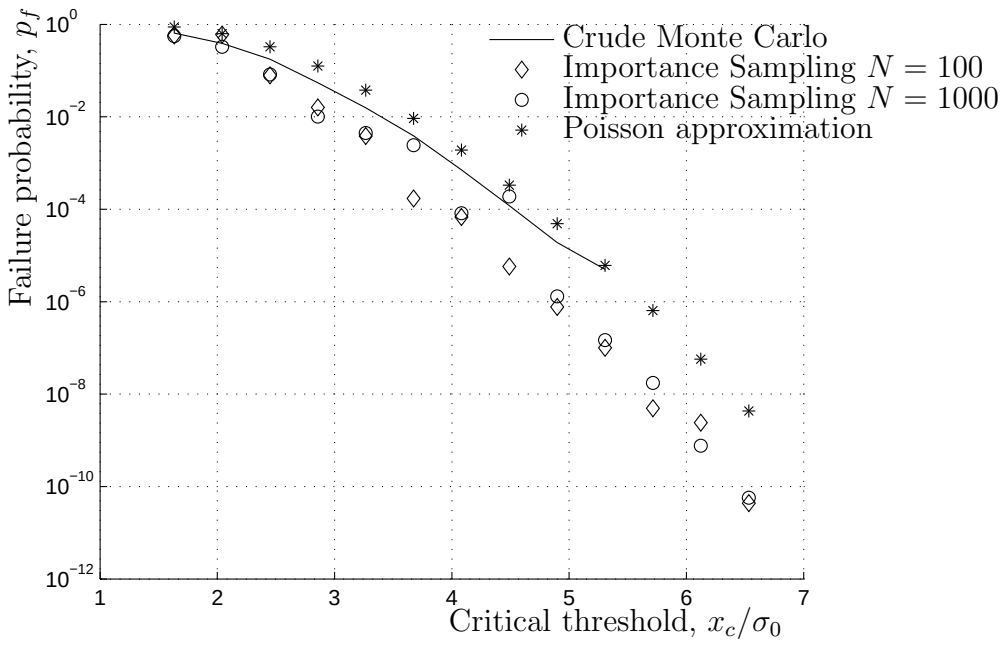

Figure 5.5: Failure probability for different threshold levels by crude Monte Carlo (number of samples, N, depends on standard error (Eq. 2.1.22) which is set to 0.05, except high thresholds ($x_c > 4 \cdot \sigma_0$) where $N = 10^6$) and importance sampling procedure using the open loop control (Eq. 5.2.24).

and the velocity $\dot{X}(t)$ of the original system (Eq. 5.2.10). Due to the choice of parameter $\omega_0 = 1\,[1/\text{sec}]$ the displacement and velocity have the same order of magnitude. These processes oscillate most likely inside the stripe $[-2\sigma_0, 2\sigma_0]$.

The b)-plots show the paths of the system (Eq. 5.2.23) controlled by the open-loop control $v(t)$ (Eq. 5.2.25). Here the design time was chosen $t_{(1)} = T$. Thus the design point oscillations force the failure event near the end of the considered time interval. The control is unaware of the system state and follows the only condition that $X(T) \geq x_c$.

The samples of the linear system controlled by the Markov control $v(X, \dot{X}, t)$ (Eq. 4.3.4) are in the c)-plots. In this case the controller is following the sample path pursuing the aim that $X(t) \geq x_c$ for $t \in (0, T]$. Thus the first passage is likely to occur anywhere on this interval. The smoothness of $v(X, \dot{X}, t)$ is a matter of accuracy of the first approximation.

In Figs. (5.9-5.10) the results of numerical experiments vs critical threshold are shown for both cases correspondingly. The critical threshold is also normalized by σ_0 (Eq. 5.2.12).

The test results were compared with estimates calculated by the crude Monte Carlo method. These are obtained with different number of samples ($> 10^3$) by the convergence criterion that the standard error SE (Eq. 2.1.22) equals 0.05, otherwise, if SE has not converged to 0.05, the number of samples is $N = 10^6$. Whereas N used by the importance sampling procedure in the two steps is $n_x \times n_{\dot{x}} \times n_t \times n_1 + n_2$, where n_x is the number of grid points in x-direction, $n_{\dot{x}}$ is in $\dot{x}$-direction, n_t is in time, n_1 is number of samples simulated with the set of initial values $(x, \dot{x}, s)$ and n_2 is number of samples on the second iteration.

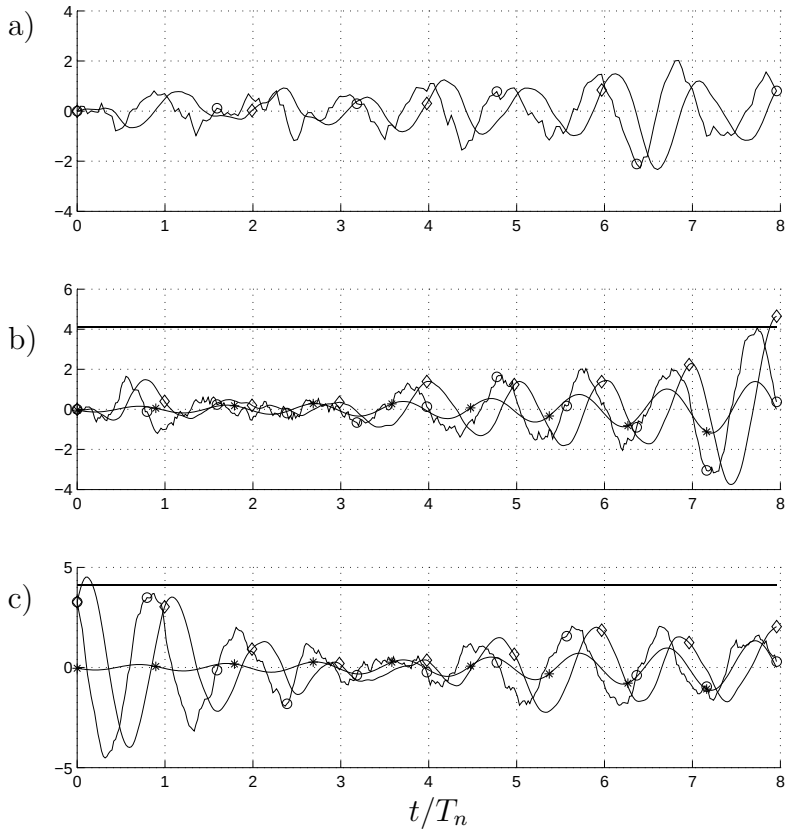

Figure 5.6: a) Displacement, ($\diamond$) $x(t)/\sigma_0$, and velocity, ($\circ$) $\dot{x}(t)/\dot{\sigma}_0$, of the original equation of motion,
b) displacement, ($\diamond$) $x(t)/\sigma_0$, velocity, ($\circ$) $\dot{x}(t)/\dot{\sigma}_0$ and deterministic control function, ($*$) $v(t)/\sigma_0$ (zero initial conditions, $x_c/\sigma_0 = 4.1$),
c) displacement, ($\diamond$) $x(t)/\sigma_0$, velocity, ($\circ$) $\dot{x}(t)/\dot{\sigma}_0$ and deterministic control function, ($*$) $v(t)/\sigma_0$ (nonzero initial conditions, $x_c/\sigma_0 = 4.1$).

The results from the first iteration are obtained with $n_1 = 100$ and two open-loop controls aimed at the failure events at $t_{(1)} = T$ and $t_{(2)} = T/2$. Due to the low number of samples the first approximation values have standard error of order $0.1 - 0.8$.

The standard error of the importance sampling estimates for whole procedure has converged to 0.05 with the number of samples used on the second iteration between $n_2 = 50 \ldots 2 \cdot 10^3$. This will not affect the total calculation time very much, because most of the computational burden is associated with the first step. For instance, for the value of the failure probability $p_f = 7.7 \cdot 10^{-3}$ estimated with the standard error $SE = 0.05$ the crude Monte Carlo method used $N = 51497$ samples and 31 sec calculation time, whereas the iterative importance sampling achieved this value with $N = 4531$ ($n_1 = 10$) on both iteration and 3 sec CPU time with the same confidence.

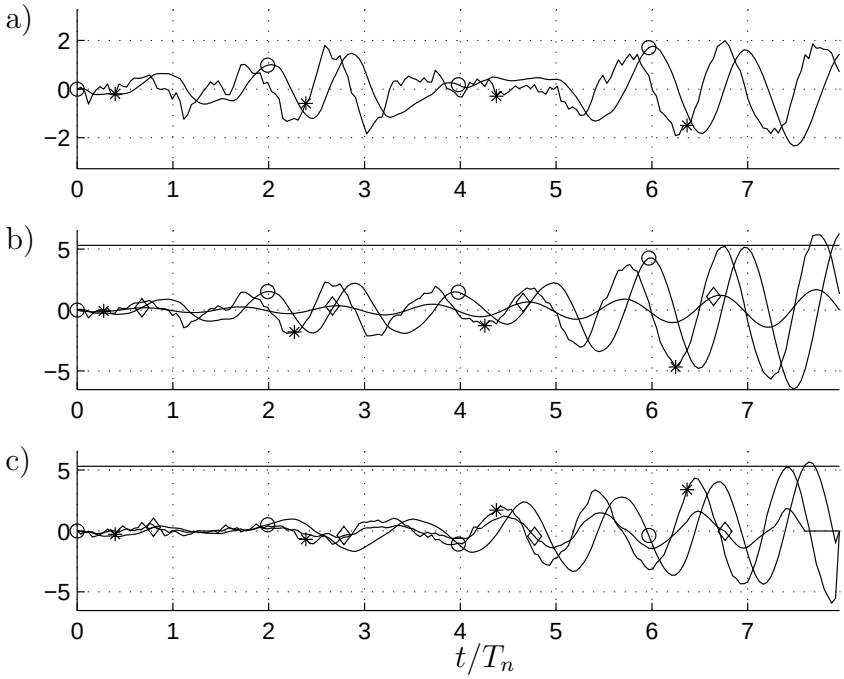

Figure 5.7: Case 1: a) ($\circ$) $x_1(t)$ and ($*$) $x_2(t)$ for the original equation (5.2.10), b) ($\circ$) $x_1(t)$ and ($*$) $x_2(t)$ for the controlled equation (5.2.23) with deterministic control ($\diamond$) $v(t)$ and c) with Markov control ($\diamond$) $v(t, x_1, x_2)$; critical threshold $x_c/\sigma_0 = 5.3$.

In Fig. (5.11), the failure probability vs damping ratio ξ is presented. The considered time interval is $T = 1.5 \cdot T_n$ which is less than the transition zone of the system with the parameter $\xi = 0.2$. This experiment shows that the procedure is applicable to the wide range of system parameters resulting from narrow-band to wide-band processes.

Figure (5.12) presents the results of the failure probability versus time. As in the previous figures, for the time $T > 0.5 \cdot T_n$ the iterative importance sampling has a better convergence to Monte Carlo results than importance sampling with the design point oscillations. Whereas for the short time intervals $T \leq 0.5 \cdot T_n$ both methods require approximately the same number of samples to achieve the chosen standard error value. This explains that for the time period of less than half a period, the system behaves as non-oscillatory and the principle of the one dominant failure point is valid.

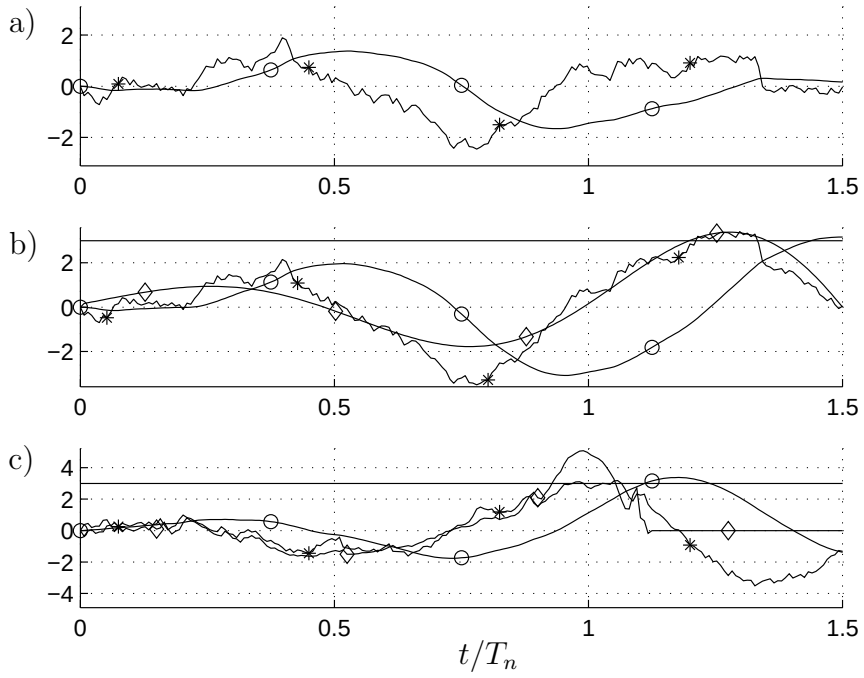

Figure 5.8: Case 2: a) ($\circ$) $x_1(t)$ and ($*$) $x_2(t)$ for the original equation (5.2.10), b) ($\circ$) $x_1(t)$ and ($*$) $x_2(t)$ for the controlled equation (5.2.23) with deterministic control ($\diamond$) $v(t)$ and c) with Markov control ($\diamond$) $v(t, x_1, x_2)$; critical threshold $x_c/\sigma_0 = 3$.

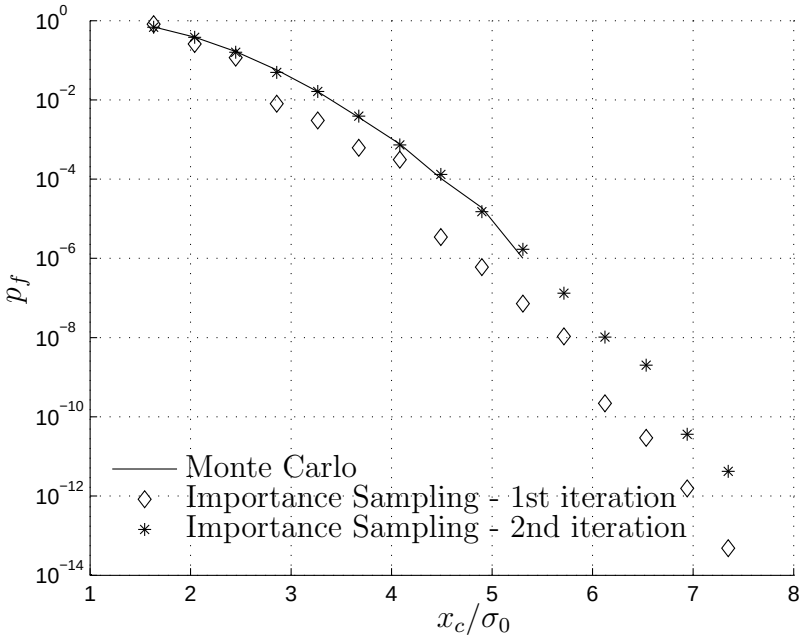

Figure 5.9: Case 1: failure probability vs critical threshold.

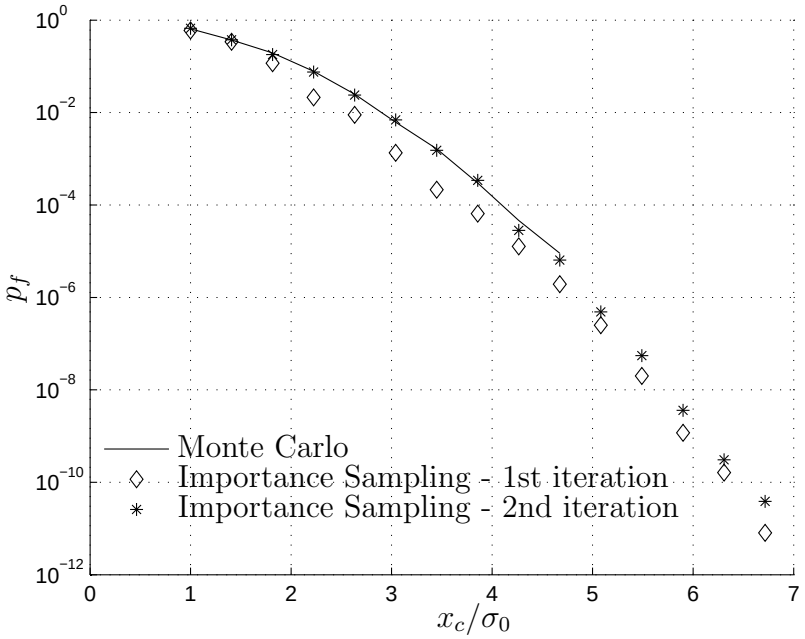

Figure 5.10: Case 2: failure probability vs critical threshold.

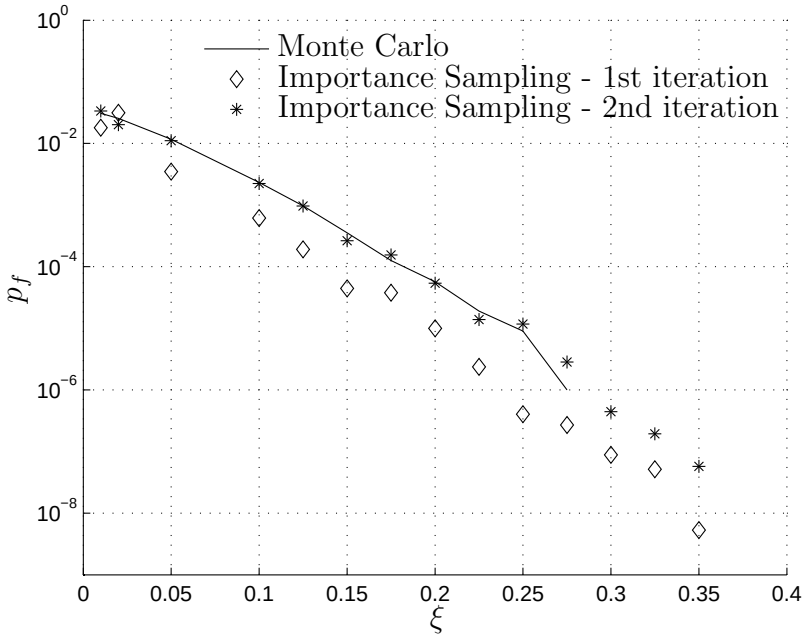

Figure 5.11: Failure probability vs damping ratio.

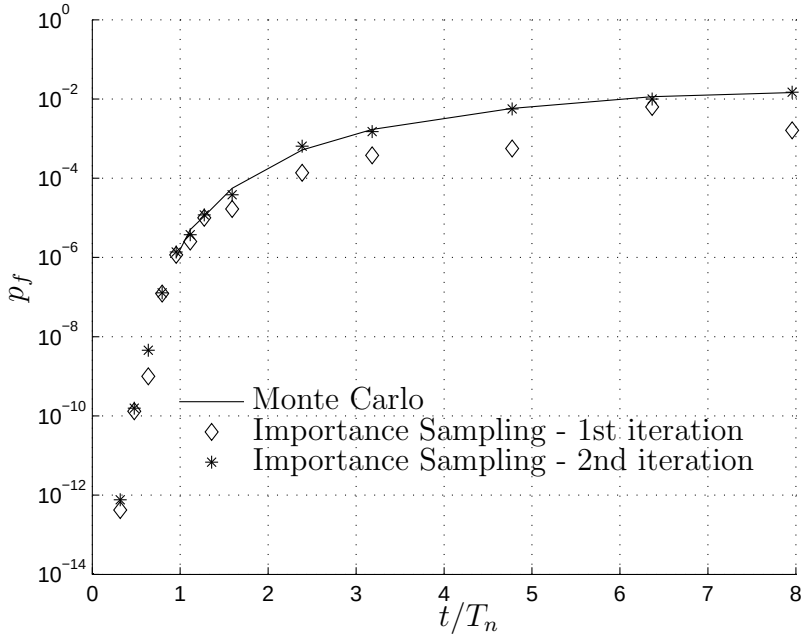

Figure 5.12: Case 1: failure probability vs time; critical threshold $x_c/\sigma_0 = 3.3$.

5.3 Duffing oscillator excited by white noise

This section is devoted to a non-linear Duffing oscillator excited by white noise (Ivanova and Naess, 2004). Consider the Duffing oscillator investigated previously by Crandall (1980):

$$\ddot{X}(t) + 2\xi\omega_0\dot{X}(t) + \omega_0^2(X(t) + \varepsilon X^3(t)) = \sqrt{\gamma}N(t), \tag{5.3.1}$$

where ξ is the damping ratio as in the case of linear oscillator, ω_0 is the frequency of free oscillations, ε is a parameter representing the degree of non-linearity and $N(t)$ is a Gaussian white noise with zero mean value and unit standard deviation. The same safe domain is considered as in Section 5.2, namely

$$D_S = \{(x, \dot{x}) : x < x_c, \dot{x} \in \mathbb{R}\}, \tag{5.3.2}$$

where x_c is a prescribed critical threshold for any $0 \leq s \leq t \leq T$.

For the further consideration the stationary joint probability density of the displacement $X(t)$ and velocity $\dot{X}(t)$ should be mentioned (Soong and Grigoriu, 1997; Lin and Cai, 1995)

$$f(x, \dot{x}) = \left\{\sqrt{2\pi}\dot{\sigma}_0 q \exp\left[-\frac{1}{2\sigma_0^2}\left(x^2 + \frac{\varepsilon}{2}x^4\right)\right]\right\}\left\{\frac{1}{\sqrt{2\pi}\dot{\sigma}_0}\exp\left(-\frac{\dot{x}^2}{2{\dot{\sigma}_0}^2}\right)\right\}, \tag{5.3.3}$$

where

$$\sigma_0^2 = \frac{\gamma}{4\xi\omega_0^3}, \quad \dot{\sigma}_0^2 = \frac{\gamma}{4\xi\omega_0} \tag{5.3.4}$$

represent stationary variances of $X(t)$ and $\dot{X}(t)$ for the linear oscillator ($\varepsilon = 0$). q is the normalization constant given by

$$q^{-1} = \sqrt{\frac{\pi\dot{\sigma}_0^2}{\varepsilon}}\left[\exp\left(\frac{1}{8\varepsilon\sigma_0^2}\right)K_{1/4}\left(\frac{1}{8\varepsilon\sigma_0^2}\right)\right], \tag{5.3.5}$$

where $K_{1/4}$ is a modified Bessel function (Lin and Cai, 1995). It is obvious that $X(t)$ and $\dot{X}(t)$ are independent with zero mean values.

The main idea is to estimate the failure probability functional (Eq. 3.3.17) on the first iteration using the simple control function (Eq. 3.3.25) for a linearized version of the non-linear Duffing oscillator (Eq. 5.3.1). Further, the different methods of linearization are compared to find the easiest and most efficient way. The objective of this exercise is to prove the efficiency of implementing a linear optimal control function to calculate the failure probability for a non-linear stochastic system.

Recently, Koo et al. (2005) showed that it is possible to obtain the design point excitation for this oscillator by one free-vibration analysis. Fortunately, this can simplify the importance sampling procedure even more.

Mean square stochastic linearization

The most widely used method of linearization which will be first considered here is the mean square stochastic linearization (MSL)(Hampl, 1985; Soong and Grigoriu, 1997). The basic idea is to minimize the difference between the mean square response characteristics of non-linear and linear oscillators. Let us consider a general non-linear dynamic system

$$g(\ddot{X}(t), \dot{X}(t), X(t)) = F(t). \tag{5.3.6}$$

Thus the equivalent linear system can be written as

$$m\ddot{Z}(t) + c\dot{Z}(t) + kZ(t) = F(t), \tag{5.3.7}$$

where the optimal values for m, c and k can be obtained by minimizing the mean square error e given

$$e = E[\epsilon^2], \tag{5.3.8}$$

where

$$\epsilon = g(\ddot{X}(t), \dot{X}(t), X(t)) - [m\ddot{Z}(t) + c\dot{Z}(t) + kZ(t)]. \tag{5.3.9}$$

So the equivalent linear oscillator which corresponds to the given Duffing oscillator is the following

$$\ddot{Z}(t) + 2\xi\omega_0\dot{Z}(t) + \omega_e^2 Z(t) = \sqrt{\gamma}N(t), \tag{5.3.10}$$

where (Soong and Grigoriu, 1997)

$$\omega_e^2 = \frac{1}{2}\omega_0^2\left(1 + \sqrt{1 + \frac{3\pi\varepsilon G_0}{\xi\omega_0^2}}\right), \tag{5.3.11}$$

where $G_0 = \gamma/\pi$ is one-sided spectral density of input excitations.

For the calculation the following parameters were used, $\omega_0 = 1.0\,1/\text{sec}$, $\xi = 0.05$, $\gamma = 0.3$. Considering different values for ε, the equivalent stiffness parameter values are given in Table 5.1.

Table 5.1: Parameters for the equivalent linear oscillator by MSL method.

ε	0.05	0.1	0.5	1
ω_e	1.091	1.156	1.443	1.637

Mean upcrossing rate linearization

The second linearization principle is proposed here because for estimating the failure probability the mean upcrossing characteristics are more crucial than the characteristics of the mean square response. It is logical to assume that if both the Duffing oscillator and equivalent linear system have the equal number of outcrossings in the same time interval then the estimate for the failure probability will be more accurate.

Incorporating the joint probability density function (Eq. 5.3.3) into the expression (3.3.8), the mean stationary upcrossing rate for the Duffing equation is given

$$\nu^+_{XD}(\zeta) = \frac{\dot{\sigma}_0^2}{q} \exp\left(-\frac{1}{2\sigma_0^2}\left(\zeta^2 + \frac{\varepsilon}{2}\zeta^4\right)\right), \tag{5.3.12}$$

where the stationary variances σ_0, $\dot{\sigma}_0$ and the normalizing coefficient q are given by Eqs. (5.3.4-5.3.5) correspondingly.

Let

$$\ddot{Z}(t) + 2\xi\omega_0 Z(t) + \omega_e^2 Z(t) = \sqrt{\gamma} N(t) \tag{5.3.13}$$

be an associated equivalent linear system.

The mean stationary upcrossing rate for the linear equation is given (Eq. 3.3.9)

$$\nu^+_{ZL}(\zeta) = \frac{\dot{\sigma}_Z}{2\pi\sigma_Z} \exp\left(-\frac{\zeta^2}{2\sigma_Z^2}\right), \tag{5.3.14}$$

where

$$\sigma_Z^2 = \frac{\gamma}{4\xi\omega_0\omega_e^2}, \quad \dot{\sigma}_Z^2 = \frac{\gamma}{4\xi\omega_0} \tag{5.3.15}$$

are standard deviations of $Z(t)$ and $\dot{Z}(t)$ respectively.

The frequency ω_e of the linearized oscillator can be found from the condition that the mean upcrossing rate ν^+_{XD} of the Duffing oscillator at steady state equals the mean upcrossing rate ν^+_{ZL} of the equivalent linear oscillator

$$\nu^+_{ZL}(\zeta) - \nu^+_{XD}(\zeta) = 0. \tag{5.3.16}$$

In the case when the mean upcrossing rate cannot be evaluated analytically, it is shown that numerical extrapolation can be implemented to assess the mean upcrossing rate for the high threshold levels. The Monte Carlo method is used for the estimation of upcrossing rates. In the case of a stationary solution, the upcrossing rate is defined

$$\hat{\nu}^+_{XD}(\zeta) = \frac{\mu_{N(T)}}{T}, \tag{5.3.17}$$

where $\mu_{N(T)}$ is the mean value of the number of outcrossings of the process from the safe domain. Further, the estimated values are approximated by the least squares method with a quadratic function and extrapolated to the desirable level taking into consideration the

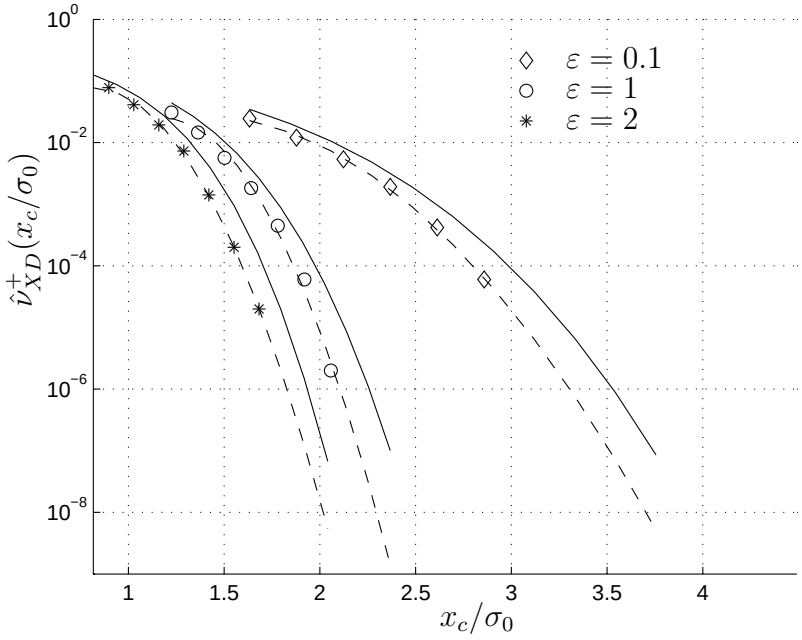

Figure 5.13: The upcrossing rate $\nu^+_{XD}(\zeta)$ vs critical threshold depending on different values of the non-linearity parameter ε is calculated in 3 different ways: method 1 (analytical) (-), method 2 (MCS) ($\diamond$,$\circ$,$*$), method 3 (approx.) (- -).

dynamic behaviour of the system. Therefore, the comparison between the analytical and numerical estimation of the mean upcrossing rate for the Duffing oscillator is given in Fig. (5.13). Method 1 (solid lines) corresponds to the calculation of the upcrossing rates by Eq. (5.3.12), method 2 (markers) is the Monte Carlo simulations (MCS), and method 3 (dashed lines) is the quadratic approximation and extrapolation.

In Fig. (5.14), the values of equivalent stiffness parameter ω_e are plotted vs the normalized values of the critical threshold. The black markers show the equivalent frequency values estimated by MSL, whereas the solid and the dashed lines with transparent markers correspond to the stiffness parameter calculated from Eq. (5.3.16) with analytically and numerically obtained Duffing oscillator upcrossing rates, respectively. The same type of markers corresponds to the same order of non-linearity. As it can be seen from Fig. 5.14 the MSL estimates give lower stiffness on the high thresholds. As a consequence the corresponding linear control function brings an insufficient contribution to the non-linear oscillatory system. Thus the failure event in this case remains something rare. The numerical estimation of the upcrossing rates gives a greater stiffness than that predicted by the analytical calculation. Moreover, features of the quadratic approximation give a curvature at the low critical levels. Though it does not very much affect the estimation of the failure probability due to the system characteristics.

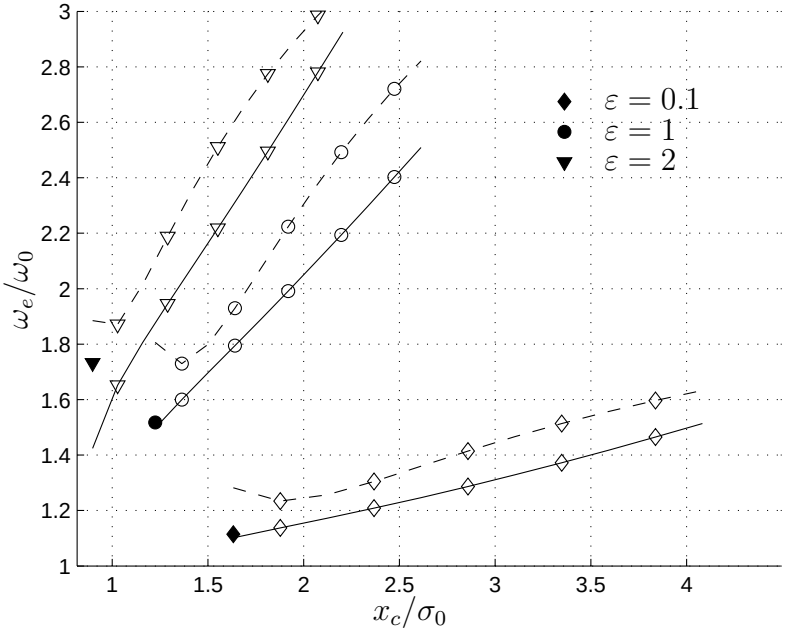

Figure 5.14: The frequency ω_e vs threshold depending on different values of the non-linearity parameter ε. Black markers (♦,●,▼) correspond to the MSL estimates. White markers (◇,○,▽) on the solid and dashed lines correspond to the analytical and numerical upcrossing rate linearization, respectively.

Procedure

The procedure for the importance sampling method is the same as for the linear oscillator in Section 5.2. On the first iteration, the failure probability functional $\widehat{p}_f(T; z, \dot{z}, t)$ is calculated for the equivalent linear equation (Eq. 5.3.13) with stiffness parameter ω_e. The simple open-loop control function is given as

$$v_Z(t) = \frac{x_c - Z_h(t_j - s)}{\sqrt{\gamma} \int_s^{t_j} h^2(t_j - \tau) d\tau} \cdot h(t_j - t), \tag{5.3.18}$$

where $Z_h(t_j - s)$ is a homogeneous solution of Eq. (5.3.13). The impulse response function has the form

$$h(t) = \frac{e^{-\xi\omega_0 t}}{\omega_d} \sin \omega_d t, \tag{5.3.19}$$

where $\omega_d = \sqrt{\omega_e^2 - (\xi\omega_0)^2}$.

Further, on the second iteration the Duffing oscillator (Eq. 5.3.1) is integrated on the corresponding time interval T. It is assumed that $\widehat{p}_f(T; x, \dot{x}, t) \approx \widehat{p}_f(T; z, \dot{z}, t)$. Thus, the importance sampling procedure is applied using the Markov control function

$$v(t, x, \dot{x}) = \frac{\sqrt{\gamma}}{\widehat{p}_f(T; x, \dot{x}, t)} \frac{d\widehat{p}_f(T; x, \dot{x}, t)}{d\dot{x}} \tag{5.3.20}$$

obtained from the previous iteration.

The simulation results are compared for the three types of estimation of the stiffness parameter ω_e, i.e., by MSL method (Eq. 5.3.11) using the analytical and numerical upcrossing rate calculation (Eq. 5.3.16).

Discussion and results

The results of the importance sampling procedure are compared with the crude Monte Carlo (MCS) in Figs. (5.15-5.16). The following parameters of the Duffing oscillator were chosen: $\xi = 0.05$, $\omega_0 = 1\,[1/\text{sec}]$, $\gamma = 0.3$, the considered time interval $T = 8 \cdot T_n$ as in case 1 in the previous section. Similarly MCS results were obtained with a different number of samples N when SE converges to 5%, if not, then $N = 10^6$.

Implementation of the MSL method to evaluate the equivalent stiffness parameter ω_e gives a good approximation for the failure probability for the small values of the non-linearity parameter ε, and low prescribed levels x_c. For the higher thresholds, this type of linearization provides a poor approximation for the control function, as was explained in the beginning of this section. Thus, during the experiments for the high thresholds, the excursions of the samples from the safe domain were still rare events as in the crude Monte Carlo method, and the importance sampling procedure fails to estimate the failure probability accurately. The results were obtained with up to $N = 50000$ with SE varying between 0.05 on low levels and up to 0.7-0.9 for tail probabilities (Fig. 5.15).

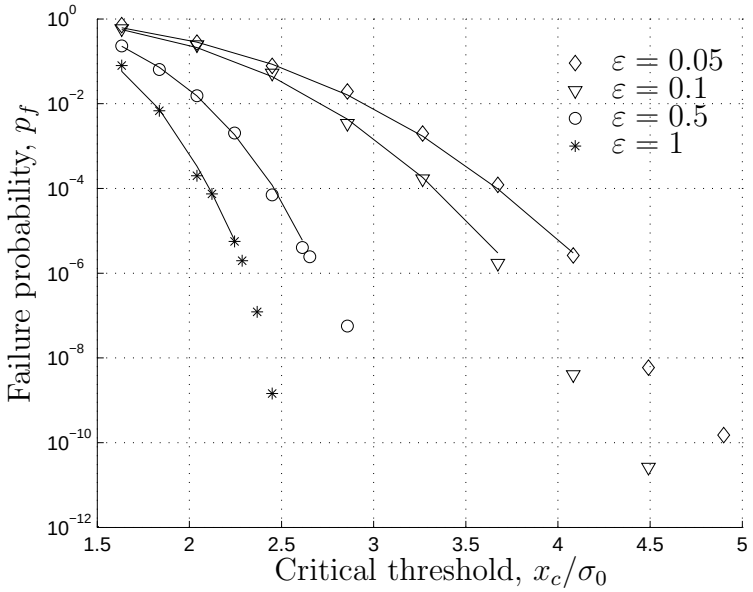

Figure 5.15: Failure probability for different threshold levels and values of non-linearity parameter ε by crude Monte Carlo and importance sampling procedure with MSL.

The failure probability values estimated by implementing mean upcrossing linearization are shown in Fig. (5.16). The results are calculated for two cases. First, the analytical

upcrossing rate linearization (AURL) was used. Second, the Monte Carlo simulations are used to estimate the upcrossing rate (NURL). The AURL estimates of the failure probability converged to the standard error $SE = 5\%$. For instance, for $\varepsilon = 2$, $x_c/\sigma_0 = 2$, the number of samples needed to estimate $p_f = 1.23 \cdot 10^{-6}$ is ca $1 \cdot 10^4$ on both iterations. The simulations run by using NURL required more samples (about $5 \cdot 10^4$) in order to achieve the same accuracy.

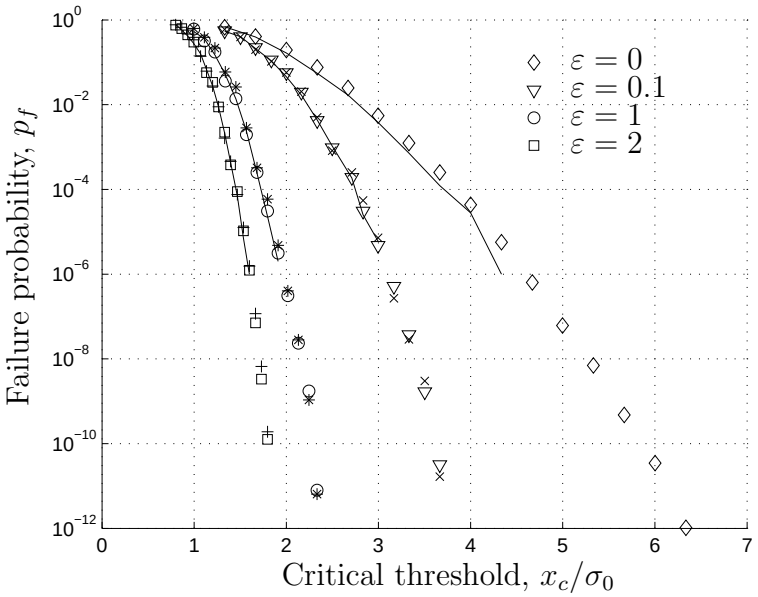

Figure 5.16: Failure probability for different threshold levels and values of non-linearity parameter ε by crude Monte Carlo and importance sampling procedure with AURL (white markerss) and NURL ($\varepsilon = 0.1$ ($\times$), $\varepsilon = 1$ ($*$), $\varepsilon = 2$ ($+$)).

The example of the realizations of the Duffing oscillator displacement $X(t)$ both with and without the control function is shown in Fig. (5.17a,b) marked with ($\diamond$). The corresponding equivalent linear system displacement $Z(t)$ is shown in Fig. (5.17a) and the corresponding control function $v(t, x, \dot{x})$ is plotted in Fig. (5.17b), both marked with ($*$).

To conclude this section it is recommended to use the equivalent linear equation and its control function on the first iteration for the non-linear problem to compose the optimal control for the second iteration. The results showed that the linearization based on the mean upcrossing rate is preferable to the traditional mean squares response linearization.

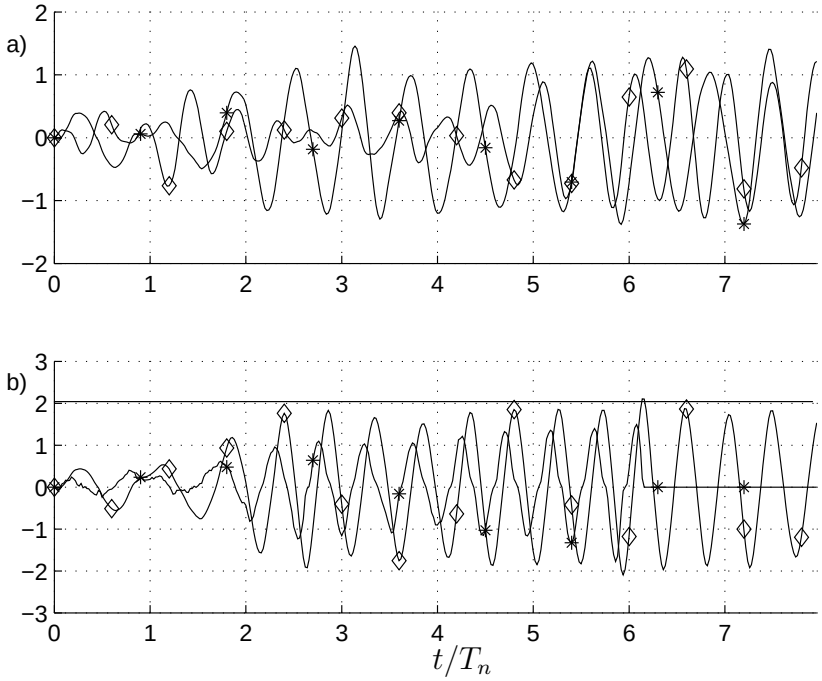

Figure 5.17: The realizations ($\varepsilon = 1$, $x_c/\sigma_0 = 2.04$): a) displacements $X(t)$ ($\diamond$) of uncontrolled Duffing oscillator and $Z(t)$ ($*$) of equivalent linear oscillator; b) displacement $X(t)$ ($\diamond$) of controlled Duffing oscillator and control $v(t, x, \dot{x})$ ($*$).

5.4 Duffing oscillator excited by coloured noise

The scope of this section is to calculate the failure probability of a Duffing oscillator excited by a filtered white noise (Olsen and Naess, 2005a). The filter is assumed to be linear, broad-banded, i.e. $\xi_z = 0.5$, whereas the system response is assumed to be a narrow-banded process in the sense of small damping, specifically $\xi = 0.02$.

$$\ddot{X}(t) + 2\xi\omega_0\dot{X}(t) + \omega_0^2 X(t)(1 + \varepsilon X^2(t)) = Z(t) \tag{5.4.1}$$

$$\ddot{Z}(t) + 2\xi_z\omega_z\dot{Z}(t) + \omega_z^2 Z(t) = \sqrt{\gamma}N(t), \tag{5.4.2}$$

where $X(s) = x$, $\dot{X}(s) = \dot{x}$, $Z(s) = z$, $\dot{Z}(s) = \dot{z}$. The safe domain to be considered in this section is as follows

$$D_S = \{(x, \dot{x}, z, \dot{z})^T : x < x_c, (\dot{x}, z, \dot{z}) \in \mathbf{R}^3\}. \tag{5.4.3}$$

The auxiliary Duffing oscillator driven by the white noise is chosen as

$$\ddot{\hat{X}}(t) + 2\xi\omega_0\dot{\hat{X}}(t) + \omega_0^2\hat{X}(t)(1 + \varepsilon\hat{X}^2(t)) = \sqrt{\gamma_e}N(t). \tag{5.4.4}$$

The parameter γ_e is engaged to compensate for the effect of the filter. It is defined by the energy which will be added to the system by the filtered noise:

$$\frac{\gamma_e}{2\pi} = S_Z(\omega_0) = \frac{S_0}{(\omega_z^2 - \omega_0^2)^2 + (2\xi_z\omega_z\omega_0)^2}, \tag{5.4.5}$$

where S_0 is the spectral density of the external excitations $\sqrt{\gamma}N(t)$, i.e., $S_0 = \gamma/2\pi$.

Furthermore, this Duffing oscillator (Eq. 5.4.4) is linearized such as

$$\ddot{Y}(t) + 2\xi\omega_e\dot{Y}(t) + \omega_e^2 Y(t) = \sqrt{\gamma_e}N(t). \tag{5.4.6}$$

The stiffness parameter ω_e is calculated from the equality of the upcrossing rate principle used in Section 5.3

$$\nu_{\hat{X}}^+(x_c) = \nu_Y^+(x_c), \tag{5.4.7}$$

where corresponding upcrossing rates are given by Eqs. (5.3.12,5.3.14). The corresponding expressions for the stationary variances (Eqs. 5.3.4 and 5.2.12) of the auxiliary Duffing and linear oscillators are given as

$$\sigma_{\hat{X}0}^2 = \frac{\gamma_e}{4\xi\omega_0^3}, \quad \sigma_Y^2 = \frac{\gamma_e}{4\xi\omega_e^3}. \tag{5.4.8}$$

The value of the parameter ω_e is plotted vs the critical threshold in Fig. (5.18) for different values of the non-linearity parameter ε. As it can be seen from the figure, the higher order of non-linearity requires a stiffer linear system.

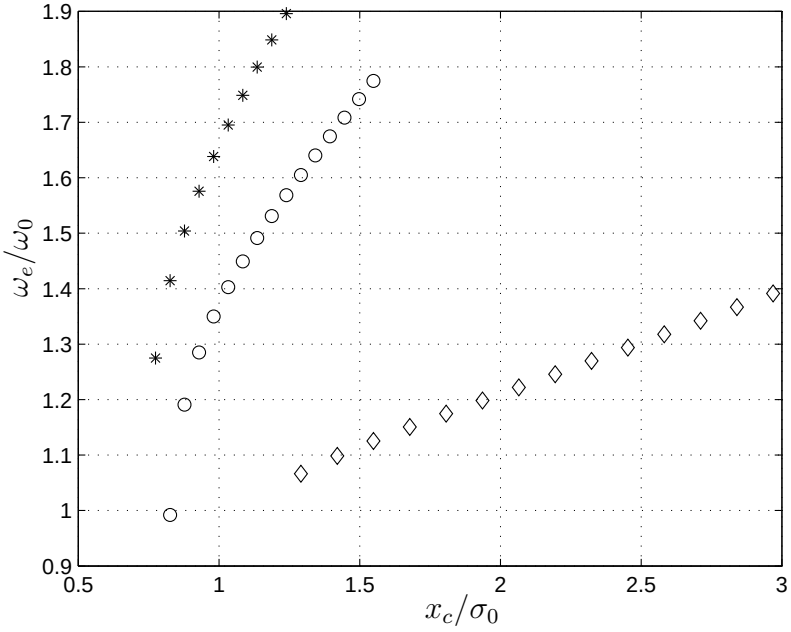

Figure 5.18: Parameter of an equivalent linear system ω_e vs critical threshold ($\varepsilon = 0.1$ ($\diamond$), $\varepsilon = 1$ ($\circ$), $\varepsilon = 2$ ($*$)).

Procedure

On the first iteration the same procedure as for the linear single degree of freedom oscillator is implemented as described in Section 5.2 for the auxiliary system (Eq. 5.4.6). The simulations using the open loop control (Eq. 5.2.25) are performed on a grid of initial values $(x, \dot{x})$ and for different values of a starting time point s.

On the second iteration according to the Girsanov transformation, the Markov control for the original system should be added as a drift to the white noise $N(t)$

$$\begin{aligned} &\ddot{\widetilde{X}}(t) + 2\xi\omega_0\dot{\widetilde{X}}(t) + \omega_0^2\widetilde{X}(t)(1 + \varepsilon\widetilde{X}^2(t)) = \widetilde{Z}(t) \\ &\ddot{\widetilde{Z}}(t) + 2\xi_z\omega_z\dot{\widetilde{Z}}(t) + \omega_z^2\widetilde{Z}(t) = \sqrt{\gamma}(v_Z(t, \widetilde{Y}) + N(t)), \end{aligned} \tag{5.4.9}$$

where $\widetilde{Y} = (\widetilde{X}, \dot{\widetilde{X}}, \widetilde{Z}, \dot{\widetilde{Z}})^T$ is the state space.

However, from the previous step the approximation of the failure probability functional is obtained only as a function of two state space variables, $\widetilde{X}(t)$ and $\dot{\widetilde{X}}(t)$, and time, i.e. $v(t, \widetilde{X}, \dot{\widetilde{X}})$.

It is important to recognize that the Markov control needed to calculate the Radon-Nikodym derivative, i.e. $v_Z(t, \widetilde{Y})$, is not the same as the process $v(t, \widetilde{X}, \dot{\widetilde{X}})$, which was derived from the white noise driven auxiliary linear system. The latter, denoted by $v_X(t, \widetilde{X}, \dot{\widetilde{X}})$, appears on the righthand side of the Duffing oscillator equation. Thus the following equations

are obtained

$$\ddot{\widetilde{X}}(t) + 2\xi\omega_0\dot{\widetilde{X}}(t) + \omega_0^2\widetilde{X}(t)(1+\varepsilon\widetilde{X}^2(t)) = Z(t) + \sqrt{\gamma_e}v_X(t,\widetilde{X},\dot{\widetilde{X}}) \tag{5.4.10}$$

$$\ddot{Z}(t) + 2\xi_z\omega_z\dot{Z}(t) + \omega_z^2 Z(t) = \sqrt{\gamma}N(t), \tag{5.4.11}$$

where, basically, due to the linearity of the filter equation

$$\widetilde{Z}(t) = Z(t) + \sqrt{\gamma_e}v_X(t,\widetilde{X},\dot{\widetilde{X}}). \tag{5.4.12}$$

Hence the original control v_Z needed for the evaluation of the Radon-Nikodym derivative (3.3.18) can be found as a result of the direct differentiation

$$\ddot{v}_X + 2\xi_z\omega_z\dot{v}_X + \omega_z^2 v_X = \sqrt{\frac{\gamma}{\gamma_e}}v_Z. \tag{5.4.13}$$

Thus, at the second step of the procedure, for each time step during the integration of the controlled system (Eq. 5.4.10), a corresponding value of the control process is chosen depending on the state space variables at this time, i.e. $v_X(t_i,\tilde{x}(t_i),\dot{\tilde{x}}(t_i))$. To recover the control v_Z, the differentiation required by Eq. (5.4.13) is performed numerically.

Discussion and results

The various stiffness parameters of the filter (Eq. 5.4.2) are considered to verify the robustness of the proposed procedure. Three following cases were studied: 1) $\omega_0 = \omega_z = 1\,[1/\text{sec}]$, 2) $\omega_0 = 1\,[1/\text{sec}]$ and $\omega_z = 0.5\,[1/\text{sec}]$, 3) $\omega_0 = 1\,[1/\text{sec}]$ and $\omega_z = 1.5\,[1/\text{sec}]$. In Fig. (5.19) the one-sided power spectral density (psd) functions of the auxiliary linear system (Eq. 5.4.6) and the original Duffing oscillator (Eq. 5.4.1) ($\varepsilon = 0$), $G_Y(\omega)$ and $G_X(\omega)$ respectively, are compared. The white approximation of the filtered noise is worse for $\omega_z < \omega_0$ (Fig. 5.19b), whereas for the case $\omega_z \geq \omega_0$ the spectra are almost identical.

The realizations of the controlled process $X(t)$ and the coloured noise $Z(t)$ for three study cases are shown in Figs. (5.20-5.22). The ordinate is normalized by corresponding values of standard deviation $\sigma_{\dot{X}0}$ (Eq. 5.4.8). As it is shown in Fig. (5.20a) the filtered process $Z(t)$ (solid line marked with asterisks) with stiffness parameter $\omega_z = 0.5\,[1/\text{sec}] < \omega_0$ has less variation and amplitude comparable with the output process $X(t)$, whereas filter process with $\omega_z = 1.5\,[1/\text{sec}] > \omega_0$ (Fig. 5.22a) is more stiff with lower amplitude and the same frequency as the main equation.

In Figs. (5.23-5.25), the failure probability versus critical threshold is plotted for different values of non-linearity parameter ε and three different filter stiffness parameters. The results from the crude Monte Carlo method (a solid line) are obtained with the standard error $SE = 0.05$ or with number of samples $N = 10^6$ if SE has not converged to 0.05. The total number of samples used in the two steps of the proposed procedure is maximum $N_{IS} = 4{\cdot}10^4$. All the simulation runs converged to the standard error 0.05. The calculation time gained compared with the crude simulation method is proportional to N_{IS}/N. The results coincide very well even in the case when the filter stiffness parameter is $\omega_z = 0.5\,[1/\text{sec}]$ (Fig. 5.24) and the proposed importance sampling procedure allows the calculation of very low probability values even when the crude method breaks up.

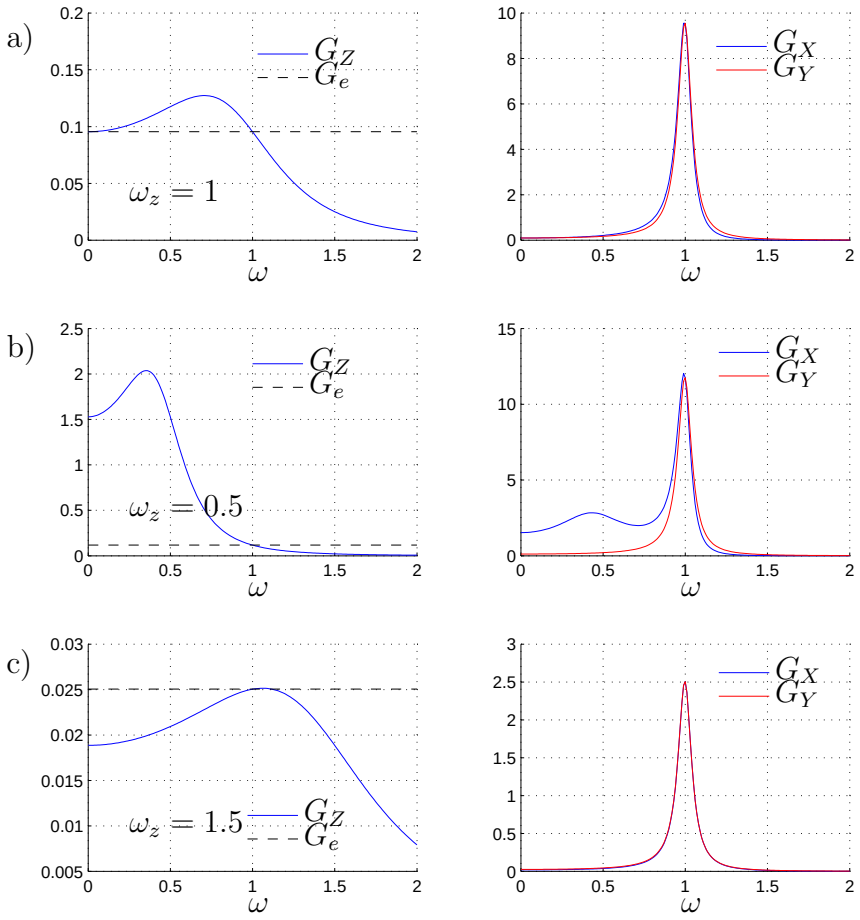

Figure 5.19: Power spectral densities G_e, G_Z, G_X and G_Y of the processes $\sqrt{\gamma_e}N(t)$, $Z(t)$, $X(t)$ ($\varepsilon = 0$) and $Y(t)$ correspondingly:
a) $\omega_0 = \omega_z = 1\,[1/\text{sec}]$, b) $\omega_0 = 1\,[1/\text{sec}]$ and $\omega_z = 0.5\,[1/\text{sec}]$, c) $\omega_0 = 1\,[1/\text{sec}]$ and $\omega_z = 1.5\,[1/\text{sec}]$.

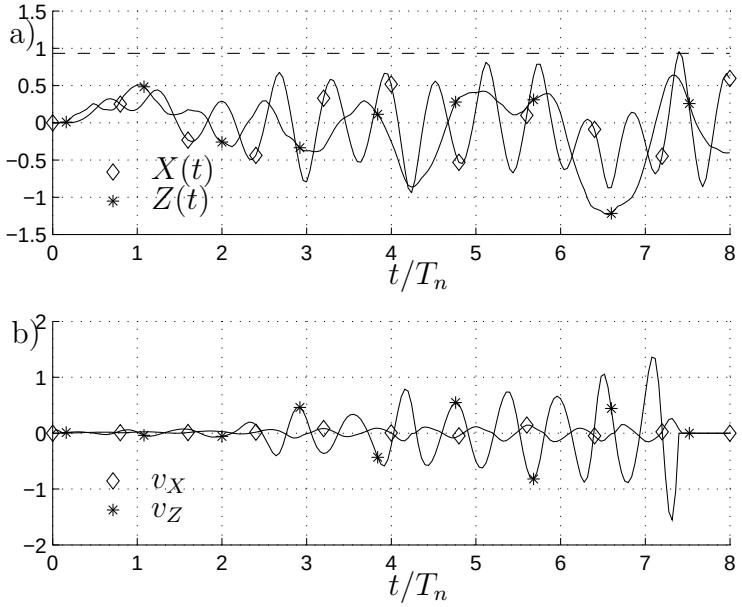

Figure 5.20: Examples on the sample paths (critical threshold $x_c = 0.93\sigma_0$, $\varepsilon = 1$, $\omega_z = 0.5$):
a) samples of controlled process $X(t)$ ($\diamond$) and filter process $Z(t)$ ($*$),
b) ($\diamond$) control function v_X, ($*$) control function v_Z.

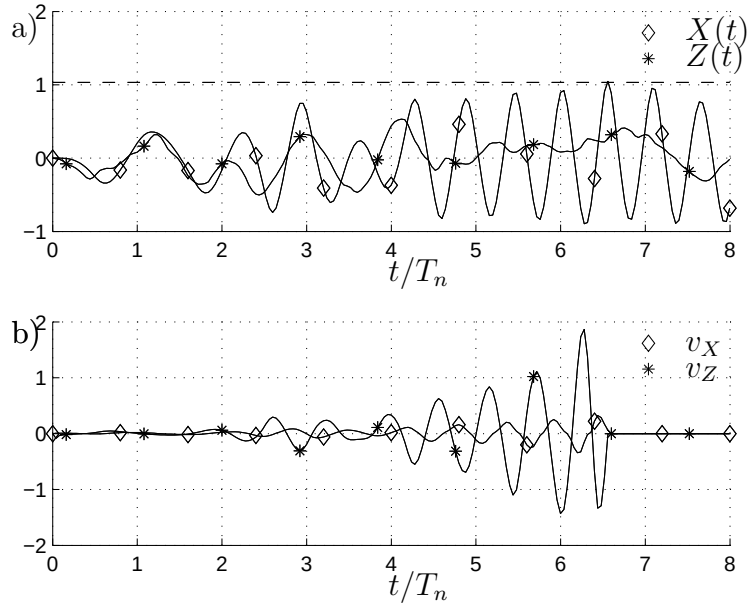

Figure 5.21: Examples on the sample paths (critical threshold $x_c = 1.03\sigma_0$, $\varepsilon = 1$, $\omega_z = 1$):
a) samples of controlled process $X(t)$ ($\diamond$) and filter process $Z(t)$ ($*$),
b) control function v_X ($\diamond$), control function v_Z ($*$).

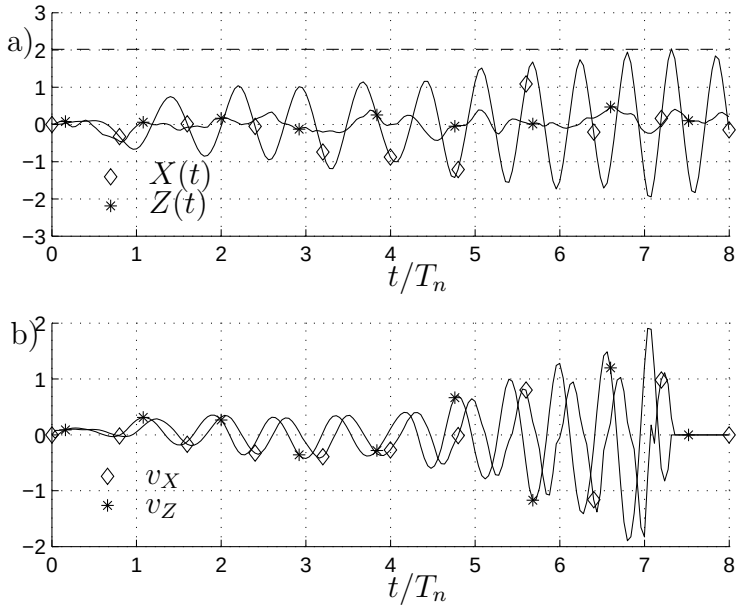

Figure 5.22: Examples on the sample paths (critical threshold $x_c = 2\sigma_0$, $\varepsilon = 1$, $\omega_z = 1.5$):
a) samples of controlled process $X(t)$ ($\diamond$) and filter process $Z(t)$ ($*$),
b) control function v_X ($\diamond$), control function v_Z ($*$).

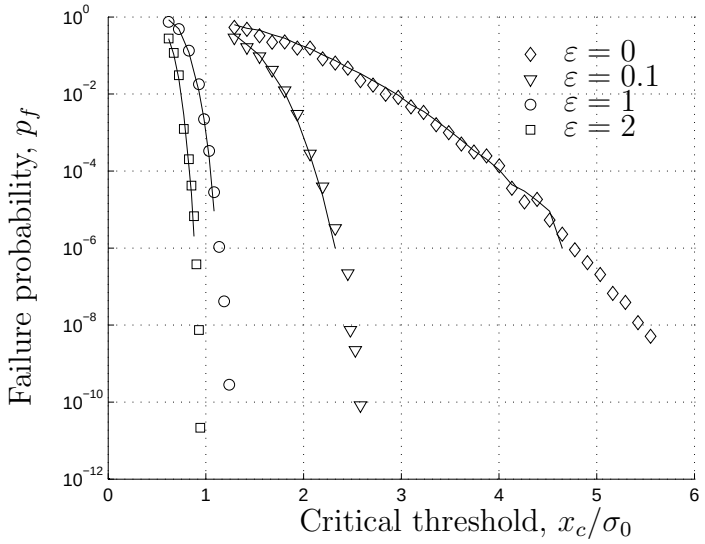

Figure 5.23: Failure probability for different values of non-linearity parameter ε (solid line - Monte Carlo method, diverse markers - present method), $\omega_z = 1\,[1/\text{sec}]$.

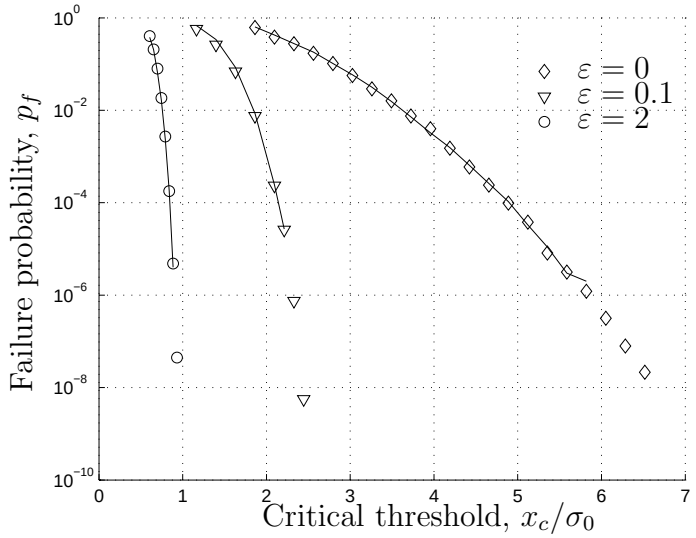

Figure 5.24: Failure probability for different values of non-linearity parameter ε (solid line - Monte Carlo method, diverse markers - present method), $\omega_z = 0.5\,[1/\text{sec}]$.

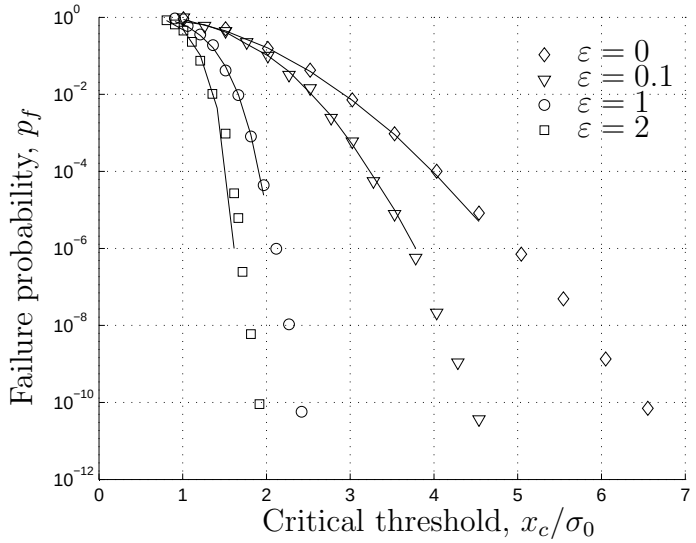

Figure 5.25: Failure probability for different values of non-linearity parameter ε (solid line - Monte Carlo method, diverse markers - present method), $\omega_z = 1.5\,[1/\text{sec}]$.

5.5 Oscillator with non-linear damping and stiffness under additive noise

The procedure described in Section 5.3 which uses the upcrossing rate as a criterion to define an auxiliary linear system is applicable to the wide class of non-linear systems given by

$$\ddot{X}(t) + g(H)\dot{X}(t) + k[X(t)] = \sqrt{\gamma}N(t), \tag{5.5.1}$$

where $H(X, \dot{X}) = \dot{x}^2/2 + K(x)$ is the system total energy with the potential energy, $K(x) = \int_0^x k(v)dv$.

For these systems an exact solution of Fokker-Planck equation is obtainable (Soong and Grigoriu, 1997)

$$f(x, \dot{x}) = q \exp\left[-\frac{2}{\pi G_0}\int_0^H g(v)dv\right] \tag{5.5.2}$$

in which q is a normalization constant.

As an example an oscillator of Caughey type is considered (Naess and Johnsen, 1993)

$$\ddot{X}(t) + 2\xi\left(1 + \lambda\sqrt{H(X, \dot{X}}\right)\dot{X}(t) + X(t) + \varepsilon X^3(t) = 2\sqrt{\xi}N(t) \tag{5.5.3}$$

with parameters ξ, λ and ε. The time parameter is non-dimensional in this formulation.

In this case, the total energy is given by the relation

$$H(x, \dot{x}) = \dot{x}^2/2 + x^2/2 + \varepsilon x^4/4. \tag{5.5.4}$$

Thus the joint probability function is

$$f(x, \dot{x}) = q \exp\left[-\frac{4\xi}{\pi G_0}\left(\frac{\dot{x}^2}{2} + \frac{x^2}{2} + \varepsilon\frac{x^4}{4} + \frac{2}{3}\lambda\left(\frac{\dot{x}^2}{2} + \frac{x^2}{2} + \varepsilon\frac{x^4}{4}\right)^{3/2}\right)\right], \tag{5.5.5}$$

where $G_0 = 4\xi/\pi$ is the one-sided spectral density of the white noise $N(t)$ and the integration constant q can be found numerically for the corresponding values of parameters ε and λ.

The same safe domain is considered as in Section 5.2

$$D_S = \{(x, \dot{x}) : x < x_c, \dot{x} \in \mathbb{R}\}, \tag{5.5.6}$$

where x_c is a prescribed critical threshold for any $0 \le s \le t \le T$.

Let

$$\ddot{Z}(t) + 2\xi\omega_e\dot{Z}(t) + \omega_e^2 Z(t) = 2\sqrt{\xi}N(t) \tag{5.5.7}$$

be an auxiliary linear system. The equivalent linear stiffness is obtained from the equality of the upcrossing rates (Eq. 5.3.16)

$$\nu_Z^+(u) - \nu_X^+(u) = 0. \tag{5.5.8}$$

The upcrossing rate of the Caughey oscillator is obtained by Rice formula (Eq. 3.3.8)

$$\nu_X^+(u) = \int_0^\infty y f(u, y; t) dy \tag{5.5.9}$$

and the mean upcrossing rate for the linear system is given by Eq. (5.3.14)

$$\nu_Z^+(u) = \frac{\omega_e}{2\pi} \exp\left(-\frac{1}{2}\omega_e^3 \cdot u^2\right). \tag{5.5.10}$$

Procedure

The procedure for the importance sampling method is the same as for the linear oscillator in Section 5.2. On the first iteration, the failure probability functional $\widehat{p}_f(T; z, \dot{z}, t)$ is calculated for the equivalent linear equation (Eq. 5.5.7) with stiffness parameter ω_e. The simple open-loop control function is given as

$$v_Z(t) = \frac{x_c - Z_h(t_j - s)}{2\sqrt{\xi} \int_s^{t_j} h^2(t_j - \tau) d\tau} \cdot h(t_j - t), \tag{5.5.11}$$

where $Z_h(t_j - s)$ is an homogeneous solution of Eq. (5.5.7). The impulse response function has the form

$$h(t) = \frac{e^{-\xi\omega_e t}}{\omega_d} \sin \omega_d t, \tag{5.5.12}$$

where $\omega_d = \omega_e^2\sqrt{1 - \xi^2}$.

Further, on the second iteration the non-linear oscillator (Eq. 5.5.3) is integrated on the corresponding time interval T. It is assumed that $\widehat{p}_f(T; x, \dot{x}, t) \approx \widehat{p}_f(T; z, \dot{z}, t)$. Thus, the importance sampling procedure is applied using the Markov control function

$$v(t, x, \dot{x}) = \frac{2\sqrt{\xi}}{\widehat{p}_f(T; x, \dot{x}, t)} \frac{d\widehat{p}_f(T; x, \dot{x}, t)}{d\dot{x}} \tag{5.5.13}$$

obtained from the previous iteration.

Discussion and results

The following set of parameter values for the Caughey oscillator has been chosen $(\lambda, \varepsilon) = (0.5, 0.1)$ and $\xi = 0.5$. The corresponding stiffness parameter of an equivalent linear oscillator is plotted vs critical threshold x_c in Fig. (5.26).

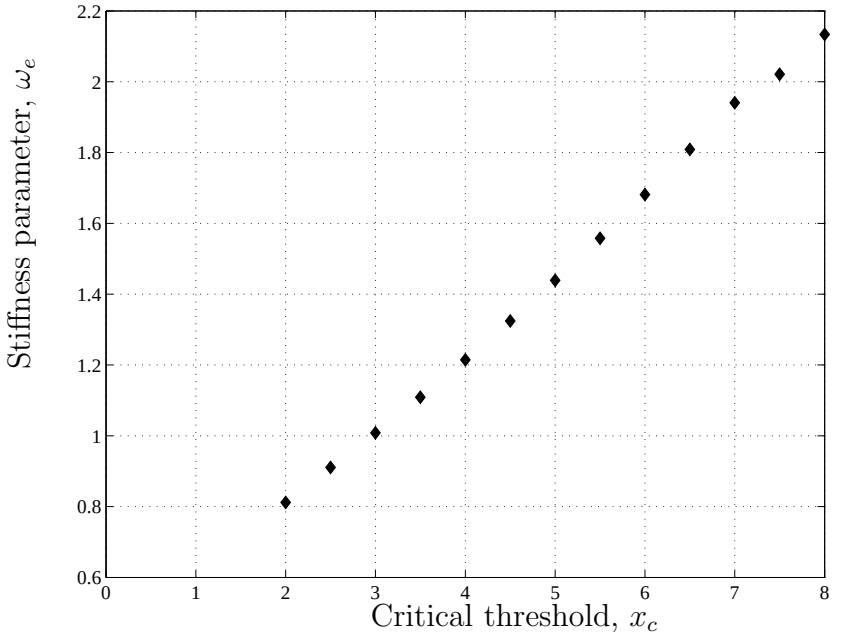

Figure 5.26: Equivalent stiffness ω_e vs critical threshold.

The realizations of the Caughey oscillator displacement $X(t)$ both with and without the control function, and the equivalent linear oscillations are shown in Fig. (5.27).

The results of the importance sampling procedure are compared with the crude Monte Carlo in Fig. (5.28). MCS results were obtained with a different number of samples N when SE converges to 5%, if not, then $N = 10^6$. The importance sampling results are calculated with different number of samples until $SE = 5\%$. The maximum number of time series on both iterations reached $N_{IS} \approx 5 \cdot 10^4$ for the lowest estimated probability.

The procedure has shown robustness and fast convergence for the first-passage probability for the Caughey oscillator.

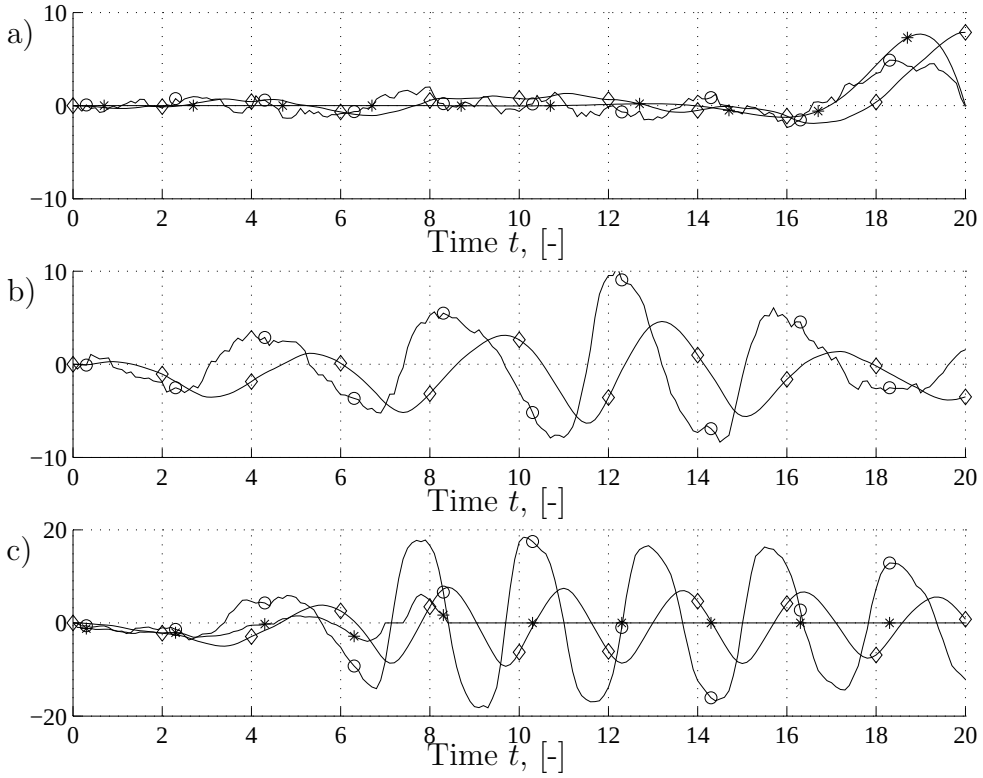

Figure 5.27: The realizations ($x_c = 7$): a) displacements $Z(t)$ ($\diamond$) and velocity $\dot{Z}(t)$ ($\circ$) of equivalent linear oscillator and its control $v_Z(t)$ ($*$); b) displacement $X(t)$ ($\diamond$) and velocity $\dot{X}(t)$ ($\circ$) of uncontrolled Caughey oscillator; c) displacement $\widetilde{X}(t)$ ($\diamond$) and velocity $\dot{\widetilde{X}}(t)$ ($\circ$) of Caughey oscillator subjected to control function $v(t, x, \dot{x})$ ($*$).

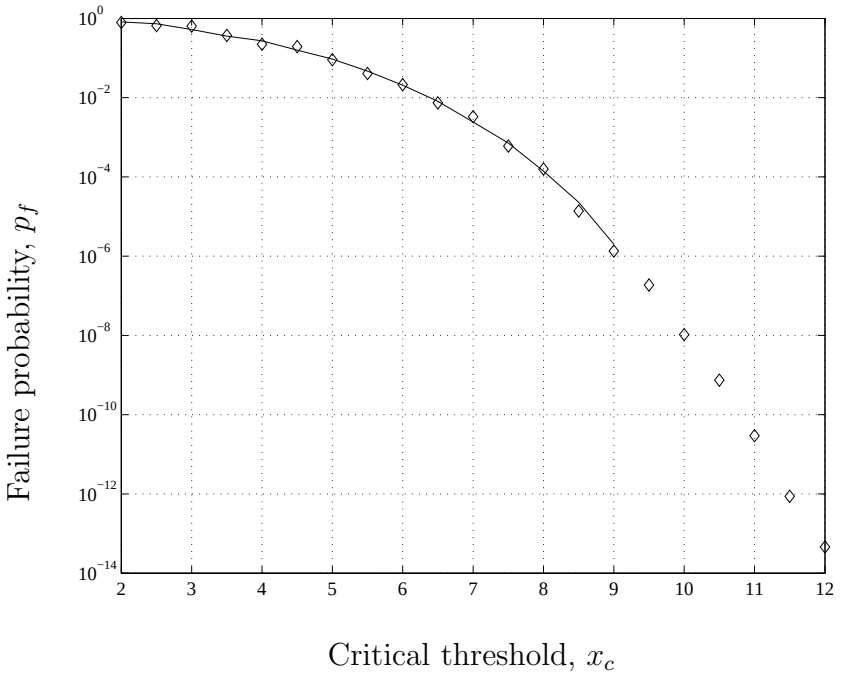

Figure 5.28: Failure probability for different threshold levels by crude Monte Carlo and importance sampling procedure.

5.6 Hysteretic systems under random excitations

Another challenging non-linear problem which is studied in this thesis is a hysteretic system. The rigorous analysis and modelling of hysteretic systems under random vibrations are presented by Wen (1980), Wen (1985). In the case of severe loads the inelastic response should be taken into consideration. The inelastic behaviour of the response has non-linear properties, which are assumed to be represented by a hysteresis of the restoring force. For the proper safety and reliability estimation these characteristics of the system have to be taken into account. The single degree of freedom hysteretic system considered here is given by

$$\ddot{X} + 2\xi\omega_0\dot{X} + \alpha\omega_0^2 X + (1-\alpha)\omega_0^2 Z = \sigma N(t), \tag{5.6.1}$$

$$\dot{Z} = -\gamma|\dot{X}|\, Z\, |Z|^{n-1} - \beta\dot{X}\, |Z|^n + A\dot{X}, \tag{5.6.2}$$

where ω_0 is a pre-yielding natural frequency, α is a ratio of post-yielding stiffness to pre-yielding stiffness, $(1-\alpha)\omega_0^2 Z$ is a hysteretic part, A governs the amplitude, γ, β control the shape of the hysteretic loop and n the smoothness of the transition from elastic to inelastic range. The external force is the Gaussian white noise with zero mean and standard deviation $\sqrt{\sigma}$. Varying the coefficients of the hysteretic member one can construct different types of restoring forces, such as hardening, narrow-band or wide-band systems.

Further on, it is assumed that there is a nearly elastic-plastic system, i.e. $A = 1.0$, $\gamma = \beta = 0.5$, $\alpha = 1/21$ and $n = 1$, where the standard deviation of the external excitations $\sigma = 0.3$ as in previous examples. The example of the sample path is shown in Fig. (5.29), together with the plot of hysteretic force (Fig. 5.30).

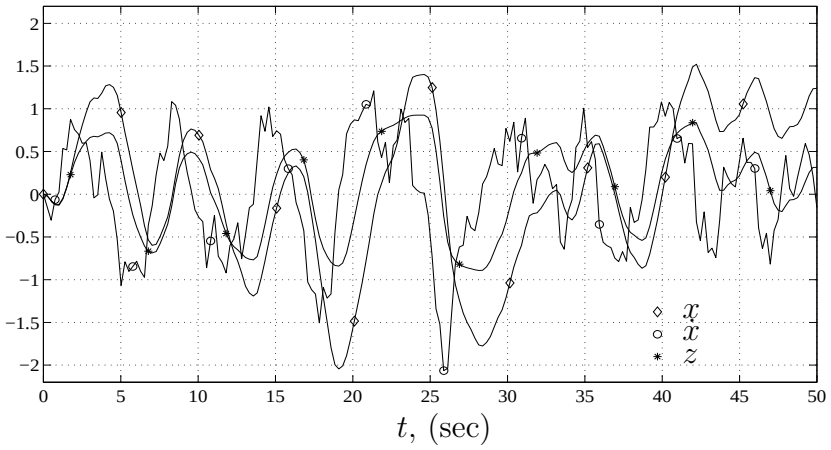

Figure 5.29: The sample path of uncontrolled hysteretic oscillator.

The safe domain is to be considered as follows

$$D_S = \{(x, \dot{x}, z)^T : x < x_c, (\dot{x}, z) \in \mathbf{R}^2\}, \tag{5.6.3}$$

where x_c is a critical threshold.

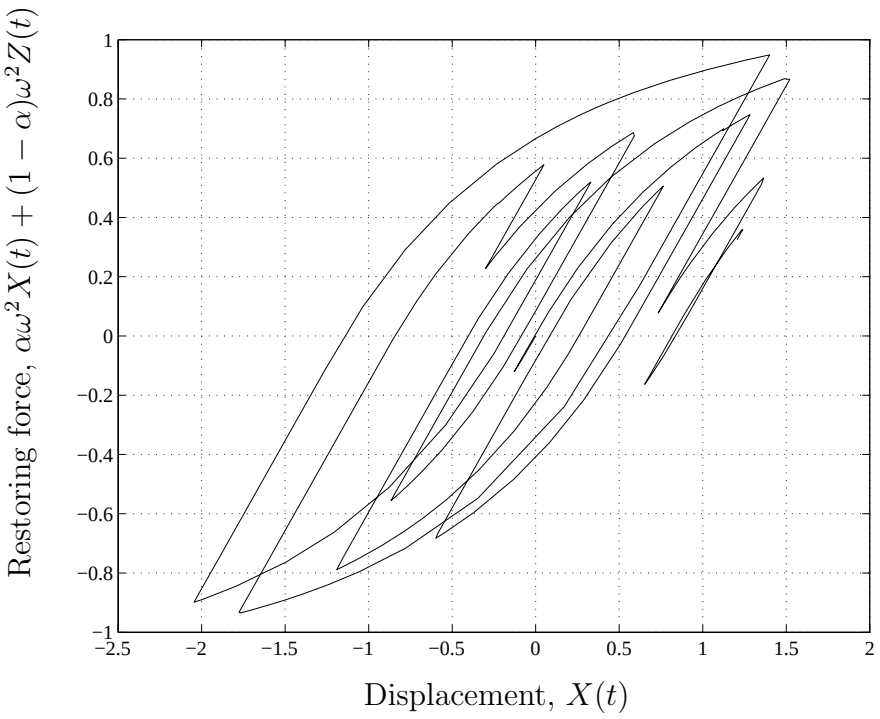

Figure 5.30: The uncontrolled hysteretic loop.

The auxiliary linear equation is given by

$$\ddot{\hat{X}}(t) + 2\xi\omega_0\dot{\hat{X}}(t) + \omega_e^2\hat{X}(t) = \sqrt{\sigma}N(t), \tag{5.6.4}$$

where an equivalent stiffness parameter ω_e is found from the assumption that the upcrossing rate $\nu_X^+(x_c)$ of the hysteretic system with zero initial conditions is the same as the upcrossing rate $\nu_{\hat{X}}^+(x_c)$ of the linear oscillator, as in Section 5.3. The upcrossing rate $\nu_X^+(x_c)$ is estimated by Monte Carlo simulations and then extrapolated to the desired level (Fig. 5.31). The estimated stiffness parameter ω_e versus critical threshold is shown in Fig. (5.32).

The controlled hysteretic system is obtained by standard Girsanov transformation

$$\ddot{\tilde{X}} + 2\xi\omega_0\dot{\tilde{X}} + \alpha\omega_0^2\tilde{X} + (1-\alpha)\omega_0^2\tilde{Z} = \sqrt{\sigma}v(t,\tilde{X},\dot{\tilde{X}}) + \sqrt{\sigma}N(t), \tag{5.6.5}$$

$$\dot{\tilde{Z}} = -\gamma|\dot{\tilde{X}}|\,\tilde{Z}\,|\tilde{Z}|^{n-1} - \beta\dot{\tilde{X}}\,|\tilde{Z}|^n + A\dot{\tilde{X}}. \tag{5.6.6}$$

Procedure

On the first iteration, due to the substantial difference in behaviour between linear and hysteretic systems started at non-zero initial values (Fig. 5.33) the mixed process is used

$$X_I(t) = \hat{X}(t) + X_h(t), \tag{5.6.7}$$

where $\hat{X}(t)$ is a solution of the linear equation (5.6.4) with zero initial conditions and $X_h(t)$ is a homogeneous solution of the hysteretic equation (5.6.1).

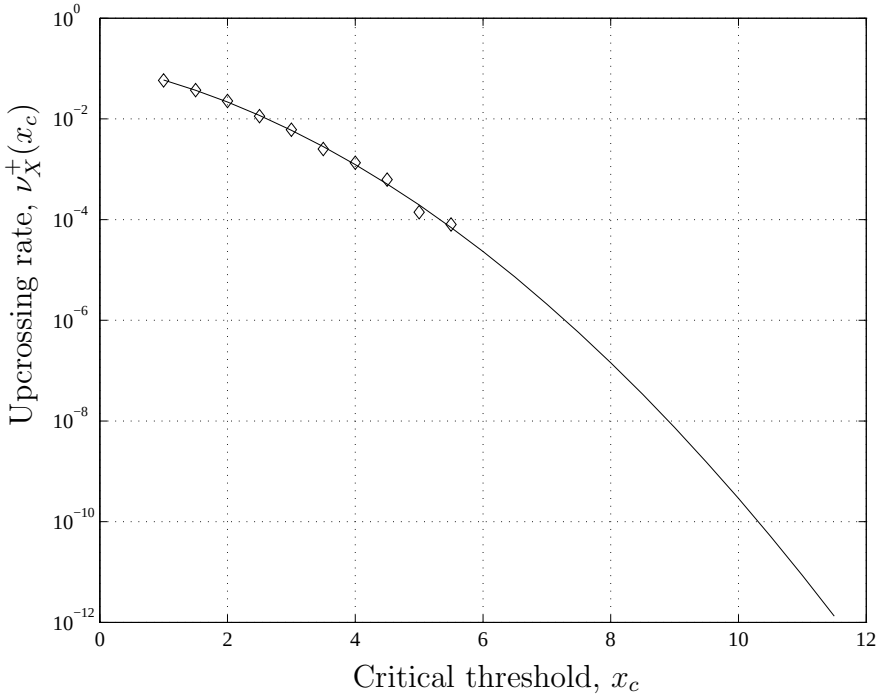

Figure 5.31: Estimated ($\diamond$) and approximated ($--$) upcrossing rate $\nu_X^+(x_c)$ for hysteretic oscillator $X(t)$ with zero initial values.

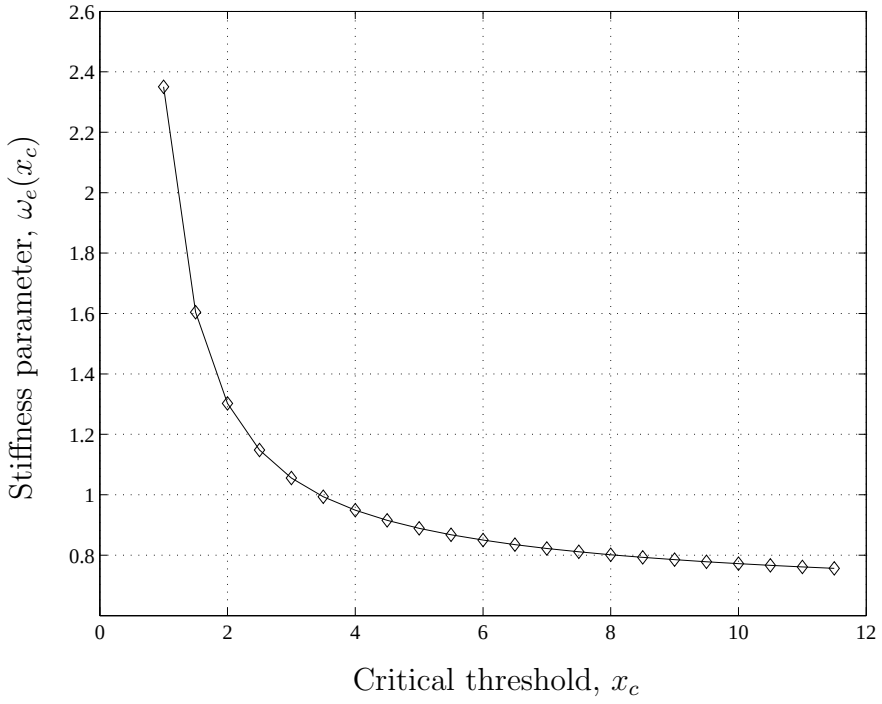

Figure 5.32: Stiffness parameter $\omega_e(x_c)$ for auxiliary linear system.

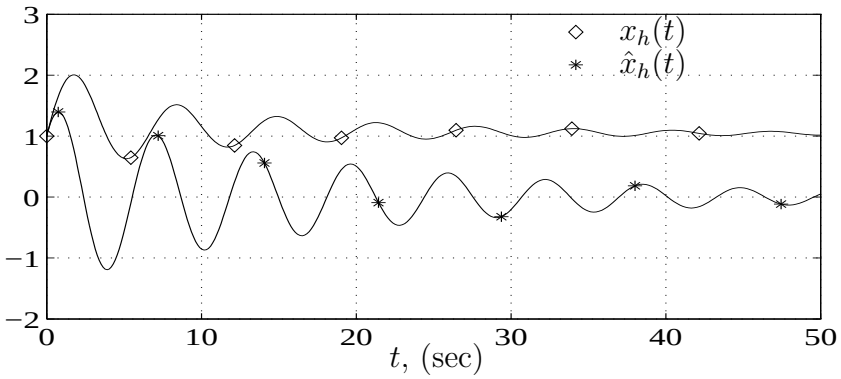

Figure 5.33: Homogeneous solutions for hysteretic system $X(t)$ and linear system $\hat{X}(t)$.

Then the simple control function on the first iteration is given by Eq. (5.2.25)

$$v_I(t) = \frac{x_c - X_h(t_j - s)}{\sqrt{\sigma} \int\limits_s^{t_j} h^2(t_j - \tau) d\tau} \cdot h(t_j - t) \tag{5.6.8}$$

where $h(\cdot)$ is the impulse response function of the linear oscillator (Eq. 5.6.4).

The failure probability functional in 2D looks completely different for the hysteretic system than for the linear oscillator due to plasticity of the response. The simulated and smoothed by B-spline 2D surface of the failure functional is shown in Fig. (5.34). The time horizon is T. Unlike the value set obtained for the linear oscillator (Fig. 5.4), the form of the failure probability functional for the hysteretic oscillator is unsymmetrical and monotonically increases up to the critical level in the x-direction and in the positive direction of the $\dot{x}$-axis.

On the second iteration the standard importance sampling procedure is applied with a Markov control function $v(t, x, \dot{x})$ given by

$$v(t, x, \dot{x}) = \frac{\sqrt{\sigma}}{\widehat{p}_f(T; x, \dot{x}, t)} \frac{d\widehat{p}_f(T; x, \dot{x}, t)}{d\dot{x}} \tag{5.6.9}$$

obtained from the previous iteration.

Discussion and results

The results of the two step iterative procedure coincide very well with the crude Monte Carlo estimates until this method breaks down. As in the previous examples, the Monte Carlo estimates are found with $SE = 5\%$ or with number of samples $N = 10^6$ when SE does not converge to 5%, whereas all the importance sampling estimates are obtained with $SE = 5\%$ and number of samples on the both iterations varying from $N_{IS} = 1000$ up to $N_{IS} = 5 \cdot 10^4$ for the probabilities of order 10^{-9}.

The samples of the controlled hysteretic system and corresponding Markov control function $v(t, x, \dot{x})$ are presented in Fig. (5.35). The restoring force is plotted versus displacement $X(t)$ in Fig. (5.36).

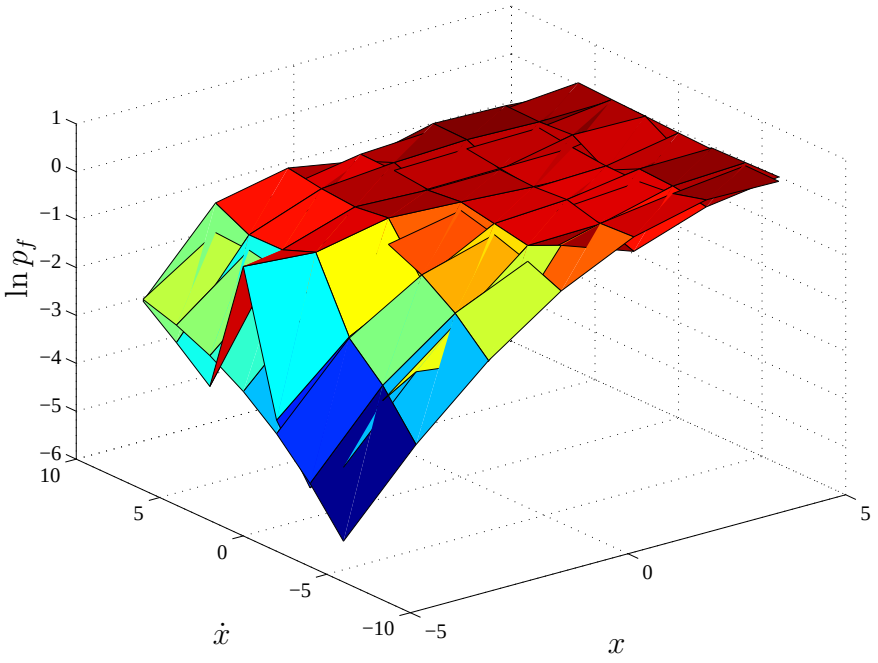

Figure 5.34: First iteration results: approximated failure probability in in $\mathbb{R}^2 = [X \times \dot{X}]$ smoothed by B-spline.

In Fig. (5.37) the resulting failure probability estimate p_f is shown versus critical threshold x_c.

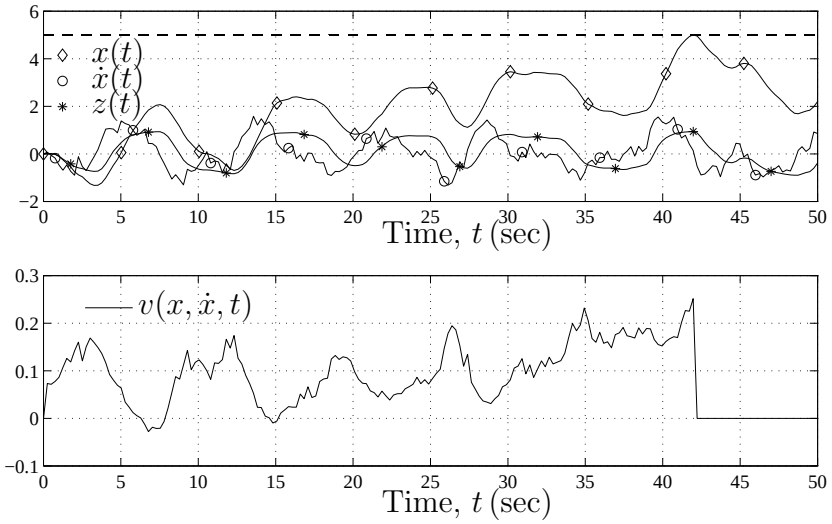

Figure 5.35: Samples of controlled hysteretic oscillator and Markov control, $x_c = 5$.

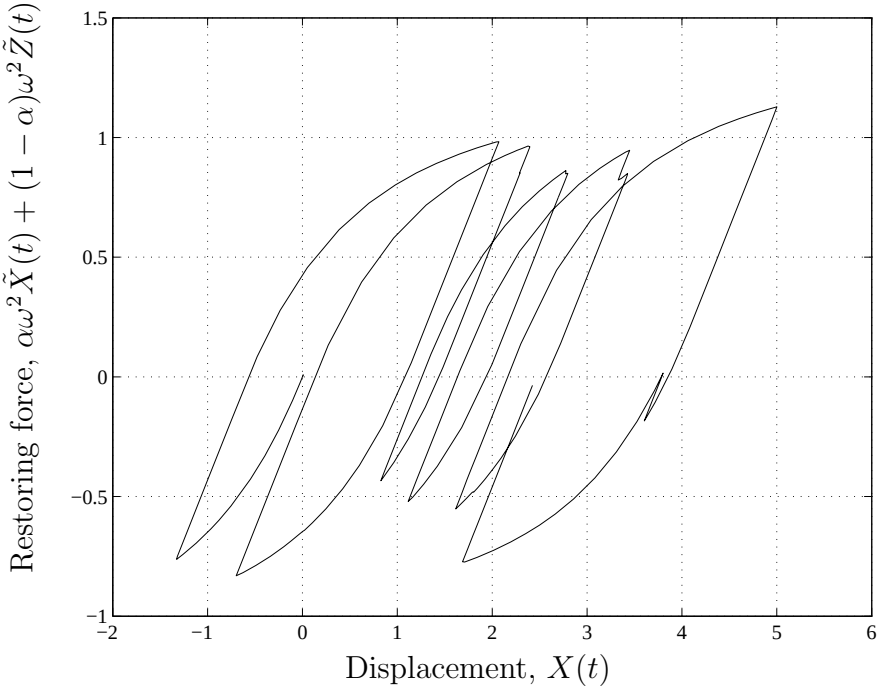

Figure 5.36: Restoring force with control.

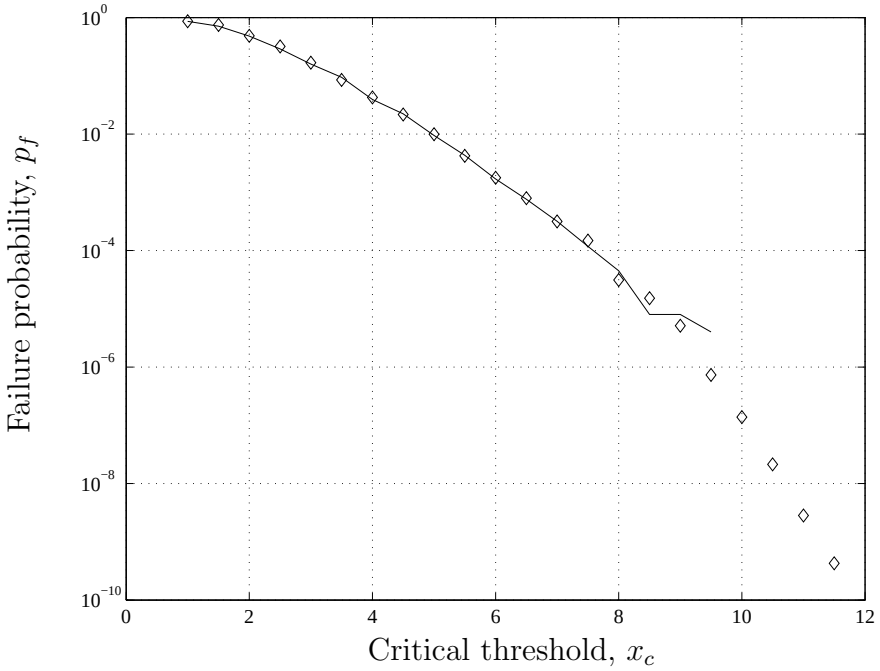

Figure 5.37: Failure probability of hysteretic system.

Chapter 6

Summary and conclusions

6.1 Results

The emphasis in the first part of this thesis is on an efficient importance sampling technique for estimating dynamic system reliability. This procedure has been proposed for solving the first excursion problem for linear and non-linear oscillatory systems excited by white and coloured noise.

The application of the importance sampling procedure was used in the framework of stochastic control theory. The considered systems were assumed to be modelled as a set of Itô stochastic differential equations where the response is a Markov process. The proposed method is a combination of known techniques such as design point oscillations and Girsanov transformation. The simulations used two types of control functions, namely the simple open-loop control and the Markov control.

The algorithm consists of two steps. On the first iteration, an auxiliary linear system with a close failure rate was used to obtain the approximation of the failure probability functional. Then the expression for the optimal control function was employed to construct the Markov control which depends on the state of the considered system. Integrating the system with this additional function allowed the calculation of the failure probability up to 10^{-10} with standard error $SE = 5 - 10\%$. The convergence rate is several orders of magnitude faster than the crude Monte Carlo simulation.

The advantage of the proposed procedure is that its implementation requires only the expression of the design point oscillations of a linear dynamic system excited by the Gaussian white noise which is obtainable in analytical form. No special algorithms for evaluation of the design point oscillations for non-linear systems are needed. Hence only minor computational time was used on the intermediate smoothing operations. As a result, the simulation time was reduced by almost the same order as a number of samples compared to the crude Monte Carlo.

The linearized system can be easily obtained for the most non-linear cases. When the linearization is not a straightforward procedure, the heuristic assumptions have to be made based on the knowledge of behaviour of the given non-linear system. The main aspect about making the correct choice for this equivalent system is to consider its upcrossing rate as a crucial characteristic of a first-passage event.

The other advantage of the iterative procedure is that designed Markov controls depends explicitly on the system state space. Thus simulated samples give unbiased estimates of the

failure probability. For example, in the case of Duffing oscillator, the right order of failure probability was achieved already with a few sample in failure domain even when mean square linearization was used. The trustworthiness of this estimate was, of course, compromised by large statistical error because outcrossings from safe domain happened so rarely.

The second part of this thesis is a probability analysis of ice loads (see Chapter 7)

6.2 New challenges

An obvious future research topic would be the investigation of the present procedure for multidegree of freedom problems and self-excited (parametric) systems. The procedure's dependance on a number of state space variables makes it unsuitable for finite element method. On the other side, different techniques to reduce the dimensionality of the system might be incorporated to obtain the approximate failure probability functional for the design of the Markov controls.

Chapter 7

Probabilistic analysis of ice loads

7.1 Introduction

This chapter describes the results of my work for two international European projects LOLEIF (Validation on **Lo**w **Le**vel **I**ce **F**orces on Coastal Structures) and its successor STRICE (Measurements on **Str**uctures in **Ice**). During the project the full-scale measurements were conducted at the Norströmsgrund lighthouse in the northern part of the Baltic Sea.

The problem of ice load definition has recently become very relevant due to the latest exploration and development of hydrocarbon production in the Arctic region. Experience showed that conventional jacket platforms are not at all the optimal solution for ice-infected regions, neither are the big artificial islands which were used in Canadian Arctic (Sanderson, 1988). The latter were found to be very labour-intensive and economically unprofitable. Thus, new technology is desired with a strong regard to the harsh environmental conditions.

Concerning the reliability and design of coastal and offshore structures in northern Europe, Arctic regions and other areas of interest the ice loads scenarios are dominating. The largest ice loads are caused by pressure ridges, level ice and rafted ice on vertical structures. Several full scale measurements have shown that the magnitudes of these forces are lower than what is recommended by several common ice codes (e.g., API, 1995).

Due to the great complexity of a probabilistic description of forces induced by ice and discrete data measurements of concomitant parameters such as ice thickness, ice strength and temperature, it is very difficult to determine the general parent probability distribution for this kind of environmental load. Nevertheless, when one comes to design standards on structures and vessels in ice-infested regions then at least estimation of the maximum load is of great interest. In the project, several probability distributions are fitted to the extreme values of local (panel) loads and the evaluated global load picked up from each day of measurements during the measuring campaign in the winter 2002. The Gumbel distribution is assumed to be the best fit in this case. The design values for 1, 5, 10, 25 year return periods are calculated and compared with the similar research found in the recent literature. From the estimated parameters, it can be concluded that the scale factor for the forces is the same as the scale of the structures. Though further research is needed to support this hypothesis.

Another objective of the project is to validate the relationship between the ice drift speed and the ice load on the structures. Sodhi et al. (1998) have shown that the ice loads increase

for decreasing indentation speed for medium and small-scale tests. However, these results have to be proven for full-scale experiments.

7.1.1 Ice-structure interaction

The nature and magnitude of the the ice load is governed by many factors, some of which relate to ice and some to structure. The load is governed either by the deformation, failure, and clearing ice in front of the structure, or by the environmental driving forces on the ice (Løset et al., 1998). Of course in both situations, the magnitude of the ice load is not constant with time. It is obvious that ice load is stochastic and only the probabilistic methodology might give reliable results.

The most important factors that govern the ice load are:

- Ice features such as level ice, rafted ice, ridges and rubbles;
- Ice properties such as crystallography, temperature, salinity, porosity, surface tension;
- Design philosophy such as limit stress, limit momentum, limit force;
- Interaction geometry such as single interaction, interaction on waterline shape, interaction with multi legged structure, on water depth and dependence on structure size;
- Failure modes such as creep, crushing, bending, buckling, splitting, shearing.

Ice appears to be an extraordinary material changing its characteristics under loading. This leads to difficulties while predicting the maximum forces induced by ice on a structure. It is a creepy ductile material at low stresses, yet an extremely brittle material at high stresses, and its behaviour is dependent on the rate of deformation and deformation history (Sanderson, 1988). Moreover, the strength of ice is scale-dependent and this makes the extrapolations and many assumptions unreliable.

To analyse the full-scale measurements properly one has to consider different ice features and their action on the structure. These issues are now briefly reviewed concerning the particular conditions in the Baltic region. There are no icebergs or multi-year ice in the Gulf of Bothnia, so these features will not be considered here.

The Norströmsgrund lighthouse is situated in the transition zone between the land-fast ice and the high dynamic drift ice of northern Bottonviken. The land-fast ice is characterized by very slow drift motion and can be considered as a static feature. Loading from the static forces are of low order and generally negligible compared with other types of ice features.

The main features of the ice cover at the lighthouse region are level ice, rafted ice and ridges. The level ice is formed by uniform freezing of the upper layer of the sea water. Hence this feature is characterized by small variation in the ice thickness. In the region where the lighthouse is situated, the typical level ice is $0.4 - 0.6\,\mathrm{m}$ thickness.

Due to flaws in the ice sheet and thickness differences in adjacent ice floes, the rafted ice might achieve 1 m thickness and more. When the rafting process is occurring, there is great compression within the ice sheet. Moreover, due to the highly dynamic situation, hummock

ice fields and pressure ridges are frequently present. In addition to the natural ridges, the artificial ice formations are common. They are usually created by leads from lighthouses, ships and icebreakers which were closed due to the wind stress.

It appears that the common failure scenarios at the site are crushing, bending and splitting. The observations showed that the prevailing mode is crushing. The similar phenomenon is also noted in Johnston et al. (1998). The cases analysed in this project were chosen by this criterion.

7.2 Instrumental site and measurements

7.2.1 Norströmsgrund lighthouse

The main ice force measurements were conducted at the Norströmsgrund lighthouse (Fig. 7.1) in the northern part of the Baltic Sea. It is located at position 65°6.6′ N and 22°19.3′ E about 35 km in an subarctic region southeast of Luleå at the edge of the land-fast ice of the Swedish coast and the drifting ice in the northern part of Bottenviken (Jochmann and Schwartz, 2000). Fig. (7.2) shows the location of the lighthouse. The water depth at the location is about 13 m depending on season. The lighthouse has an overall height of 42.3 m, 9 levels and a helicopter platform on top (during wintertime the lighthouse can be reached only by helicopter). The data collection equipment is installed on level 7. Level 8 is used as a storage place, while on level 9 living quarters were built. Entering of the lighthouse is possible at level 4 and level 9. At the waterline the lighthouse is equipped with a polygon steel shield of 20 segments. The diameter at the waterline, including the load measuring panels, is 7.52 m.

7.2.2 Climate conditions in the Baltic Sea area

As usual, offshore installations at sea have to sustain severe environmental loading. All equipment must be corrosion resistant to withstand the impact of salty seawater and spray. Waves hitting offshore structures (Fig. 7.3) can create very high instantaneous forces. Temperature differences between summer and winter in the northern Baltic Sea can reach 70°C and more, and pose additional stress on materials.

As it was mentioned above during normal winters, the Norströmsgrund lighthouse is located in the transition zone of land-fast ice and the high dynamic drift ice. The keel depth of the ridges in the area often exceeds 6 m. This depth causes grounding of the ridges on the caisson of the lighthouse.

Following warming in the late winter and spring season the ice breaks up and is transported by currents and wind throughout the area. At this time one can frequently encounter ice free periods, shortly afterwards strong ice drift and once again low drift and even no ice drift. This is the most interesting period for the measurements as then the most variable forces are found under different ice conditions and thus interesting scenarios occur when ice hits the lighthouse.

Figure 7.1: Norströmsgrund lighthouse (Photo: Luleå University of Technology).

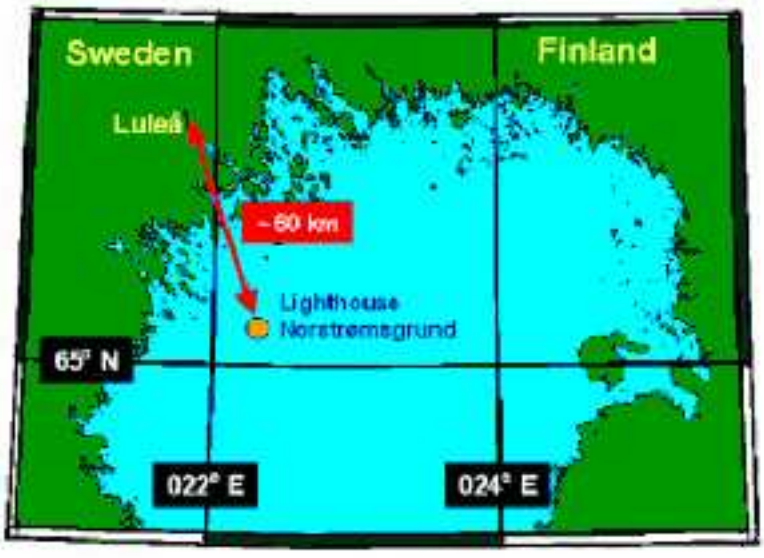

Figure 7.2: Map of a location of the lighthouse Norströmsgrund.

Ice conditions in natural waters are very variable. Fig. (7.4) gives a brief presentation of this.

Figure 7.3: Panels in waves (Photo: Luleå University of Technology).

The above-mentioned forces and actions cause very variable ice conditions and formations with corresponding heterogeneous mechanical and physical properties. The upper left photo in Fig. (7.4) shows a piece of packed ice with rubble in the front and relatively thin areas of recently frozen open water. The upper right photo displays the track of an icebreaker that visited the lighthouse. The channel is filled with broken ice (rubble) which is already freezing together again. The lower left photo shows some cracks in a piece of ice which hit the lighthouse before the ice came to rest - also note the formation of very thin plain ice at the sheet edge formed due to freezing of open water. Cracks typically form before the ice fails and breaks when hitting a structure, but also when ice sheets collide or when a ship moves through ice. The lower right photo shows the formation of ridges and plates which were frozen together again and thus form closed ice cover.

7.2.3 Instrumentation

The lighthouse is equipped with different types of sensors and a video observation system to determine the ice forces acting on the structure, document the force parameters and describe the ice structure interaction process.

Figure 7.4: Ice formation (Photo: Luleå University of Technology).

Ice force measuring system

Fifteen rigid ice force sensing panels were installed at the lighthouse. They were mounted on the polygon steel shield using special designed and manufactured clamping pieces at the waterline of the structure. The panels were designed to measure ice loads with maximum estimated pressure of up to 3 MPa. Each panel accommodates sensors (load cells) which measure the ice pressure. The sensors were individually adjusted and calibrated and mounted in a watertight steel case. Each panel has a size of approximately 1.2 m by 1.6 m and a weight of about 3.5 tonnes.

Two different kinds of panels were used, both are completely watertight. Eight large panels, each equipped with 4 load cells, were installed around the basement of the lighthouse "looking" in the direction from which the most probable ice drift can be expected. The linearity error of the load cells is smaller than 0.1% within the measurement range. The linearity error of the total panels was found to be better than 2%. The eight smaller panels are assembled in one segmented panel of almost the same size as the other panels. This arrangement covers an area of 162 degrees, the direction of ice-attack from North to South-South-East (Figs. 7.5-7.6).

Measuring of ice forces on the panels installed at the lighthouse (Fig. 7.7) was one of the key field activities in the LOLEIF and STRICE projects. Very large amounts of data were registered by the panels equipped with a total of 32 load cells. The evaluation of gigabytes of registered data to seek and identify interesting and relevant events comprised extensive work.

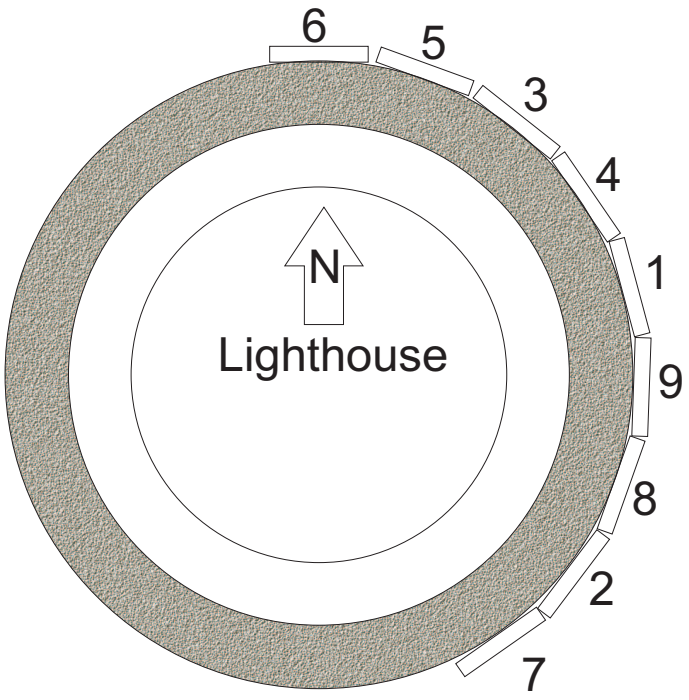

Figure 7.5: Panel arrangement (plane).

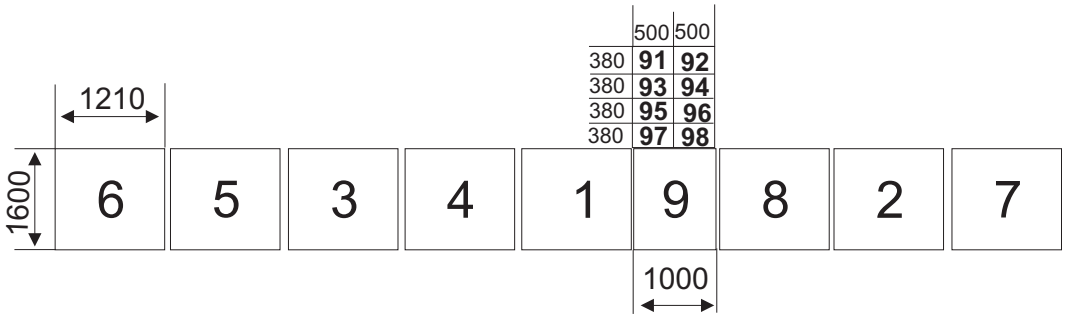

Figure 7.6: Panel arrangement (front).

The loads cells are connected via a cable connection box placed at the first level of the lighthouse with the front end measuring system Spider 8 consisting of carrier amplifiers, filters and ADCs. Eight units can be a cascade leading to a total amount of 64 channels - the channels are scanned by the 16 bit ADC simultaneously with a maximum frequency of 9600 Hz. During the measurement at the lighthouse the scanning frequency was set to 1200 Hz. The cut off frequency of the low pass filter, Bessel characteristic, was 150 Hz.

Video observation

Two video cameras placed in heated weather housing were mounted to the reeling of the north and south balcony (Fig. 7.8). Cameras were mounted to observe the ice features and calibrated to measure the ice velocity.

Figure 7.7: Panels installed at the lighthouse (Photo: Luleå University of Technology).

A third camera placed at the highest balcony, mounted to a pen and tilt head and equipped with an electronic lens picked up the overall ice situation and could be focused on special ice features or ice structure interaction events. All video signals were distributed to a multiplex unit, recorded in time lapse mode on a long time video recorder and monitored on a TV-screen. Existing lights were rearranged and new lights installed to make video observation possible during night time.

Ice thickness measurements

Two different methods were applied to determine the thickness of the ice interacting with the lighthouse. Method 1 uses a low range upward looking echo sounder, type *Mesotech MS 808A*, mounted underwater by a driver team in north-east direction about 5 m away from the panels on the concrete caisson in about $6 - 7$ m water depth. This transducer profiles the subsurface of the ice cover while the ice sheet is passing. The main technical information is listed below (Jochmann and Schwartz, 2000):

- Frequency 200 kHz
- Transducer Beam 10° Cone
- Max. Range 30 m
- Resolution 8.4 mm

Figure 7.8: Camera mounted on reeling (Photo: Luleå University of Technology).

The surface of ice cover is profiled by a laser scanner system, type *Sick LMS 210*, mounted at the upper balcony of the lighthouse using aluminium pipes. The beam of this laser is focusing on the same point as the echo sounder. The maximum range of this device is 50 m while the resolution is better than 50 mm. Method 2 uses the electromagnetic induction principle. The method as well as the installation and calibration procedure is reported in LOLEIF report No.9 (Jochmann and Schwartz, 2000).

The further evaluation, analysis and adequacy of ice thickness data is reported in Haas and Jochmann (2003).

7.2.4 Meteorological data measurements

Meteorological conditions in the Gulf of Bothnia were recorded at the pilot-station at Marjaniemi. This area has practically neither tide nor currents. Only in storm surge the water level can rise. The maximum at Marjaluoto has been 1.8 m in the summer and 1.2 m during the winter, while most of the sea is covered. Ice movements are caused by winds. During the wintertime, winds over 30 m/s are extremely rare. Temperatures during the winter can drop well below 30°C, normally a few weeks with temperatures around −25°C

Table 7.1: Statistical properties of air temperature and pressure during the measuring campaigns 2001-2002.

Period	26 Feb - 10 Apr 2001	19 Feb - 11 Apr 2002
Mean T_{air}, °C	-5.7	-2.3
Std T_{air}, °C	5.7	4.5
Max T_{air}, °C	0.6	8.5
Min T_{air}, °C	-18.6	-13.9
Mean P_{air}, hPa	1005.3	1004
Std P_{air}, hPA	7.7	19.1
Max P_{air}, hPa	1020	1038
Min P_{air}, hPA	987	962

are common. The water salinity is low, from 0 to 6 ppt. There are several rivers discharging to Gulf of Bothnia. They bring cold fresh water that is stratifying under the ice cover and can build strong ice with zero salinity at the bottom of the level ice. The software packages Diadem and MATLAB were used for data collection, analysis and presentation. The single loads of each load cell, four for one panel, were collected and stored together with the time channel as raw data in binary format on the hard disk of the data collection computer.

Air temperature and pressure

The sensor of a digital thermometer was installed at the outside North wall of the level at height about 20 m above sea level. The display of this sensor was located in the measuring room of the lighthouse. The main characteristics of temperature and air pressure during two measuring campaigns in the period February to April are showed in Table 7.1. 4-hour measurements (solid line) and daily mean (dashed lines with markers) of air temperature and pressure are plotted in Figs. (7.9-7.10). As it is seen from the table and figures the mean winter February-April Temperature is increasing.

Wind speed and direction

A wind speed and direction indicator was installed on the helicopter deck of the lighthouse about 28 m above sea level. The display of this sensor was located in the measuring room of the lighthouse. Figs. (7.11-7.14) represent the plots of wind speed and direction accordingly versus date. In the rose diagrams 0° corresponds to the North and 90° is to the East. The wind pictures for the winters 2001-2002 are similar with the most frequent winds from the North, East and South-West and speed of less than 10 m/s.

Ice drift velocity

The ice drift speed and direction was determined by manual image analysis by the video pictures. A $10 \times 10\,\mathrm{m}^2$ grid was marked on the ice, recorded and painted on the video screen.

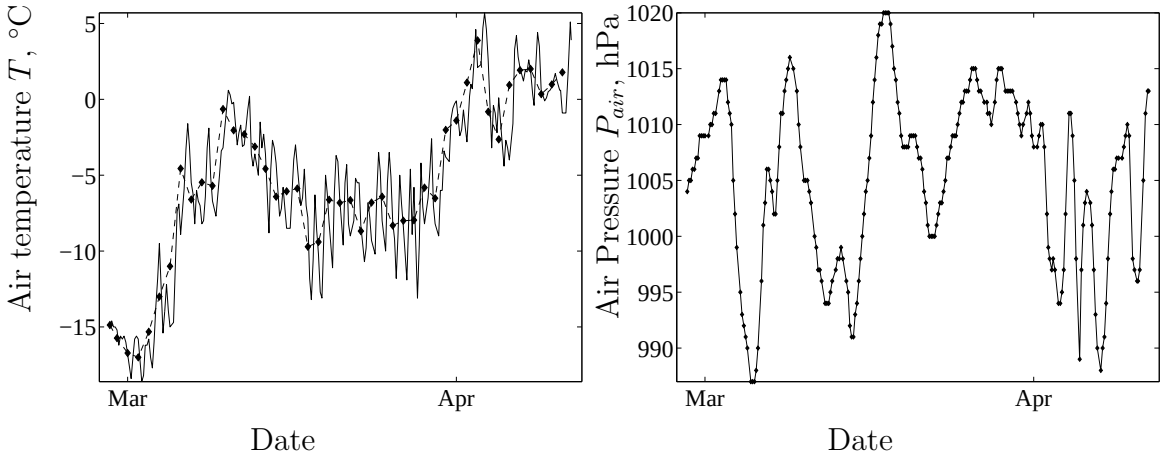

Figure 7.9: Air temperature and pressure, 2001.

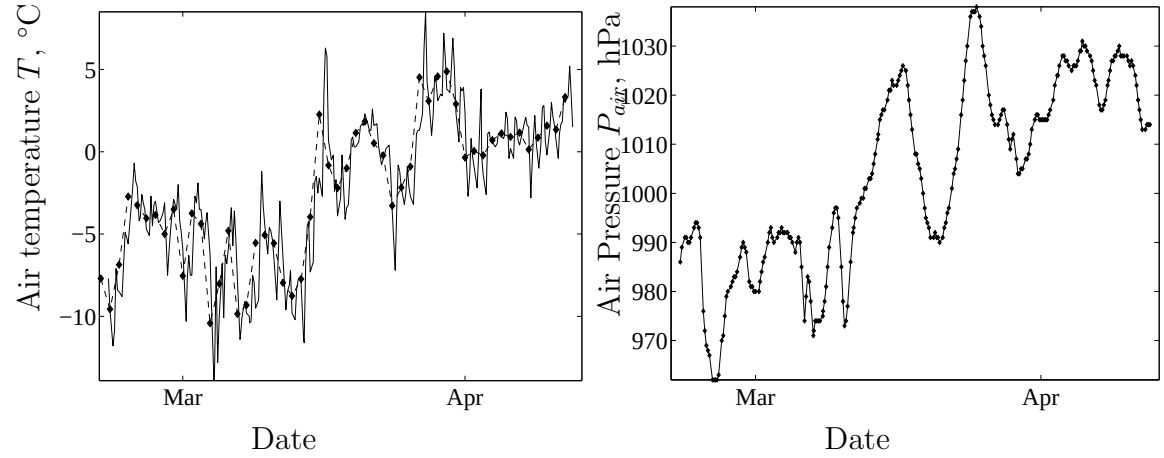

Figure 7.10: Air temperature and pressure, 2002.

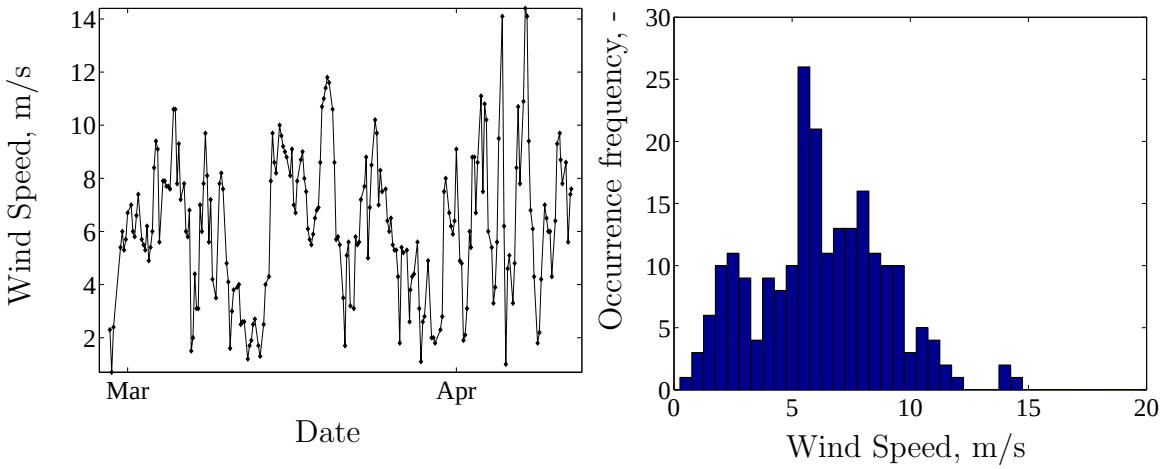

Figure 7.11: Wind speed, 2001.

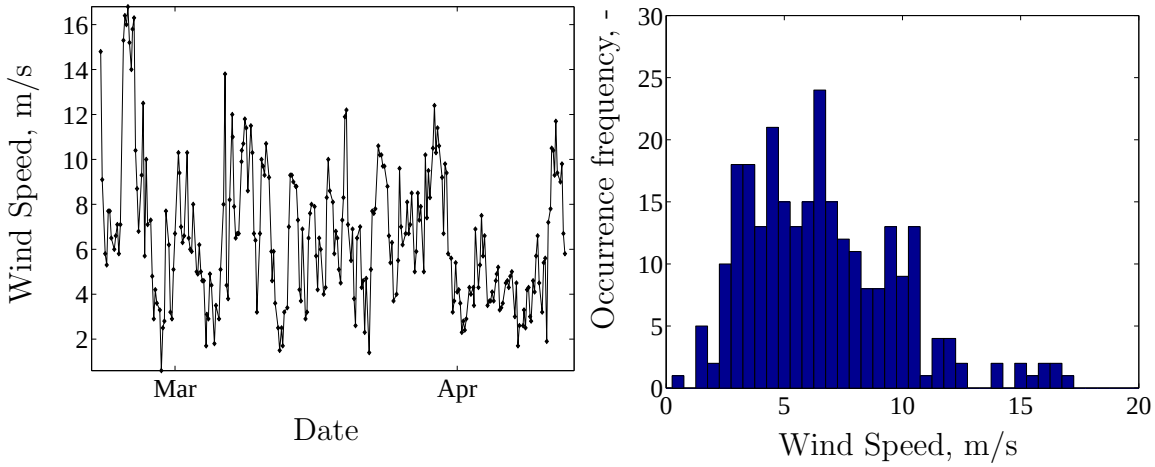

Figure 7.12: Wind speed, 2002.

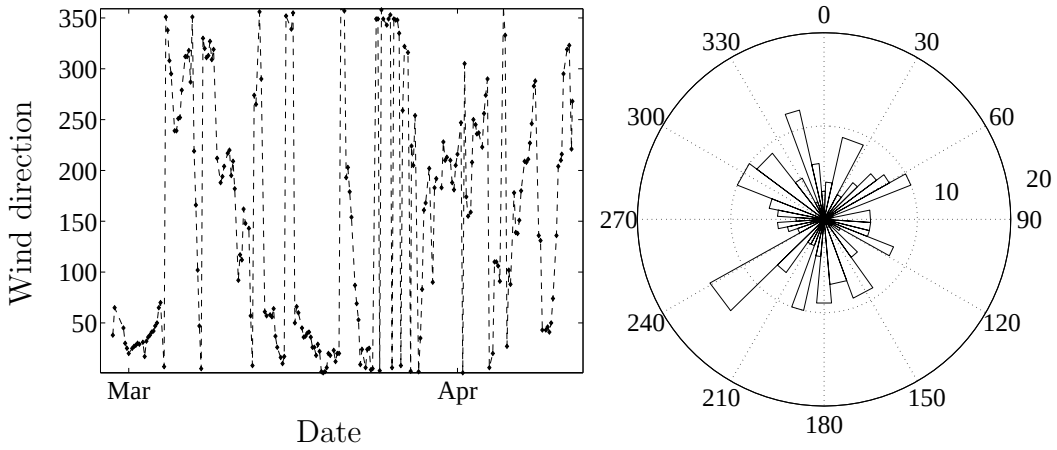

Figure 7.13: Wind direction data and rose diagram, 2001.

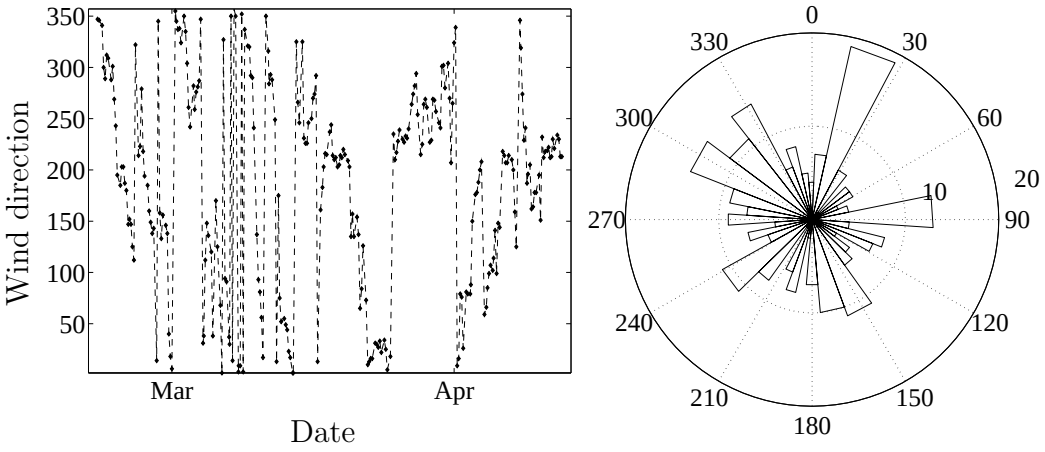

Figure 7.14: Wind direction data and rose diagram, 2002.

Ice drift speed and direction were determined by following single significant ice features passing the grid lines. A mean speed value was calculated from the observed distance and measured time. The results are documented in the logbook. Figs. (7.15-7.18) represent the plots of ice drift speed and ice drift direction accordingly versus date. The measured ice drift velocity is in the range $0 - 0.6\,\mathrm{m/s}$. For winter 2002 the prevailing ice drift direction is South-West, which unfortunately produced a small amount of data because the measuring panels are facing North to South-East.

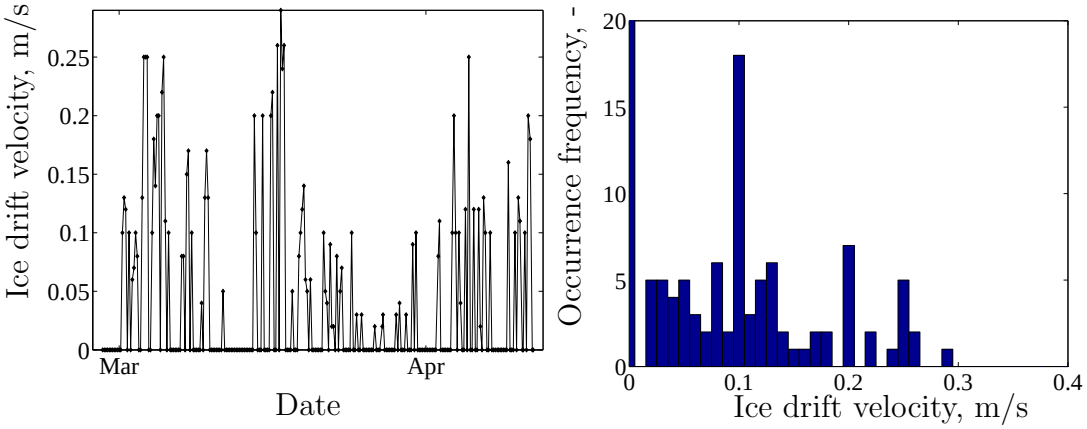

Figure 7.15: Ice drift velocity, 2001.

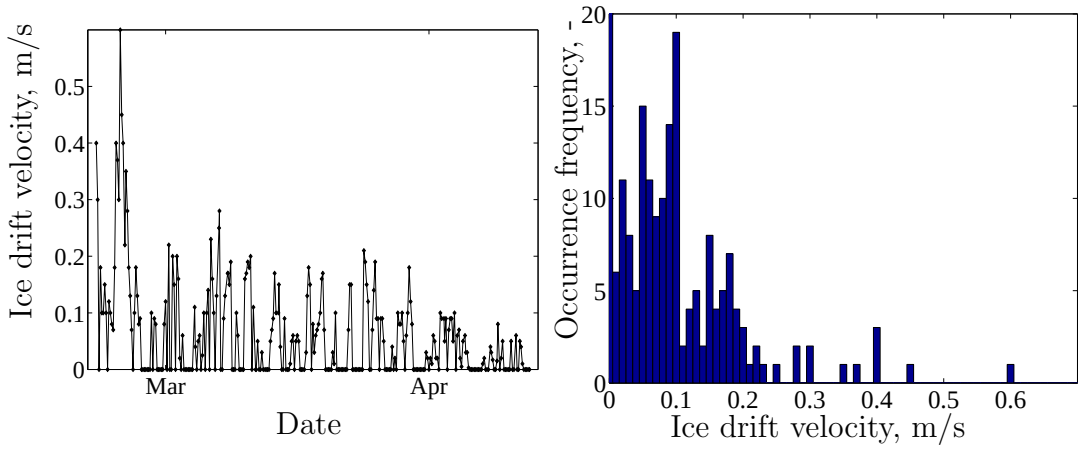

Figure 7.16: Ice drift velocity, 2002.

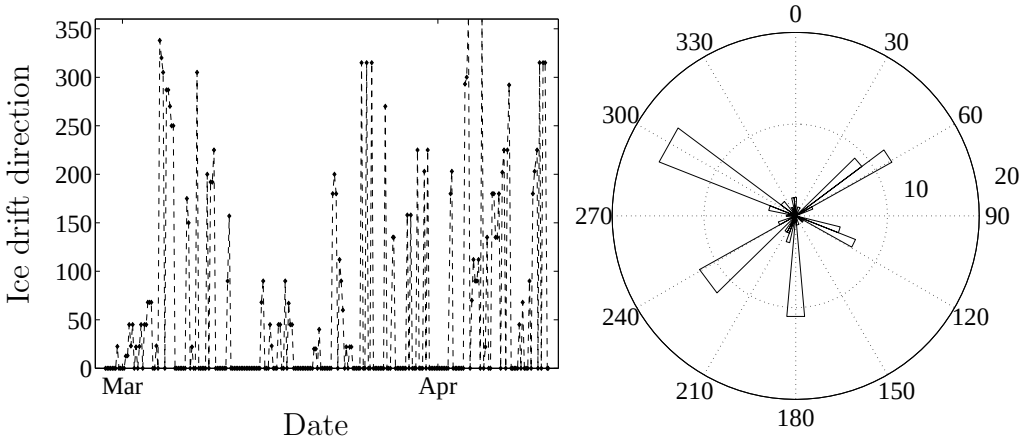

Figure 7.17: Ice drift direction data and rose diagram, 2001.

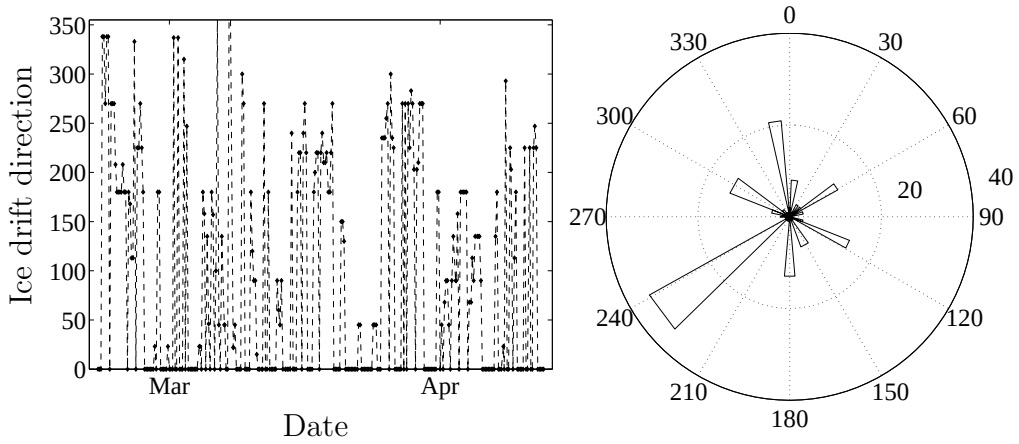

Figure 7.18: Ice drift direction data and rose diagram, 2002.

7.2.5 Calculation of global loads

This section is from Bjerkås et al. (2003). The authors suggested the following methodology to assess the global loads on the structure. Since the load measuring panels cover a cylindrical pile only partly, then some assumptions have to be made in order to estimate those loads. Firstly, the observed ice drift direction θ_{obs} is correct and unchanged during the event of interest. Secondly, the ice cover acts on exactly the half cross-section perimeter of the cylindrical structure. Thirdly, only normal forces are taken into account, the shear stress between ice sheet and structure are neglected.

The ice drift direction angle θ is calculated from the North where the x axis points. Thus North-West direction defines (x, y)-coordinates. The new $\xi - \eta$ coordinates change with the ice drift direction, where axis ξ points towards the direction θ. Each panel covers α° (18°) of the perimeter. It is assumed that the drift direction is the multiple of α and it crosses in

the middle of the panel. Hence the drift direction is given by

$$\theta = \alpha \cdot n, \quad n \approx \frac{\theta_{obs}}{\alpha}. \tag{7.2.1}$$

For convenience, the numeration of the panels in the new coordinates is altered so that panel 1 faces in the ξ direction. On its left there are even-numbered panels and on its right odd-numbered ones, looking from above. There are 9 panels all together. In the new numeration the normal and shear components of the force is given by

$$F_\xi = \sum_{i=2}^{5} \cos((i-1)\alpha)(F_{2i-1} + F_{2i-2}) + F_1 \qquad [\alpha = 18^\circ] \tag{7.2.2}$$

$$F_\eta = \sum_{i=2}^{5} \cos((i-1)\alpha)(F_{2i-1} - F_{2i-2}) = 0 \qquad [\alpha = 18^\circ]. \tag{7.2.3}$$

Although the shear force F_η as it was mentioned above cancels out due to symmetry.

Thus, the global force F_g is given by

$$F_g = F_\xi. \tag{7.2.4}$$

To estimate the zones where the force measurements are not available due to the existing panel installation the mirroring technique and interpolation/extrapolation along the cosine distribution curve is used (Bjerkås et al., 2003).

Further calculations of the global load are made according to this scheme.

7.3 Correlation

In the literature on ice crushing, effective pressure is defined as the total interaction force divided by the contact area, which is usually taken to be the product of structure width and ice thickness. Sanderson (1988) attributed the trend of decreasing effective pressure with increasing contact area to non-simultaneous failure of ice. Sodhi (1998) in his work referred the decreasing of the effective pressure to the dependence on the ductile and brittle modes of failure which are affected by the indentation speed. One of the main goals of this section is to verify these results on data obtained from the Norströmsgrund lighthouse. The other objective is to estimate the correlation effects on local force during the indention process of ice loading.

Furthermore, Sodhi (1998) proposes a correlation model for the indentation process. He saw a definite effect of indentation velocity on the mode of deformation or failure that takes place within the ice sheet. Let a random function $f(x,t)$ be a local force per unit width of the structure at a point x at a time instant t. Then the global force on the structure is given by

$$g(t) = \int_W f(x,t)dx. \tag{7.3.1}$$

In the Sodhi's experiments the indentor was flat. In the case of other surface types the projected coordinate along surface should be used.

Non-simultaneous failure will cause force variation not only with respect to time at a point, but also across the structure at any instant. The size of contact areas, or crushing zones, results in spatial correlation of local forces in the neighbourhood of a point on the structure. Assuming the failure process is the same across the width of the structure, we see that the expected (or average) local force per unit width is independent of the location of a point on the structure, implying

$$E[g(t)] = WE[f(x,t)]. \tag{7.3.2}$$

We can express the second moment in terms of the integral of the local force (Sodhi, 1998):

$$E[g^2(t)] = \iint_W E[f(x_1,t)f(x_2,t)]dx_1dx_2 = \iint_W R_{f(x,t)}(x_2-x_1)dx_1dx_2, \tag{7.3.3}$$

where $R_{f(x,t)}(x_2-x_1)$ is the auto-covariance function of the local force $f(x,t)$ caused by the random crushing process. Based on Dunwoody (1991), Sodhi proposes a spatial correlation function in terms of a negative exponential function:

$$R_{f(x,t)}(x_2-x_1) - (E[f(t)])^2 = \sigma^2_{f(t)} \exp(-|x|/L), \tag{7.3.4}$$

where x is the distance between points x_1 and x_2 on the structure, $\sigma_{f(t)}$ is the standard deviation of the local force per unit width and L is a correlation length, which has relationship to the size and the number of contact areas, or the crushing zones.

7.3.1 Results

From all available time series the crushing events were chosen (Table 7.7). The total resultant forces are calculated as summarized effect of all panel normal forces. The projections on x-axis (positive in East direction) and y-axis (positive in North direction) are obtained

$$F_x = \sum_{i=1}^{9} F_{xi}, \qquad F_y = \sum_{i=1}^{9} F_{yi}. \tag{7.3.5}$$

Thus the total force is given as

$$F_{tot} = \sqrt{F_x^2 + F_y^2}. \tag{7.3.6}$$

The global forces F_g are calculated by mirroring technique according to Bjerkås et al. (2003) described in Section 7.2.5.

The effective pressure was calculated by dividing the total resultant force F_{tot} by the contact area as follows

$$p_{eff} = F_{tot}/A. \tag{7.3.7}$$

For the whole structure the contact area A is calculated multiplying the projection of the circular shape of the lighthouse, being equipped with panels and contacted by ice, by the ice thickness as follows

$$A = D_{eff} \cdot h_I. \tag{7.3.8}$$

If the ice thickness exceeded the height of the panel, the water level was taken into account. Further the mean value μ_p with twice standard deviation σ_p of effective pressure p_{eff} will be used for comparison of different events.

The panel, total and estimated global forces from event 0203-091 are shown in Fig. (7.19). Frequency plots and empirical cumulative distribution functions (CFDs) are calculated for these forces (Figs. 7.20-7.23). The average values with corresponding standard deviations are plotted in Fig. (7.24). The ice drift direction is approximately 40°, corresponding to the direction which panel 5 is facing.

Table 7.2: Crushing events, 2001.

Event	Ice Thick. h_I [m]	Ice Forma-tion	Ice Speed [m/s]	Air Temp. [°C]	D_{eff} [m]	A [m^2]	Aspect Ratio D_{eff}/h_I	Mean p_{eff} MPa	Max p_{eff} MPa
0103-002	0.85	hummock	0.07	-16.2	7.20	6.12	8.47	0.059	0.265
0103-003	0.46	level ice	0.05	-16.0	7.48	3.44	16.26	0.207	0.493
0103-004	0.48	level ice	0.05	-15.8	7.48	3.56	15.70	0.255	0.476
0103-006	0.45	level ice	0.08	-16.0	7.48	3.37	16.62	0.258	0.441
0203-030	0.37	level ice	0.13	-17.2	7.48	2.79	20.08	0.345	0.683
0203-040	0.34	level ice	0.18	-16.8	7.48	2.58	21.71	0.330	0.543
0203-051	0.31	level ice	0.20	-16.4	7.48	2.30	24.35	0.366	0.519
0203-052	0.22	level ice	0.20	-16.4	7.48	1.61	34.68	0.523	0.740
0203-060	0.30	level ice	0.25	-15.8	7.48	2.22	25.23	0.365	0.801
0203-070	0.30	level ice	0.25	-14.4	7.48	2.24	24.99	0.305	0.681
0203-080	0.65	hummock	0.25	-13.8	7.48	4.86	11.51	0.266	0.593
0203-091	0.40	level ice	0.25	-13.0	7.48	2.96	18.89	0.314	0.520
0203-092	0.65	hummock	0.25	-13.0	7.48	4.86	11.51	0.177	0.529
0203-100	0.48	hummock	0.33	-12.6	6.13	2.95	12.73	0.122	0.579
0203-110	0.48	hummock	0.23	-11.8	7.20	3.44	15.07	0.247	0.734
0303-020	0.30	level ice	0.12	-15.2	6.13	1.83	20.49	0.382	0.752
0303-031	0.29	level ice	0.17	-11.0	6.13	1.76	21.39	0.385	0.852
0303-032	0.29	level ice	0.17	-11.0	5.36	1.54	18.71	0.437	0.971
0303-040	0.29	level ice	0.16	-14.0	5.36	1.58	18.21	0.319	0.792
0603-060	0.22	level ice	0.15	-7.0	6.13	1.35	27.92	0.936	1.638
0603-070	0.30	level ice	0.15	-7.0	6.75	2.03	22.50	0.674	1.165
0603-081	0.17	level ice	0.15	-7.3	6.13	1.03	36.41	0.193	0.883
0603-082	0.28	level ice	0.15	-7.3	6.13	1.72	21.89	0.857	1.544
0703-011	0.28	level ice	0.17	-8.2	5.36	1.50	19.14	0.608	1.221
0703-012	0.32	level ice	0.17	-8.2	5.36	1.72	16.75	0.502	1.044
0703-013	0.28	level ice	0.17	-8.2	5.36	1.50	19.14	0.479	1.224
1303-031	0.46	level ice	0.08	-3.9	7.48	3.48	16.10	0.056	0.289
1303-032	0.40	level ice	0.08	-3.9	7.48	2.97	18.87	0.034	0.279
1303-041	0.36	level ice	0.20	-2.2	7.48	2.68	20.87	0.028	0.396
1303-042	0.51	level ice	0.10	-2.8	7.48	3.82	14.66	0.027	0.182
1303-050	0.46	level ice	0.08	-2.9	7.48	3.42	16.37	0.030	0.265
1303-060	0.48	level ice	0.12	-2.7	7.48	3.59	15.58	0.205	0.819
1303-070	0.69	level ice	0.10	-3.2	7.48	5.17	10.82	0.052	0.319
1303-080	0.97	hummock	0.20	-3.1	7.48	7.26	7.71	0.079	0.229

Analysing the effective pressure versus the aspect ratio (Fig. 7.25), the obtained picture showed more scatter than the results obtained by Sodhi (1998). The data was divided in two

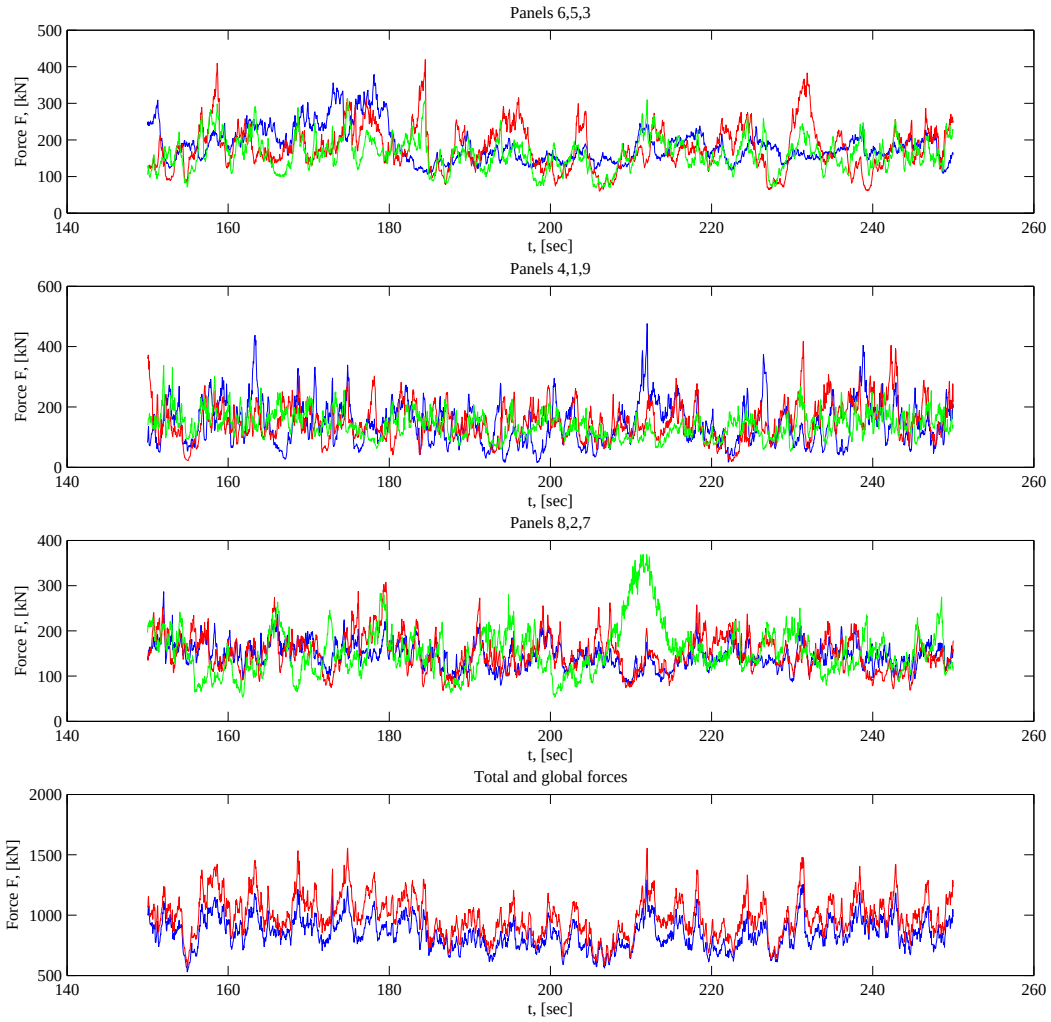

Figure 7.19: Local, total and global forces on the lighthouse, event 0203-091.

groups. The first group included the effective pressure values for the ice drift velocities V_I less than 0.1 m/s and the second group is for the values with ice drift velocities V_I greater than 0.1 m/s. Unlike Sodhi (1998), it was found that the lower ice drift velocity V_I produced lower pressure on the structure than the events with estimated ice drift velocity V_I greater than 0.1 m/s. Due to the large scatter it is difficult to establish the character of this relationship. The effective pressure $(\mu_p + 2\sigma_p)$ is shown versus the contact area in Fig. (7.26). A decreasing behaviour of indentation pressure with increase in the contact area is present. The effect of ice drift velocity is similar as for effective pressure relationship on aspect ratio. The events with low drift velocity are characterized by lower pressure than events with a higher drift velocity.

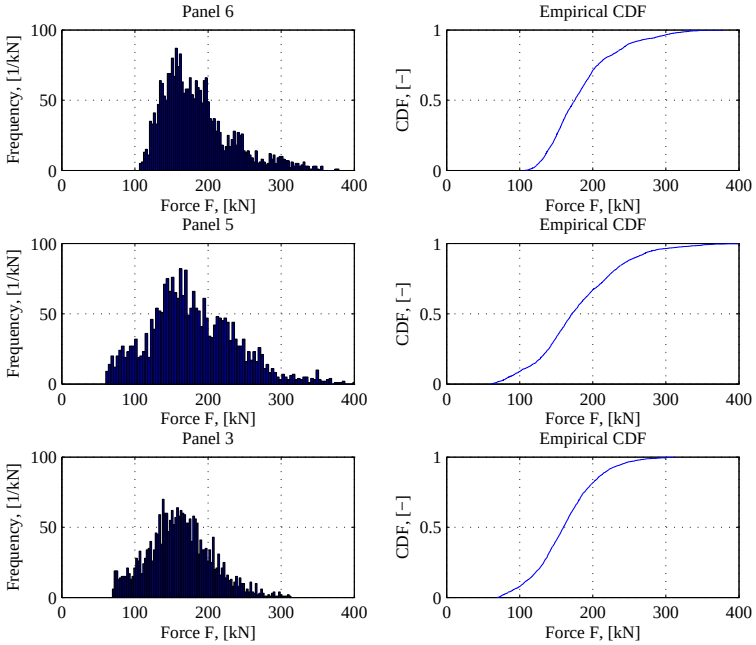

Figure 7.20: Histograms and empirical CFDs for panels 6,5,3, event 0203-091.

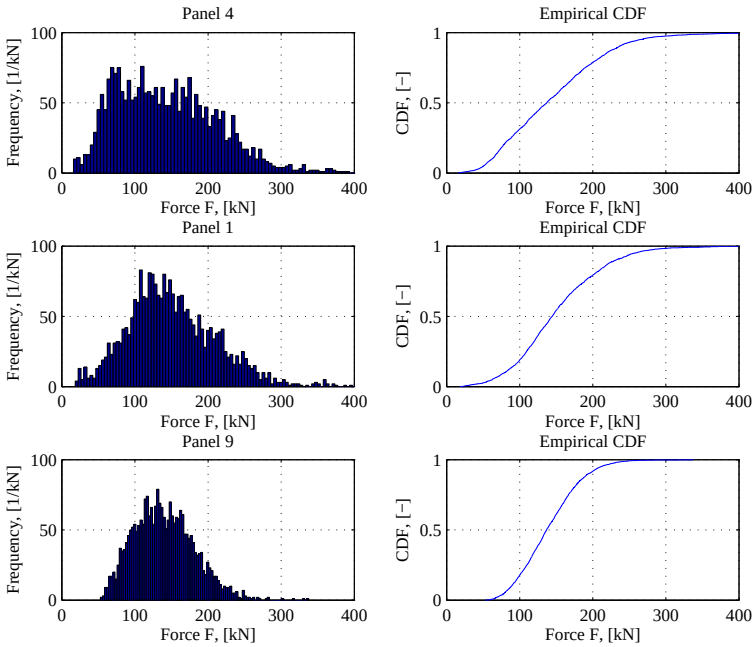

Figure 7.21: Histograms and empirical CFDs for panels 4,1,9, event 0203-091.

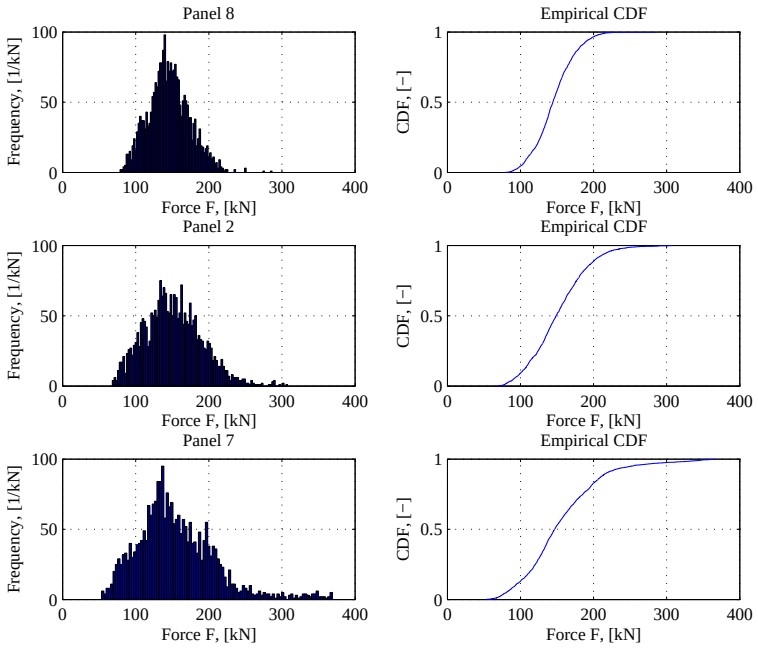

Figure 7.22: Histograms and empirical CFDs for panels 8,2,7, event 0203-091.

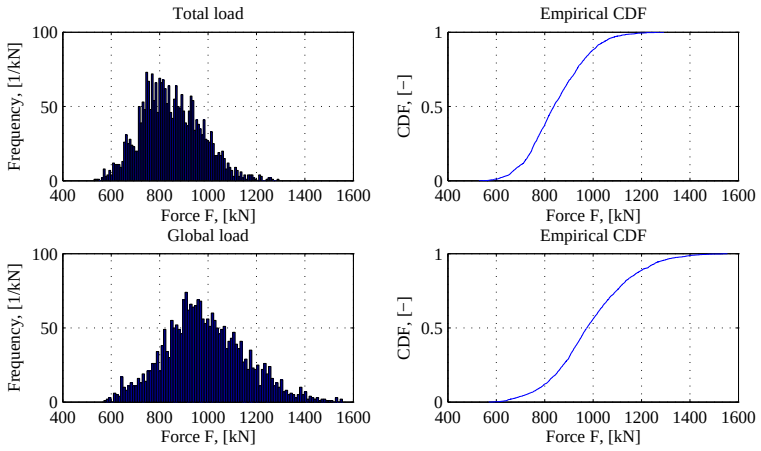

Figure 7.23: Histograms and empirical CFDs for total and estimated global forces, event 0203-091.

Considering the relationship of the effective pressure on the meteorological conditions, the dependencies on air temperature and wind speed are shown in Figs. (7.27-7.28). A high wind speed corresponded to the low effective pressure values, and again the events with lower ice drift velocity are characterized by the lower estimated pressure on the structure. In addition, a high air temperature caused a decrease in the effective pressure. Higher pressures were estimated for the events with the ice drift speed $V_I > 0.1\,\mathrm{m/s}$ than the events with velocities

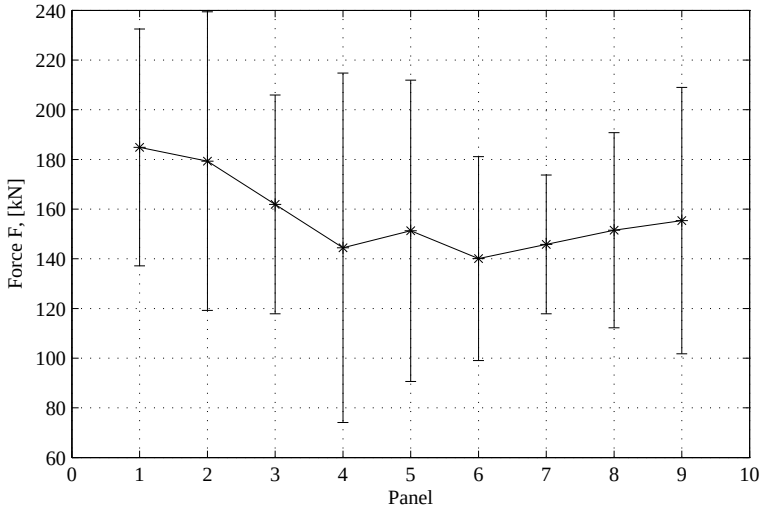

Figure 7.24: Mean values of panel forces with standard deviation, event 0203-091. Panel numeration is in natural order from North to South East clockwise, see Fig. (7.5).

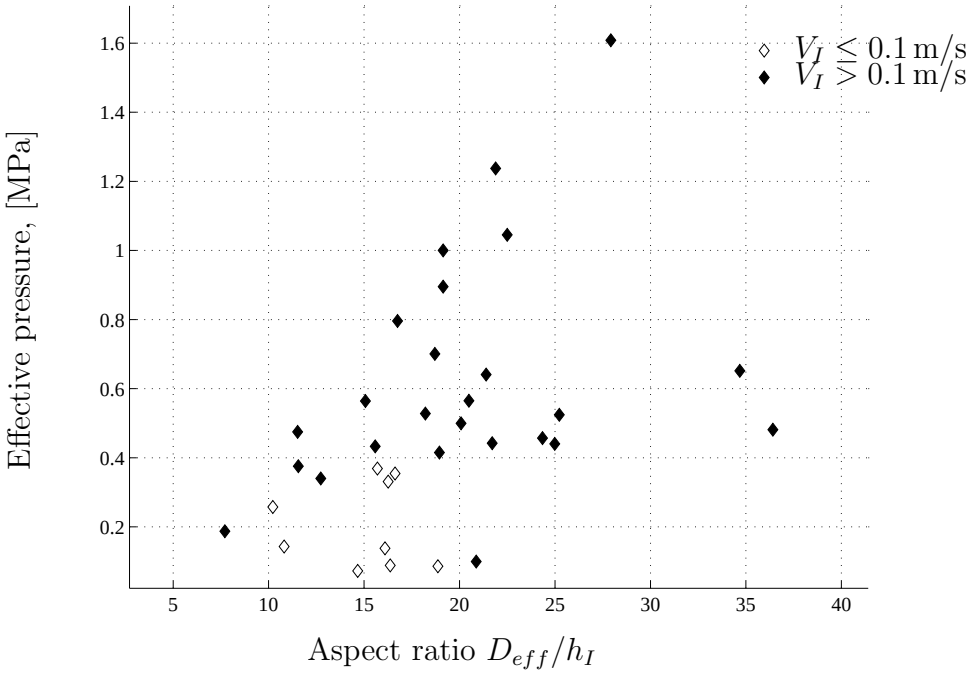

Figure 7.25: Effective pressure ($\mu_p + 2\sigma_p$) vs aspect ratio.

$V_I \leq 0.1\,\mathrm{m/s}$ at low temperature less than $-10^\circ\,\mathrm{C}$. The same relationship applies also for temperatures above $-10^\circ\,\mathrm{C}$.

Fig. 7.29 shows effective pressure dependency on ice drift velocity. This relationship corresponds well with results presented by Sodhi (2001). The decreasing behaviour of effective pressure versus ice thickness is shown in Fig. 7.30.

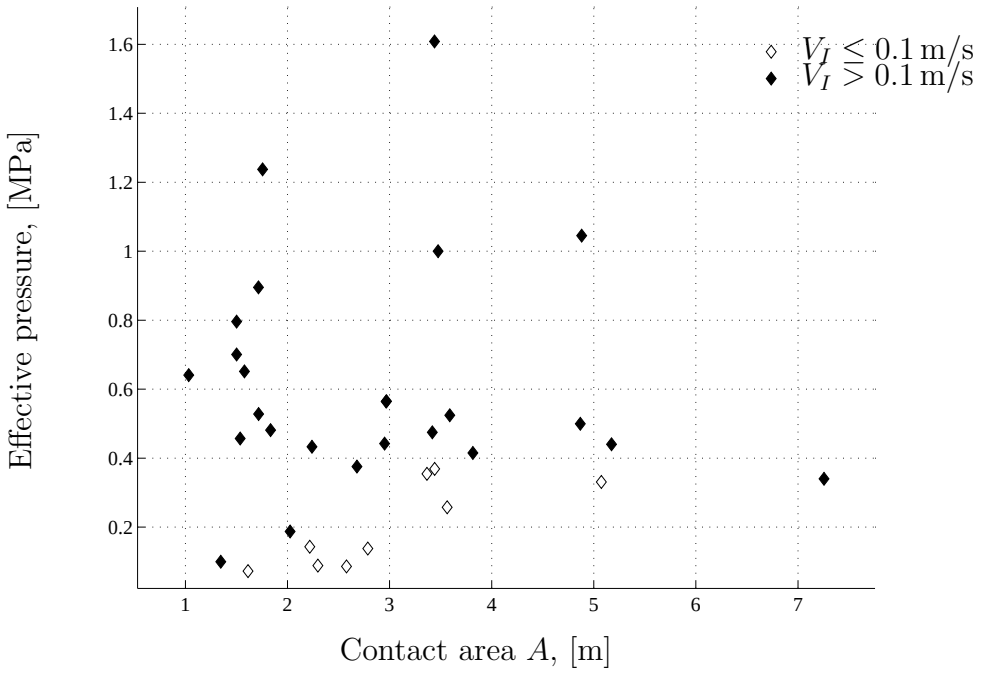

Figure 7.26: Effective pressure ($\mu_p + 2\sigma_p$) vs contact area.

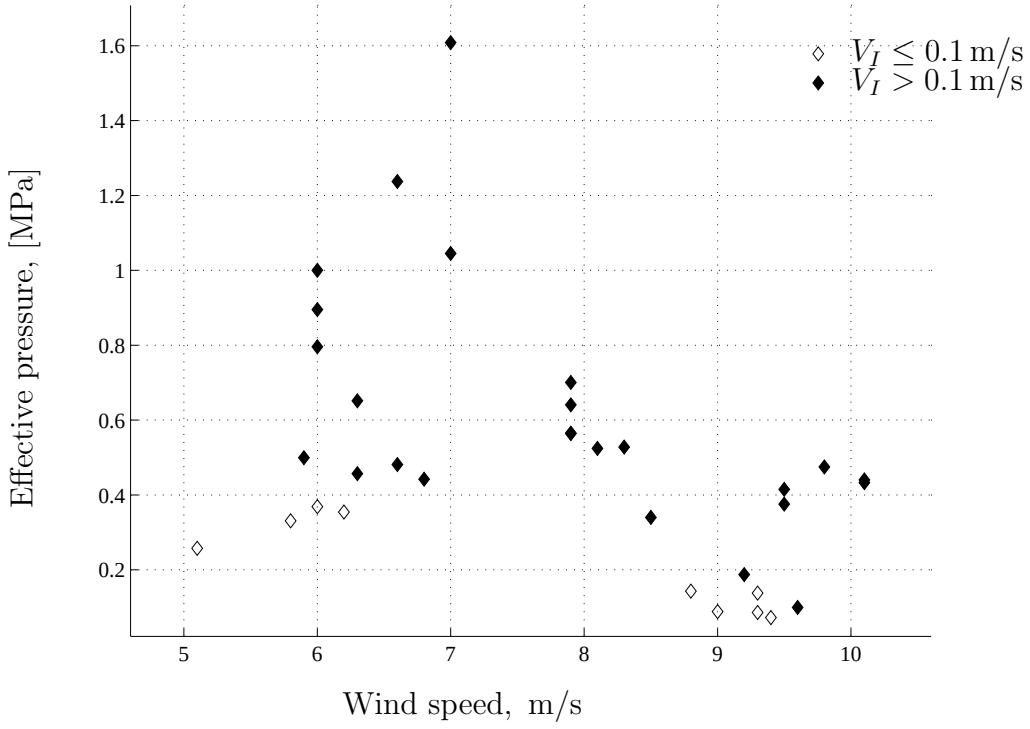

Figure 7.27: Effective pressure ($\mu_p + 2\sigma_p$) vs wind speed.

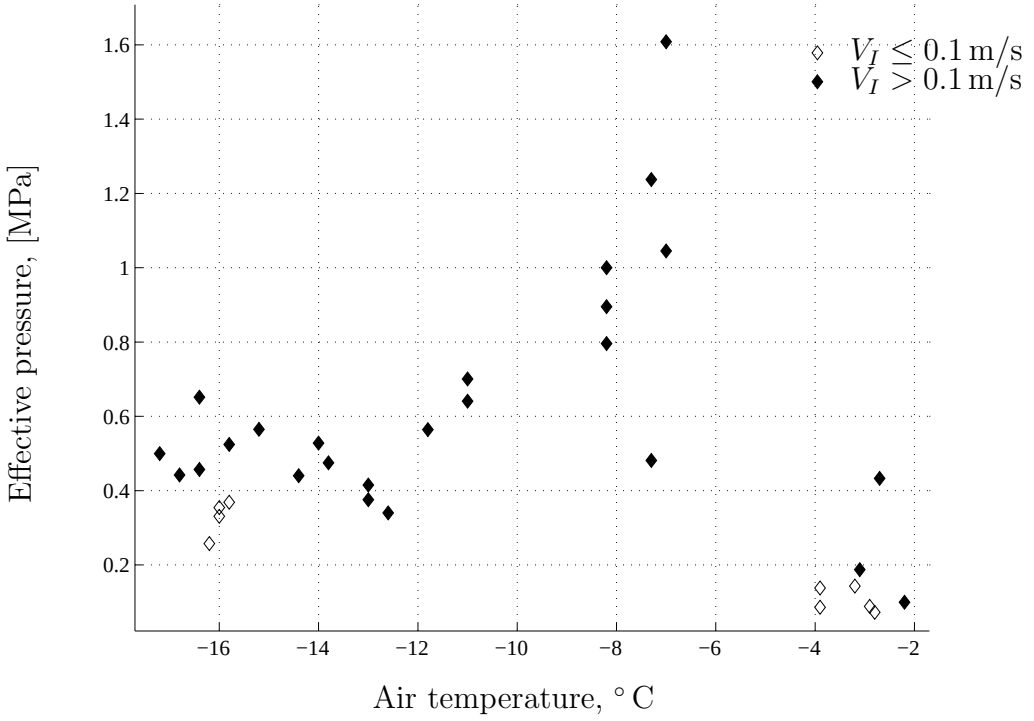

Figure 7.28: Effective pressure ($\mu_p + 2\sigma_p$) vs air temperature.

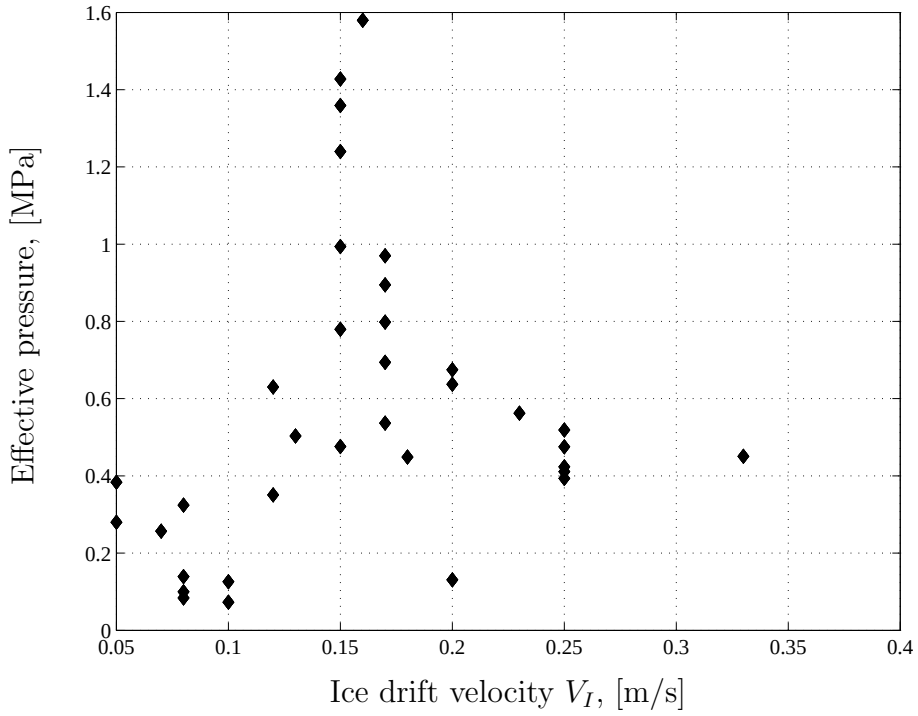

Figure 7.29: Effective pressure ($\mu_p + 2\sigma_p$) vs ice drift velocity.

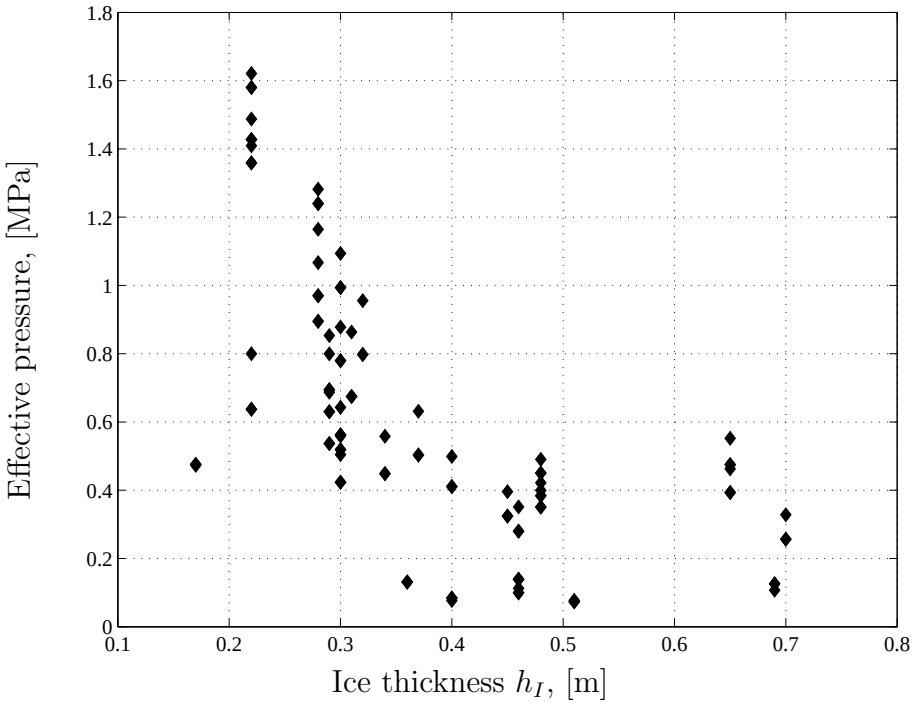

Figure 7.30: Effective pressure ($\mu_p + 2\sigma_p$) vs ice thickness.

Further the correlation of the local forces on the structure along the contact area is considered. The correlation coefficients are given by

$$\rho_{i,j} = \frac{Cov(p_i, p_j)}{\sigma_{p_i}\sigma_{p_j}} \tag{7.3.9}$$

where p_i is an effective pressure for the i^{th} panel and σ_{p_i} is a standard deviation of p_i. $Cov(p_i, p_j)$ is a cross-covariance of the effective pressures on the i^{th} and j^{th} panels. Stronger correlation between the panel forces corresponds to higher ice drift velocities (Sodhi, 1998). Fig. (7.31) shows correlation coefficients calculated for two events characterised by ice drift velocities $V_I = 0.05\,\text{m/s}$ (⧫) and $V_I = 0.16\,\text{m/s}$ (•) which correspond to minimum and maximum values of parameter L (Eq. 7.3.4).

Data for the characteristic length parameter versus velocity and air temperature are presented in Fig. (7.32) and Fig. (7.33), respectively. A least squares fit is shown as solid lines on both figures and given as

$$L(V_I) = 1.46V_I + 1.52, \qquad L(T_a) = 0.03T_a + 2.11.$$

In spite of highly scattered data, both fitted lines indicate that the characteristic length parameter shows a tendency for increase with increasing values of the drift velocity and temperature, although the increase with temperature is rather weak, which is caused by the two very large values at $-14°\text{C}$. Sodhi (2001) explains this increase by different fracture modes, changing from brittle crushing at low values of L to ductile crushing at large values of L.

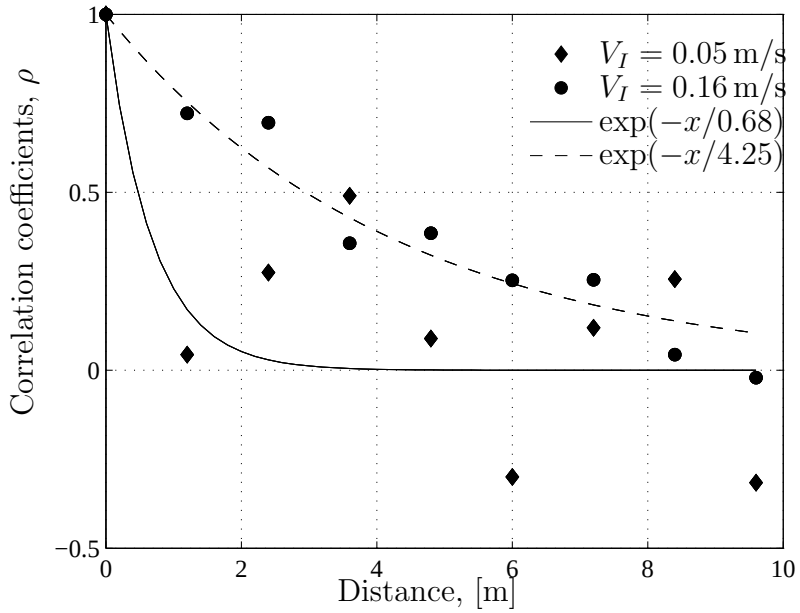

Figure 7.31: Correlation coefficients between local forces from the events, during which the estimated ice-drift velocity was 0.05 m/s and 0.16 m/s. Solid lines are the corresponding functions $exp(-x/L_i)$ fitted to these coefficients.

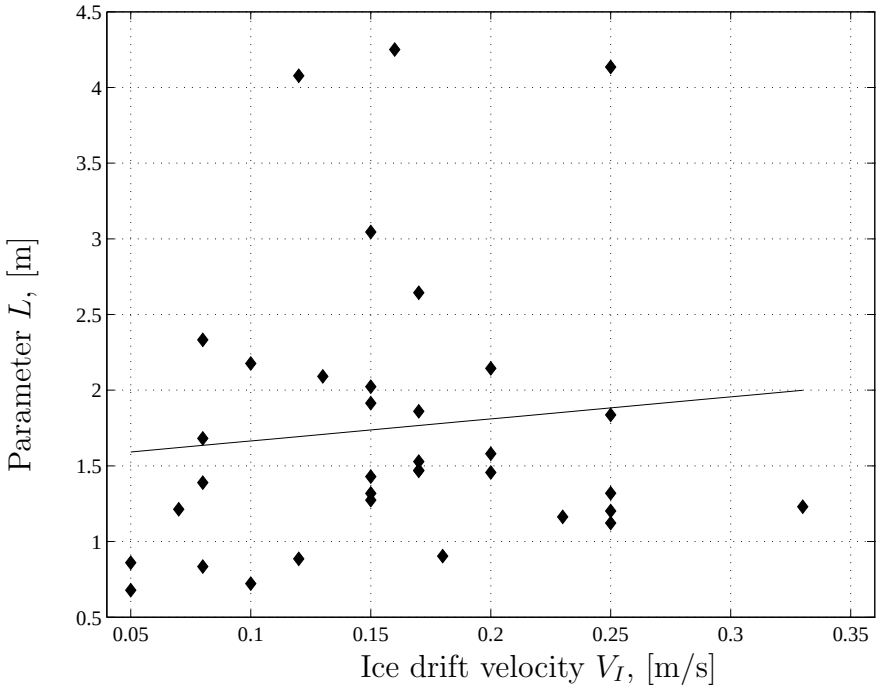

Figure 7.32: Correlation parameter L vs the ice-drift speed. The solid line is linear least squares fit to these data.

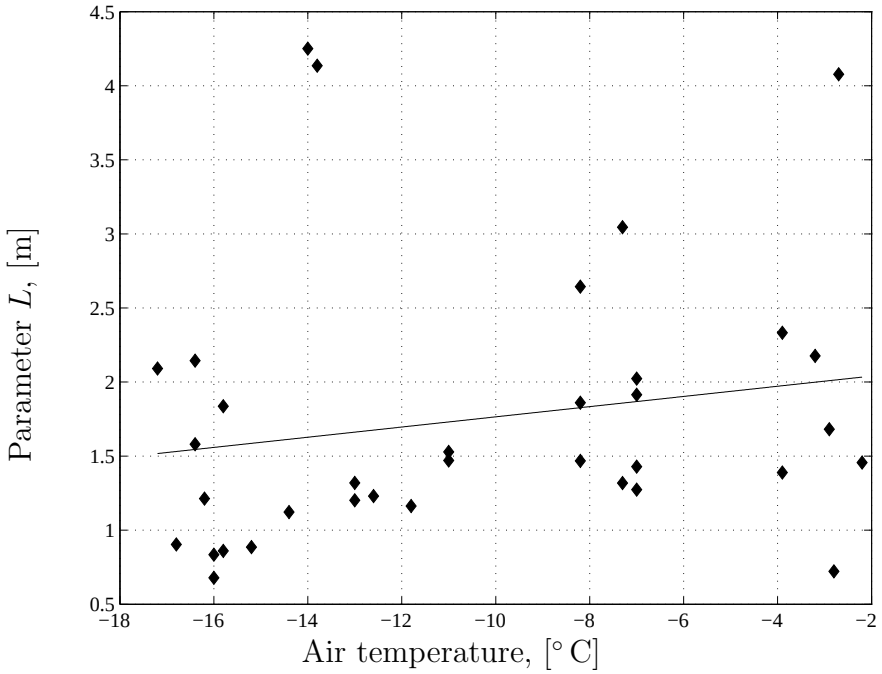

Figure 7.33: Correlation parameter L vs air temperature. The solid line is linear least squares fit to these data.

7.4 Extreme value distribution

The extreme probability distribution is one of the most important aspects of stochastic analysis in many engineering problems. Knowledge of this distribution for the appropriate process allows the analyst to calculate the probability that in this particular case, the ice force on a structure has exceeded some critical level during the time interval of interest.

Usually, as in wave and wind statistics, the annual extremes are used in order to estimate the design value. Unfortunately, in our case only five years of measurements are available, which is not enough to provide annual extremes. Thus it is assumed that the daily maximum ice load has an extreme value distribution which can be used afterwards to calculate the design value. Hence the events happened in two consecutive days are supposed to be independent. This is possible because of highly dynamic ice drift situation near the lighthouse. The new ice fields are entering the area at least once a day. This assumption was checked with the time series and logbooks of direct observations.

A simple way to formulate the extreme value problem is to define a new stochastic process $Y(t)$ which is the extreme value of $X(t)$, the original time series, during some specified period of time of length t. Specifically, we let

$$Y(t) = \max_{0 \le s \le t} X(s). \tag{7.4.1}$$

The extreme value distribution for $X(t)$ is then simply the distribution of the $Y(t)$ random variable. Letting $F_{Y(t)}(u)$ denote the cumulative distribution function of Y(t) gives

$$F_{Y(t)}(u) = P[Y(t) \le u] = P[X(s) \le u : 0 \le s \le t]. \tag{7.4.2}$$

The extreme distribution related to the original distribution of $X(t)$ is

$$F_{Y(t)}(x) = [F_X(x)]^n \tag{7.4.3}$$

where n is the number of data in the $Y(t)$ series, in our case n is the number of days. Therefore the different kinds of asymptotical extreme value distributions are developed over the years (generalized extreme value distribution GEV, Gumbel, Weibull and Pareto distributions, cf. Appendix C).

7.4.1 Return period and design value

The general procedure of statistical extrapolation on the basis of the limited set of extreme value data is to plot data on the probability paper corresponding to the considered distribution under the assumption that the experimental extreme value distribution converges to some known (for example, Gumbel, Weibull etc.) extreme value distribution. Then some sort of linear regression can be carried out in order to fit the data to the analytical expression. Within this approximation, an extrapolation may be needed in order to reach a desirable design value.

The extreme value distribution is intimately related to the mean upcrossing rate $\nu_x^+(t)$ of the original process $X(t)$ (Lutes and Sarkani, 1997). Moreover, if it is assumed that upcrossings of high levels for the original process are independent events (Poisson assumption, cf. Section 3.3), the extreme value distribution is given as

$$F_{Y(T)}(\zeta) = P[Y(T) \leq \zeta] = \exp\left(-\int_0^T \nu_x^+(t,\zeta)dt\right) \tag{7.4.4}$$

where the upcrossing rate $\nu_x^+(t,\zeta)$ can be evaluated in the general case by the Rice formula (Eq. 3.3.8).

Further, it is assumed that the mean upcrossing rate does not depend explicitly on time $\nu_x^+(t,\zeta) = \nu_x(\zeta)$, i.e. the underlying distribution is stationary (Mathiesen, 1991). Then the probability distribution is expressed as

$$F_{Y(t)}(\zeta) = \exp\left(-\nu_x(\zeta)t\right). \tag{7.4.5}$$

Since generally the distribution $F_{Y(t)}(\zeta)$ is unknown for any time period t, the extrapolation can be applied from the available short-term distribution. Let the chosen average duration $\tau = \tau(\zeta)$ between exceedings of the threshold level ζ and corresponding distribution $F_{Y(\tau)}(\zeta)$ be known then the average upcrossing rate $\nu_x(\zeta)$ is following

$$\nu_x(\zeta) = \frac{-\ln(F_{Y(\tau)}(\zeta))}{\tau}. \tag{7.4.6}$$

Finally, the return period R of interest, the time interval for the threshold level ζ to be exceeded on an average once, is now given as

$$R(\zeta) = \frac{1}{\nu_x(\zeta)} = -\frac{\tau}{\ln(F_{Y(\tau)}(\zeta))}. \tag{7.4.7}$$

Then the design threshold corresponding to the given return period $R(\zeta)$ is obtained as

$$\zeta(R) = F^{-1}_{Y(\tau)}\left[\exp\left(-\frac{\tau}{R}\right)\right]. \tag{7.4.8}$$

For example, if the extreme value distribution is chosen to be the Gumbel distribution, then the design value will be given by the Eq. (C.3.3) with parameters correspondingly estimated from the experimental data. For long return periods $R \geq 1$ year the common procedure has been to set the exceeding duration τ at a constant value typical for given area (about 20-24 hours). In our case τ is chosen to be $\tau = 1$ (day) thus the return period R is in days as well.

7.4.2 Results and discussion

In this section the various extreme value distributions are fitted to the daily maximum ice loads in order to estimate the design values by extrapolation. Extreme values for forces on panels and estimated global load are extracted from data files for each day of measurements in year 2002. As it was discussed in Section 7.2.5, the global load was estimated by mirroring techniques described in Bjerkås et al. (2003). The data were chosen so that the time between the two adjacent values is more than 12 hours (half of one day period) otherwise it was manually checked by the time series and logbooks that these extremes belong to the different events. In addition to prove the independence of the extreme values, the scatter plots for the global force with lags 1, 2, 3 and 4 days were plotted (Fig. 7.34). The values are normalized by the maximum load for the whole of 2002. Fig. (7.34) indicates that there is no obvious tendency in the scatter. Additionally the autocorrelation function (ACF) for global force was calculated (Fig. 7.35). All values lay inside the interval $\pm u_{\alpha/2}/\sqrt{n}$, where $u_{\alpha/2}$ denotes the value of the standard normal variable u with $P(|u| > u_{\alpha/2}) = \alpha$, $\alpha = 0.05$ is chosen in our case (Shumway and Stoffer, 2000). This proves also that the available daily maximum ice loads can be considered as independent.

Four discussed types of distributions are fitted to the data. The estimates for parameters of the Gumbel distribution for extremes of the extrapolated global load are given in Table 7.3 and the plot on the Gumbel paper is shown in Fig. (7.36). The goodness-of-fit test gave acceptance of initial hypothesis about Gumbel distribution at 99% significance level. The same methodology was implemented for estimating parameters for Weibull, GEV and GPD distributions (Tables 7.4, 7.5, 7.6 and Figs. 7.36, 7.37, 7.38). In order to estimate parameters for GEV distribution, two methods were used, namely, the method of maximum likelihood "ML" and the method of probability weighted moments "PWM". The ML method gives usually lower covariance in estimates, but it seems that the fitting curve for PWM method is closer to experimental data. For parameter estimation for the GPD, also two methods were used: the method of moments "mom" and the maximum likelihood method "ML". A description of the different statistical methods used, such as ML and PWM, will not be given here. All the calculations were performed in the Matlab program in toolbox WAFO http://www.maths.lth.se/matstat/wafo/.

Goodness-of-fit tests for all panels (1 to 9) had confirmed the hypotheses about the Gumbel distribution with probability of 99%. Results are given in Table 7.3 and distributions

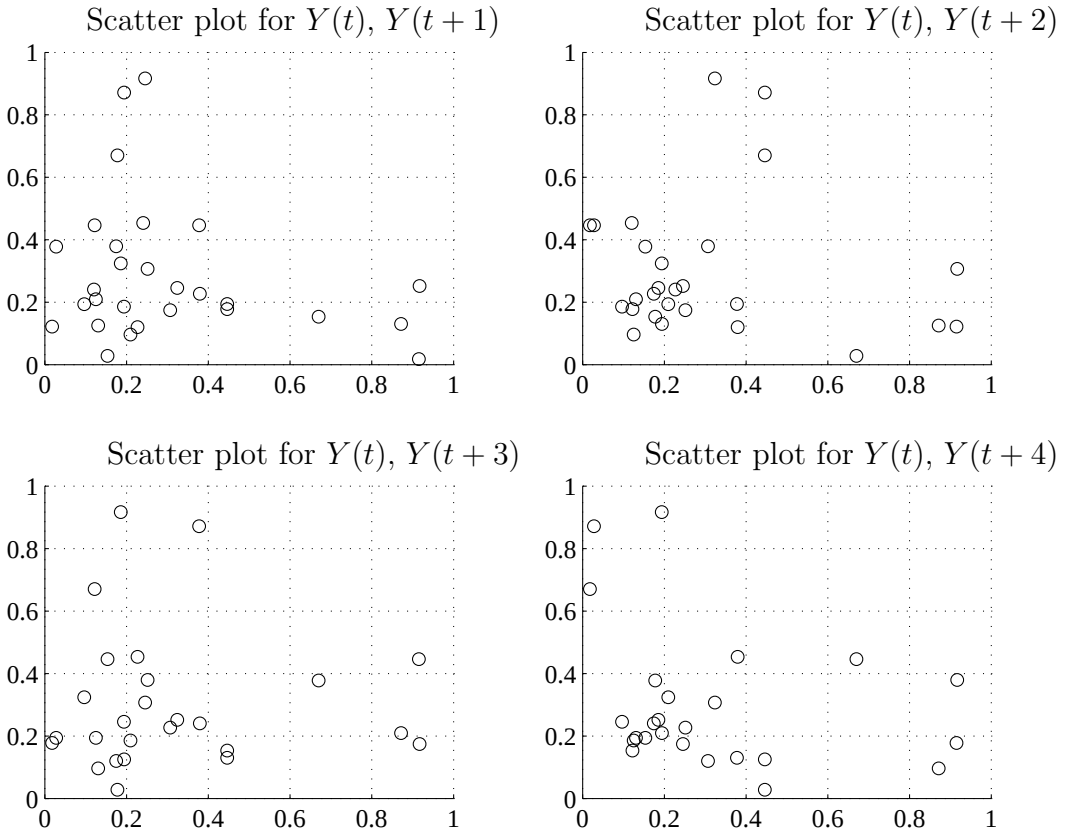

Figure 7.34: Scatter plots for global force with lag 1, 2, 3 and 4 days (data from 2002).

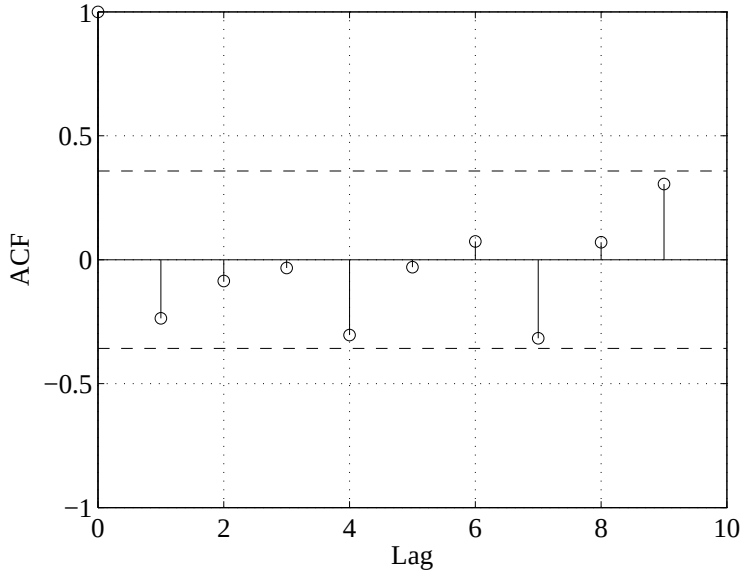

Figure 7.35: Autocorrelation function for global force (data from 2002).

plotted in Fig. (7.39). Parameters for the Weibull, GEV and GPD distributions were estimated (Tables 7.4, 7.5, 7.6 and Figs. 7.40, 7.41, 7.42, respectively). The PWM method was used for estimatition of the GEV parameters, and the Pickands' method was used for GPD parameters. It is remarkable that for the first panel the shape parameter k almost equals zero which confirms the hypothesis about the Gumbel distribution. Other parameters, location c and scale λ, have relative differences 6% and 2% correspondingly. It can be noticed that for other panels the shape parameter k differs from zero and has different signs even though the Gumbel test gave the positive results on acceptance of the null-hypothesis. Thus the shape of the probability distribution curve is changing, although the difference is not substantial. More data is needed in order to make a best choice between those two distributions.

Table 7.3: Estimated parameters for Gumbel distribution for global loads and panel loads.

	$1/\alpha$, kN	b, kN	$\alpha_{global}/\alpha_{panel}$	b_{global}/b_{panel}
Panel 1	240.15	213.97	0.25	0.17
Panel 2	236.45	171.68	0.25	0.13
Panel 3	253.83	198.8	0.27	0.16
Panel 4	263.01	252.8	0.28	0.20
Panel 5	281.53	288.23	0.30	0.22
Panel 6	228.81	235.89	0.24	0.18
Panel 7	189.23	129.4	0.20	0.10
Panel 8	154.77	108.52	0.17	0.08
Panel 9	207.97	139.64	0.22	0.11
Average	228.4167	193.2144	0.24	0.15
Global load	946.21	1280.1	-	-

Table 7.4: Estimated parameters for Weibull distribution for global and panel loads.

	u, MN	k, $-$	u_{panel}/u_{global}
Panel 1	0.278	1.033	0.14
Panel 2	0.169	1.22	0.09
Panel 3	0.192	1.97	0.10
Panel 4	0.323	1.19	0.16
Panel 5	0.383	1.24	0.19
Panel 6	0.348	1.02	0.18
Panel 7	0.250	0.89	0.13
Panel 8	0.261	0.92	0.13
Panel 9	0.422	1.20	0.21
Average	0.292	1.19	0.15
Global load	2.0797	1.3652	-

Table 7.5: Estimated parameters for GEV distribution for global and panel loads.

	k, $-$	λ, kN	c, kN
Panel 1	0.0060464	256.36	210.18
Panel 2	-0.16571	223.45	148.25
Panel 3	0.026921	269.04	201.28
Panel 4	0.18184	294.74	276.8
Panel 5	0.32253	323.65	335.94
Panel 6	0.23425	265.67	262.11
Panel 7	-0.13605	183.4	113.84
Panel 8	-0.15094	148.7	94.273
Panel 9	-0.21617	188.25	113.96
Average	0.011413	239.25	195.18
Global load (PWM)	-0.26887	807.89	1139.5
Global load (ML)	-0.23104	841.91	1170.4

Table 7.6: Estimated parameters for GPD distribution for global and panel loads.

	k, $-$	λ, kN
Panel 1	0.16243	414.56
Panel 2	-0.04866	305.01
Panel 3	0.086524	379.83
Panel 4	0.34061	537.98
Panel 5	0.49898	662.53
Panel 6	0.44703	527.33
Panel 7	-0.056631	233.94
Panel 8	-0.052634	195.13
Panel 9	-0.10962	243.29
Average	0.140892	388.8444
Global load (mom)	0.29173	2447.5
Global load (ML)	0.28905	2449.3

It is of interest to notice that scale factors between the distribution parameters estimated for load on panels and for global load are between $[0.1, 0.3]$ (Table 7.3). Meanwhile, the scale factor for panel width $w_p = 1.2\,\text{m}$ to diameter of structure $D = 7.52\,\text{m}$ is 0.16. The average scale factor for the location parameter b in the Gumbel distribution equals 0.15. For other distributions, the scale factor for panel loads and global loads is also comparable with this value. Unfortunately, the shape factor for the GEV and GPD showed large discrepancy between the individual parameters, and is thus questionable to compare.

For calculation of design values and comparison with other sources, the Gumbel distri-

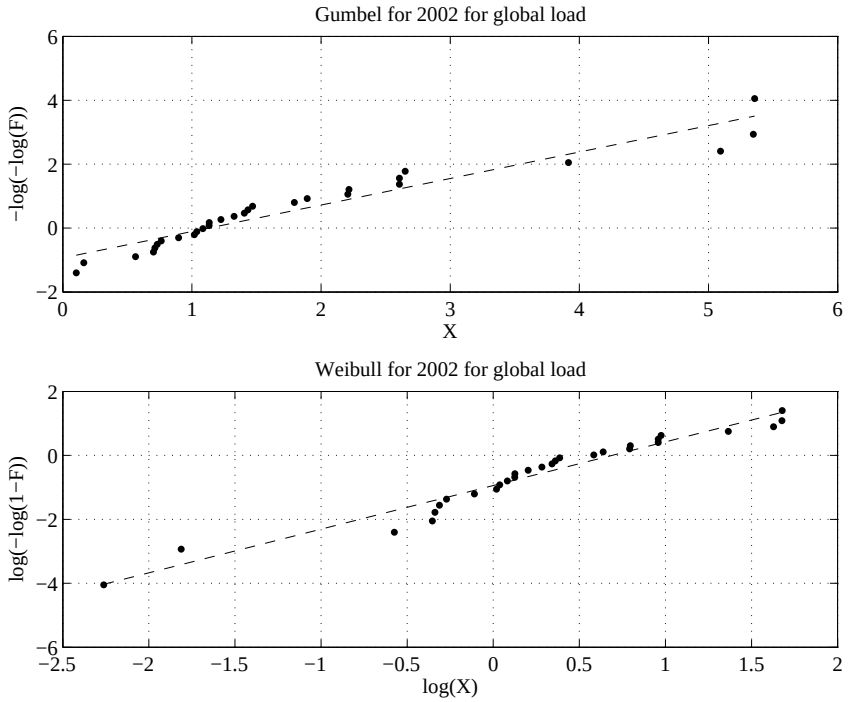

Figure 7.36: The global load data (year 2002) on Gumbel and Weibull paper.

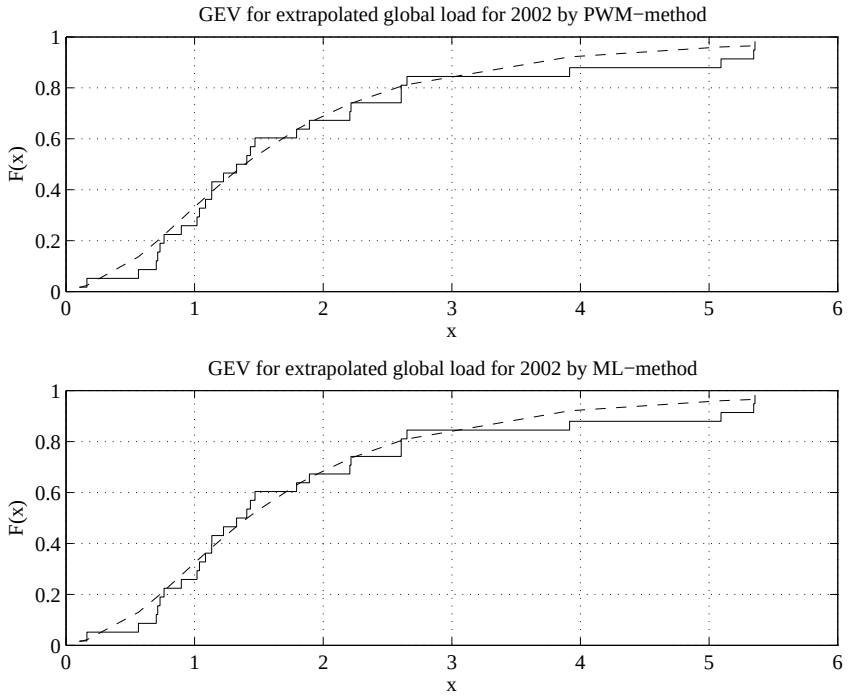

Figure 7.37: The estimated GEV distribution ($--$) and empirical distribution on the global load data (year 2002).

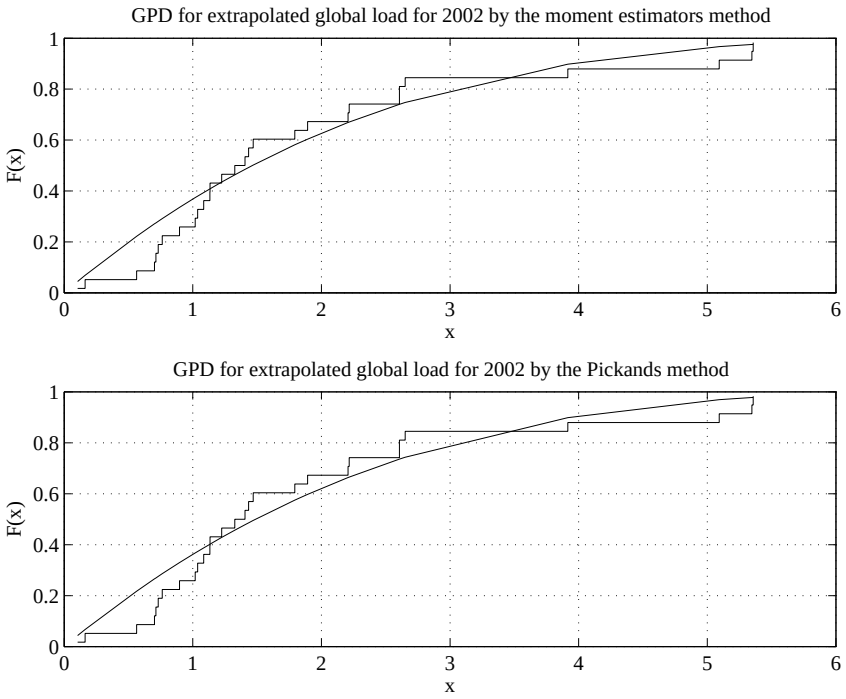

Figure 7.38: The estimated GPD (-) and empirical distribution on the global load data (year 2002).

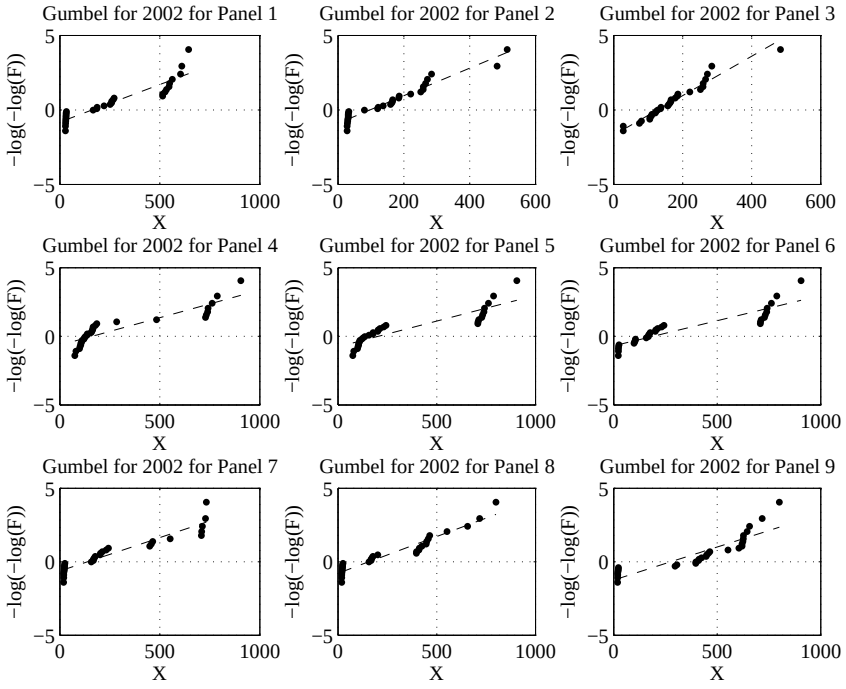

Figure 7.39: The panel load data (year 2002) on Gumbel paper.

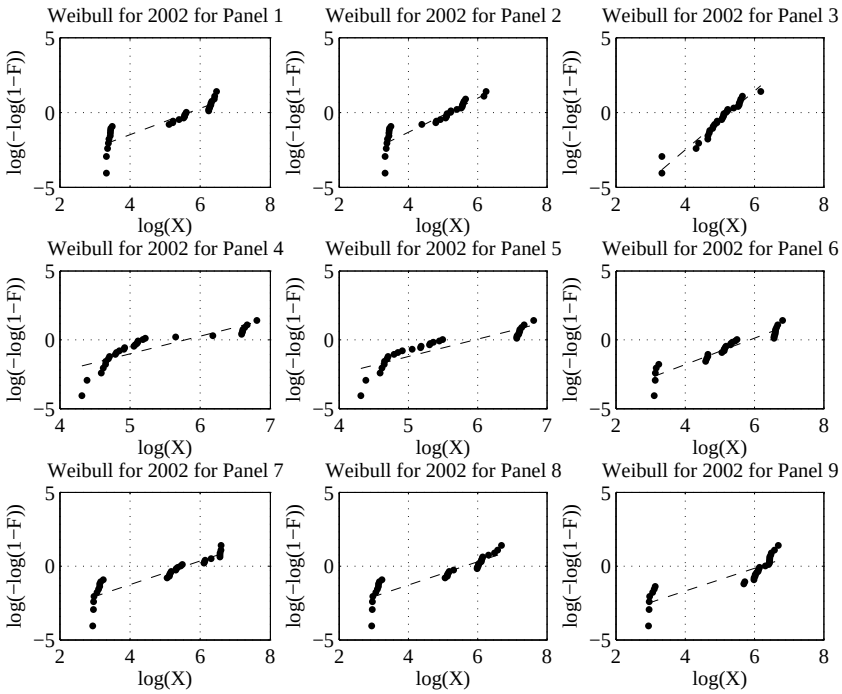

Figure 7.40: The panel load data (year 2002) on Weibull paper.

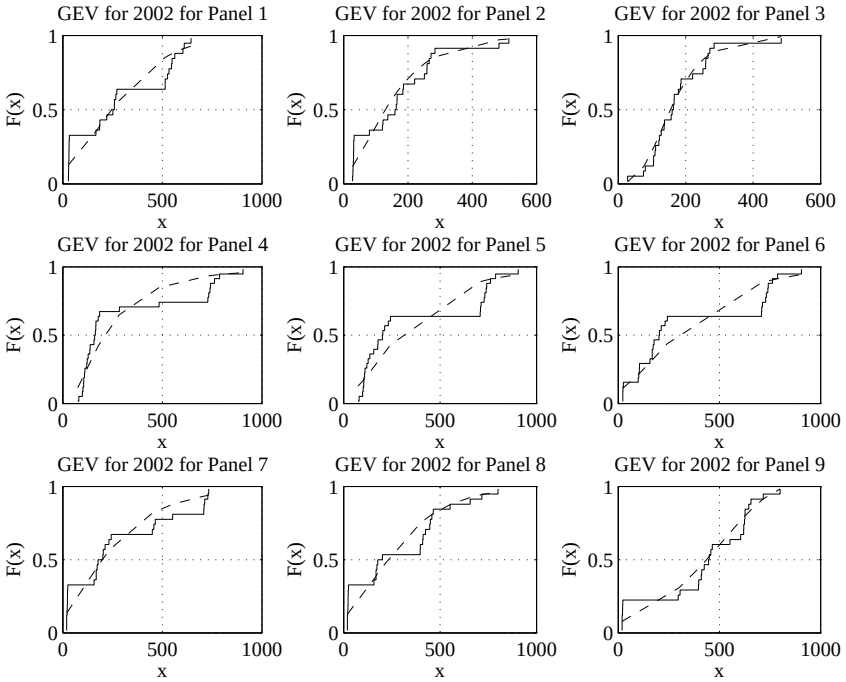

Figure 7.41: The estimated GEV distribution (− −) and empirical distribution on panel load data (year 2002).

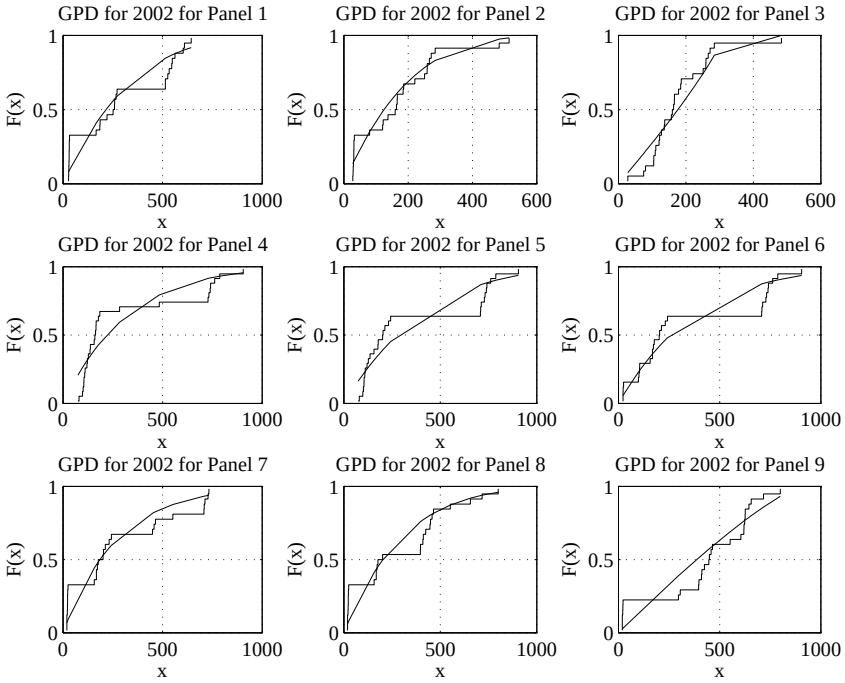

Figure 7.42: The estimated GPD (–) and empirical distribution on panel load data (year 2002).

bution was chosen. The design values were calculated by Eq. (C.3.3), where the exceeding duration $\tau = 1$ day and the return period $R = 1, 5, 10, 25$ years in days (the number of years multiplied by 365 days) was used. It corresponds to probability of exceedance P_e that is given in Table 7.7 together with estimated forces (the design value for panels calculated on the average parameters for all panels).

Table 7.7: Design values derived from the Gumbel distribution.

	Panel load, MN	Global load, MN	Probability P_e
$\zeta(1\,\text{year})$	1.54	6.86	2.74E-03
$\zeta(5\,\text{year})$	1.91	8.39	5.48E-04
$\zeta(10\,\text{year})$	2.07	9.04	2.74E-04
$\zeta(25\,\text{year})$	2.28	9.91	1.10E-04
Maximum (2002)	1.42	5.84	-

To conclude this section, it can be mentioned that the data can be transformed in order to fit some of proposed distributions as it was done in Naess (1998). For instance, it may be the effective pressure. Unfortunately, the ice thickness data is unreliable for this period making the method presentation impossible.

It should be noted that in spite of disregarding the ice interaction scenarios, the method is reliable because the Baltic Sea area is not experiencing the most extreme ice loads. The

ice conditions in the area adjacent to the Norströmsgrund lighthouse are primarily first year level and rafted ice, and first year ridges. Moreover, the ice cover is often disturbed artificially by icebreakers and the structure itself is affecting the ice strength. As mentioned in Simiu and Hackert (1996), the extreme value distribution is described with reference only to ordinary winds and storms, not including the extreme wind events like hurricanes.

The Gumbel distribution gave the best fit and clear dependencies for the data among other distributions. Though it would be unwise to reject some of them. For example, probably the GEV (Generalized Extreme Value) distribution may give more general statistical estimate for ice forces under further consideration because it possesses more universal structure. This kind of distribution was regarded in Morse (2000) as well. In this source (Morse, 2000), an analogous study is performed concerning the ice booms on the St. Lawrence River in Canada. Several different distributions were used. However, no particular preference was made except the Normal distribution, which was rejected in the hypothesis. It is mentioned in Section 7.1 that the maximum recorded loads follow the Gumbel distribution well. Nevertheless, the Gumbel distribution may overestimate loads on the structure as it is shown in Table 7.7 the yearly maximum values for panel load and global load are less than predicted by the Gumbel distribution (7% and 15% correspondingly).

Further, the analysis results of similar structures are reviewed. The conical formation on the piles of the Confederation Bridge was investigated in Brown et al. (2001). The ice loads are determined from the computer simulations based on the parameters given statistically by their specific distributions. The exceedance probability is plotted for two different cone materials. For $P_e = 10^{-4}$, the design value for the concrete cone is about 11.5 MN, for the steel cone approximately 9 MN. The difference in the numbers is due to different coefficients of friction on the cone surface. In Table 7.7 the value for the Norströmsgrund lighthouse estimated in this report for the same probability is given as 9.91 MN. Consider that the diameter of the pile with cone structure on it at the waterline is approximately 12.48 m. Thus the scale factor between the Norströmsgrund and the Confederation Bridge is $7.52/12.48 = 0.6$. Thus if the force on the concrete cone is taken as reference value, then the estimated force for the structure with diameter 7.52 m would be 6.9 MN. These values lie in the same range, and the relative difference is about 30%. However, it should be taken into account that generally forces on a conical structure are less than on cylindrical structures due to different ice failure scenarios. On a cone the prevailing failure mode is bending, on cylindrical structures it is crushing as it was shown in Schwarz (2001) and Schwarz and Jochmann (2001).

7.5 Summary and conclusions

Ice force measurements and determination of parameters affecting the ice force were carried out at the Norströmsgrund lighthouse in winters 2001-2002. The lighthouse is located in a subarctic region in the Baltic Sea. For the force determination the structure was equipped at the water line with eight rigid ice force sensing panels of size 1.21×1.60 m and a load capacity of 3 MN including an overload range of 50% and with segmented panel assembled from 8 small panels with a load area 0.50×0.37 m and a normal load capacity of 1 MN. To

determine the ice force parameters, an echo sounder, em device, laser distance sensors and video cameras were installed.

The data from the 2001 campaign was chosen for verification of the assumption that the effective pressure depends on the indentation velocity proposed by Sodhi (1998). 34 events, which were characterized as crushing, were extracted. During these incidents the estimated ice drift velocity varied from 0.05 m/s up to 0.33 m/s. The measuring period of campaign started on 25 February 2001. The logbooks were used to document visual observation results as well as meteorological data together with information on date and time. The greatest ice loads were documented during the crushing events.

Analysis of the data showed that the highest effective pressure was caused by the ridges. Unlike the medium-scale experiments conducted by Sodhi (1998), the ice with low drift speed produced low interaction pressure on the structure.

The spatial stationarity of the crushing process and a negative exponential function for correlation function was assumed in terms of the mean and the standard deviation of the local force and a correlation length parameter. Analysis of measured data showed that these parameters depend on ice drift speed, air temperature and ice features.

The extreme value analysis of the data from the 2002 measurement campaign revealed that the daily maximum forces were best fitted to the Gumbel distribution. In addition, it was shown that the forces on the panel and estimated global force had a scale factor that was comparable with the scale factor of the structure and panel geometry. Comparison with relevant literature was conducted and good agreement was found with the present study.

References

Adomian, G. (1983). *Stochastic Systems*. Academic Press.

Aoki, S. and Suzuki, K. (1985). First excursion probability estimation of mechanical appendage system subjected to nonstationary earthquake excitations. In *Proc. 4th Int. Conf. on Structural Safety and Reliability, ICOSSAR'85*, 1, pages 201–210.

API (1995). *Planning, Designing and Constructing Structures and Pipelines for Arctic Conditions. Recommended Practice 2N*. Washington D.C.

Au, S.-K. (2001). *On the Solution of First Excursion Problems by Simulation with Application to Probabilistic Seismic Performance Assessment*. Ph.D. thesis, California Institute of Technology.

Au, S. K. and Beck, J. L. (2001). First excursion probabilities for linear systems by very efficient importance sampling. *Probabilistic Engineering Mechanics*, 16(3), pages 193–207.

Au, S. K. and Beck, J. L. (2003). Important sampling in high dimensions. *Structural Safety*, 25, pages 139–163.

Ayyub, B. M. and Haldar, A. (1985). Improved simlulation techniques as structural reliability models. In *4th Int. Conf. on Structural Safety and Reliability ICOSSAR'85*, 1, pages 17–26.

Bauer, W. F. (1958). The Monte Carlo method. *SIAM J. Appl. Math.*, 6, pages 438–451.

Bayer, V. and Bucher, C. (1998). An importance sampling procedure for first passage problems. In N. Shiraishi, M. Shinozuka, and Y. Wen, editors, *Proceedings of ICOSSAR'97 - the 7th International Conference on Structural Safety and Reliability*, 1, pages 501–504, Kyoto. A.A. Balkema, Rotterdam.

Bellman, R. E. (1957). *Dynamic Programming*. Princeton University Press.

Bellman, R. E. and Dreyfus, S. (1962). *Applied Dynamic Programming*. Princeton University Press.

Bergman, L. A. and Spencer Jr., F. (1985). First passage of a rigid structure on a sliding foundation. In *4th Int. Conf. on Structural Safety and Reliability ICOSSAR'85*, 1, pages 181–190.

Bjerkås, M., Moslet, P., Jochmann, P., and Løset, S. (2003). Global ice loads on the lighthouse Norströmsgrund in the winter 2001. In *POAC'03*, Trondheim, Norway.

Bolotin, V. V., Frolov, K. V., and Chirkov, V. (1999). *Vibrations in Engineering. Vibrations of Linear Systems (Vibratsii v tekhnike)*, 1. Mashinostroenie, Moscow, 2nd edition. In Russian.

Bronshtein, I. N. and Semendyaev, K. A. (1956). *Handbook of Mathematics (Spravochnik po Matematike)*. Gos. Izd-Vo Tekhniko-Teoreticheckoy Literatury, Moscow, 6th edition. In Russian.

Brown, T. G., Jordaan, I. J., and Croasdale, K. R. (2001). A probabilistic approach to analysis of ice loads for the confederation bridge. *Can. J. Civ. Eng.*, (28), pages 562–573.

Bucher, C. (2002). Numerical solution of the first-passage problem by FORM and importance sampling. In Grundmann and Schuëller, editors, *Structural Dynamics, EURODYN2003*, pages 749–754. Swets and Zeitlinger, Lisse.

Bury, K. V. (1975). *Statistical Models in Applied Science*. John Wiley and Sons.

Carpenter, M. and Kennedy, C. (1994). Fourth-order 2N-storage Runge-Kutta schemes. Technical Report NASA TM-109112, Langley Research Center, Hampton, VA.

Chung, K. L. and Williams, R. J. (1990). *Introduction to Stochastic Integration*. Birkhäuser Boston, 2nd edition.

Cornell, C. A. (1969). A probability-based structural codes. *Journal of American Concrete Institute*, 66(12), pages 974–985.

Crandall, S. H. (1970). First-crossing probabilities of the linear oscillator. *Journal of Sound and Vibration*, 12(3), pages 285–299.

Crandall, S. H. (1980). Non-gaussian closure for random vibration of non-linear oscillators. *International Journal of Non-linear Mechanics*, 15(4-5), pages 303–313.

der Kiureghian, A. and Dakessian, T. (1998). Multiple design points in first and second-order reliability. *Structural Safety*, (20), pages 37–49.

Dey, A. and Mahadevan, S. (1998). Time-variant system reliability. In N. Shiraishi, M. Shinozuka, and Y. Wen, editors, *Proceedings of ICOSSAR'97 - the 7th International Conference on Structural Safety and Reliability*, 1, pages pages 647–654, Kyoto. A.A. Balkema, Rotterdam.

Ditlevsen, O. and Madsen, H. O. (2003). *Structural Reliability Methods*. 2.2 Internet Edition.

Dunwoody, A. B. (1991). Non-simultaneous ice failure. Report, Amoco Production, Tulsa, OK.

Fishman, G. S. (1996). *Monte Carlo: Concepts, Algorithms, and Applications*. Springer-Verlag New York, Inc.

Fleming, W. H. and Rishel, R. O. (1975). *Deterministic and Stochastic Optimal Control*. Springer-Verlag New York, Inc.

Gao, Z., Moan, T., and Heggelund, S. E. (2005). Time variant reliability of mooring system considering corrosion deterioration. In *Proceedings of 24th Int. Conf. on offshore Mechanics and Arctic Engineering (OMAE 2005)*, pages OMAE2005–67429.

Girsanov, I. V. (1960). On transforming a certain class of stochastic processes by absolutely continuous substitution of measures. *Theory of Probability and its Applications*, V(3), pages 285–301.

Grey, W. and Melchers, R. E. (2003). A comparison of some numerical methods for estimating time-invariant reliability. In A. Der Kiureghian, S. Madanat, and J. Pestana, editors, *Applications of Statistics and Probability in Civil Engineering*, pages 57–62, Rotterdam. Millpress.

Haas, C. and Jochmann, P. (2003). Continuous EM and ULS thickness profiling in support of ice force measurements. In *Proc. of the 17th Int. Conf. On Port and Ocean Engineering under Arctic Conditions POAC'03*, pages 849–856, Trondheim, Norway.

Hampl, N. C. (1985). Stochastic analysis of nonlinear systems under dynamic loading. In *4th Int. Conf. on Structural Safety and Reliability ICOSSAR'85*, 1, pages 615–619.

Han, S. M. and Benaroya, H. (2002). *Nonlinear and Stochastic Dynamics of Compliant Offshore Structures*. Kluwer Academic Publishers.

Hasofer, A. M. and Lind, N. C. (1974). Exact and invariant second-moment code format. *Journal of the Engineering Mechanics Division, ASCE*, 100, pages 111–121.

Ivanova, A. and Naess, A. (2004). An importance sampling procedure for estimating failure probabilities of dynamic systems. In *Proceedings 9th ASCE Joint Specialty Conference on Probabilistic Mechanics and Structural Reliability, July 2004*, Albuquerque, New Mexico, USA.

Jochmann, P. and Schwartz, J. (2000). Ice force measurement at lighthouse Norströmsgrund - winter 2000. Report 9, Hamburgische Schiffbau-Veruchsansalt GmbH, Hamburg, Germany.

Johnston, M. E., Croasdale, K. R., and Jordaan, I. J. (1998). Localized pressures during ice-structure interaction: Relevance to design criteria. *Cold Regions Science and Technology*, 27, pages 105–117.

Karamchandani, A. and Cornell, A. C. (1991). Adaptive hybrid conditional expectation approaches for reliability estimation. *Structural Safety*, 11, pages 59–74.

Karlin, S. and Taylor, H. M. (1975). *A First Course in Stochastic Processes*. Academic Press, Inc., 2nd edition.

Karlin, S. and Taylor, H. M. (1981). *A Second Course in Stochastic Processes*. Academic Press, Inc.

Khan, R. A., Ahmad, S., and Datta, T. K. (2003). First passage failure of cable stayed bridge under random ground motion. In A. Der Kiureghian, S. Madanat, and J. Pestana, editors, *Applications of Statistics and Probability in Civil Engineering*, pages 1659–1666, Rotterdam. Millpress.

Kloeden, P. E. and Platen, E. (1999). *Numerical Solution of Stochastic Differential Equations*. Springer.

Knuth, D. E. (1981). *The Art of Computer Programming*, V.2. AddisonWesley, 2nd edition.

Koo, H. and Der Kiureghian, A. (2003). Importance sampling of first-excursion probability for nonlinear systems. In A. Der Kiureghian, S. Madanat, and J. Pestana, editors, *Applications of Statistics and Probability in Civil Engineering*, pages 329–336, Rotterdam. Millpress.

Koo, H., Der Kiureghian, A., and Fujimura, K. (2005). Design-point excitation for nonlinear random vibrations. *Probabilistic Engineering Mechanics*, 20, pages 136–147.

Koutsourelakis, P. S., Pradlwater, H. J., and Shuëller, G. I. (2004). Reliability of structures in high dimensions, Part I: Algorithms and Applications. *Probabilistic Engineering Mechanics*, 19, pages 409–417.

Lange, K. (1999). *Numerical Analysis for Statisticians*. Springer-Verlag New York, Inc. online.

Li, C.-C. and Der Kiureghian, A. (1995). Mean out-crossing rate of non-linear response to stochastic input. In M. Lemaire, L. Favre, and A. M. Mébarki, editors, *Proceedings of the 7th International Conference on Applications of Statistics and Probability (ICASP) in Civil Engineering Reliability and Risk Analysis*, page 295, Paris, France.

Lin, Y., Kozin, F., Wen, Y., Casciati, F., Schuëller, G., Der Kiureghian, A., Ditlevsen, O., and Vanmarcke, E. (1986). Methods of stochastic structural dynamics. *Structural Safety*, 3, pages 167–194.

Lin, Y. K. (1967). *Probabilistic Theory of Structural Dynamics*. McGraw-Hill, Inc.

Lin, Y. K. and Cai, G. Q. (1995). *Probabilistic Structural Dynamics. Advanced Theory and Applications*. McGraw-Hill, Inc.

Liu, J. S. (2001). *Monte Carlo Strategies in Scientific Computing*. Springer.

Liu, J. S. and Chen, R. (1998). Sequential Monte Carlo methods for dynamic systems. *Journal of the American Statistical Association*, 93(443), pages 1032–1044.

Løset, S., Shkhinek, K., and Høyland, K. (1998). *Ice Physics and Mechanics*. Norwegian University of Science and Technology, Trondheim, 1st edition.

Lutes, L. D. and Sarkani, S. (1997). *Stochastic Analysis of Structural and Mechanical Vibrations*. Prentice-Hall, Inc.

Macke, M. (1999). Variance-reducing simulation of nonlinear dynamic systems. In N. Jones and R. Chanem, editors, *Proc. 13th ASCE Engineering Mechanics Division Conference*, Baltimore, Maryland, USA.

Macke, M. (2000). Variance reduction in Monte Carlo simulation of dynamic systems. In R. Melchers and M. Stewart, editors, *Proc. 8th Int. Conf. on Applications of Statistics and Probability*, pages 797–804, Sydney, Australia.

Macke, M. and Bucher, C. (2003). Importance sampling for randomly excited dynamical systems. *Journal of Sound and Vibration*, 268, pages 269–290.

Maclaren, N. M. (1989). The generation of multiple independent sequences of pseudorandom numbers. *Appl. Statist.*, 38, pages 351 – 359.

Madsen, H. O., Krenk, S., and Lind, N. C. (1986). *Methods of Structural Safety*. Prentice-Hall, Inc.

Mathiesen, M. (1991). Long-term wave and wind statistics. Report STF60 A91084, SINTEF Norwegian Hydrotechnical Laboratory.

McKay, M. D., Conover, W. J., and Beckman, R. (1979). A comparison of three methods for selecting values of input variables in the analysis of output from a computer code. *Technometrics*, 21, pages 239–245.

Melchers, R. E. (1999). *Structural Reliability Analysis and Prediction*. John Wiley & Sons Ltd, 2nd edition.

Melchers, R. E. and Ahammed, M. (2002). Gradient estimation for applied Monte Carlo analyses. *Reliability Engineering and System Safety*, 78, pages 283–288.

Metropolis, N. and Ulam, S. (1949). The Monte Carlo method. *Journal of the American Statistical Association*, 44(247), pages 335–341.

Milstein, G. N. (1995). *Numerical Integration of Stochastic Differential Equations*. Kluwer Academic Publishers.

Morse, B. (2000). Forces on wide structures - an analysis of ice loads on the St. Lawrence River ice booms from 1994 to 2000. Report 10-56, PERD/CHC.

Naess, A. (1990). Approximate first-passage and extremes of narrow-band Gaussian and non-Gaussian random vibration. *Journal of Sound and Vibration*, 138, pages 365–380.

Naess, A. (1995). Prediction of extreme response of nonlinear structures by extended stochastic linearization. *Probabilistic Engineering Mechanics*, 10, pages 153–160.

Naess, A. (1998). Estimation of long return period design values for wind speeds. *Journal of Engineering Mechanics*, 124(3), pages 252–259.

Naess, A. (1999). Comments on importance sampling for time variant reliability problems. *Stochastic Structural Dynamics*, 4, pages 197–202.

Naess, A. and Johnsen, J. M. (1993). Response statistics of nonlinear, compliant offshore structures by the path integral solution method. *Probabilistic Engineering Mechanics*, 8, pages 91–106.

Næss, A. and Skaug, C. (2000). Importance sampling for dynamical systems. In *ICASP Applications of Statistics and Probability*, 8, pages 749–755. A.A. Balkema.

Newton, N. J. (1994). Variance reduction for simulated diffusions. *SIAM J. Appl. Math.*, 54, pages 1780–1805.

Noori, M., Dimentberg, M., Hou, Z., Christodoulidou, R., and Alexandrou, A. (1995). First-passage study and stationary response analysis of a BWB hysteretic model using quasi-conservative stochastic averaging method. *Probabilistic Engineering Mechanics*, 10, pages 161–170.

Øksendal, B. (1998). *Stochastic Differential Equations: an Introduction with Application.* Springer, 5th edition.

Olsen, A. I. and Naess, A. (2005a). Estimating failure probabilities of nonlinear dynamic systems subjected to coloured noise by an importance sampling procedure. In G. Augusti, G. Schuëller, and M. Ciampoli, editors, *ICOSSAR, Joint Specialty Conference on Probabilistic Mechanics and Structural Reliability*, pages 1971–1977. Millpress, Rotterdam.

Olsen, A. I. and Naess, A. (2005b). Importance sampling for dynamic systems by approximate calculation of the optimal control function. In A. Wilson, N. Limnios, S. Keller-McNulty, and Y. Armijo, editors, *Modern Statistical and Mathematical Methods in Reliability* of *Series on Quality, Reliability and Engineering Statistics*, 10, pages 339–352. World Scientific.

Olsen, A. I. and Naess, A. (2006). An importance sampling procedure for estimating failure probabilities of dynamic systems. *SADHANA, Academy Proceedings in Engineering Sciences*, Accepted.

Olsson, A., Sandberg, G., and Dahlblom, O. (2003). On latin hypercube sampling for structural reliability analysis. *Structural Safety*, 25, pages 47–68.

Paz, M. (1980). *Structural Dynamics, Theory and Computation*. Van Nostrand Reinhold Company.

Pradlwater, H. J. and Schuëller, G. I. (2004). Excursion probabilities of non-linear systems. *Int. Journal of Non-Linear Mechanics*, (39), pages 1447–1452.

Rackwitz, R. (2001). Reliability analysis - a review and some perspectives. *Structural Safety*, 23, pages 365–395.

Rice, S. O. (1954). Mathematical analysis of random noise. In N. Wax, editor, *Selected Papers on Noise and Stochastic Processes*, pages 133–294. Dover Publications, Inc.

Roberts, J. (1976). First passage time for the envelope of a randomly excited linear oscillator. *Journal of Sound and Vibration*, 46, pages 1–14.

Roberts, J. B. and Spanos, P. (1990). *Random Vibration and Statistical Linearization*. John Wiley & Sons Ltd.

Rubenstein, R. Y. (1981). *Simulation and the Monte Carlo Method*. John Wiley & Sons, Inc.

Rubenstein, R. Y. and Melamed, B. (1998). *Modern Simulation and Modeling*. John Wiley & Sons, Inc.

Rudin, W. (1987). *Real and Complex Analysis*. McGraw-Hill, Inc.

Sanderson, T. (1988). *Ice mechanics. Risk of offshore structures*. Graham and Trotman.

Schuëller, G. I., Pradlwarter, H. J., and Koutsourelakis, P. S. (2004). A critical appraisal of reliability estimation procedures for high dimensions. *Probabilistic Engineering Mechanics*, 19, 463–474.

Schwarz, J. (2001). Lolief summary report: Validation of low level ice forces on coastal structures. Technical report, Hamburgische Schiffbau-Veruchsansalt GmbH, Hamburg, Germany.

Schwarz, J. and Jochmann, P. (2001). Ice force measurements within the loleif-project. In *Proceedings of the 16th Int. Conf. on Port and Ocean Engineering under Arctic Conditions*, pages 669–680, Ottawa, Canada.

Shiao, M. C. (1991). First passage problem: a probabilistic dynamic analysis for hot aerospace components. *Probabilistic Engineering Mechanics*, 6, pages 139–147.

Shumway, R. H. and Stoffer, D. S. (2000). *Time Series Analysis and Its Applications*. Springer.

Simiu, E. and Hackert, N. (1996). Extreme wind distribution tails: A "peaks over threshold" approach. *Journal of Structural Engineering*, 122(5), pages 539–547.

Skaug, C. (2000). *Random Vibration and the Path Integral Method*. Dr. ing. thesis, Department of Structural Engineering, Norwegian University of Science and Technology.

Sobol', I. M. (1973). *Monte Carlo Numerical Methods*. Nauka. In Russian.

Sodhi, D. (1998). Non-simultaneous crushing during edge indentation of freshwater ice sheets. *Cold Regions Science and Technology*, 27, pages 179–195.

Sodhi, D., Takeuchi, T., Nakasawa, N., Akagawa, S., and H., S. (1998). Medium-scale indentation tests on sea ice at various speeds. *Cold Regions Science and Technology*, 28, pages 161–182.

Sodhi, D. S. (2001). Crushing failure during ice-structure interaction. *Engineering Fracture Mechanics*, 68, pages 1889–1921.

Soong, T. T. and Grigoriu, M. (1997). *Random Vibration of Mechanical and Structural Systems*. Prentice-Hall, Inc.

Takada, T. (1998). Application of important sampling technique to first passage problem for gaussian or non-gaussian processes. In S. Shiraishi and Y. Wen, editors, *Structural safety and Reliability*, pages 419–426. Balkema, Rotterdam.

Tanaka, H. (1997). Application of an importance sampling method to time-dependent system reliability analyses using the Girsanov transformation. In N. Shiraishi, M. Shinozuka, and Y. Wen, editors, *Proceedings of ICOSSAR'97 - the 7th International Conference on Structural Safety and Reliability*, 1, pages 411–418, Kyoto. A.A. Balkema, Rotterdam, 1998.

Tanaka, H. (2000). Importance sampling simulation for a stochastic fatigue crack growth model. In R. E. Melchers and M. B. Stewart, editors, *Proceedings of the 8th International Conference on Applications of Statistics and Probability*, Sydney, Australia. Balkema, Rotterdam.

Vijalapura, P. K., Conte, J. P., and Meghella, M. (2000). Time-variant reliability analysis of hysteretic sdof systems with uncertain parameters and subjected to stochastic loading. In R. E. Melchers and M. G. Stewart, editors, *Applications of Statistics and Probability*, 2, pages 827–834.

Wadsworth, H. M. (1997). *Handbook of Statistical Methods for Engineers and Scientists*. McGraw-Hill, 2nd edition.

Wang, L. and Moan, T. (2003). *Modeling Wave Loads On Ships Using Peaks Over Threshold Method. Applications of Statistics and Probability in Civil Engineering*. Millpress, Rotterdam.

Wen, Y. (1980). Equivalent linearization of hysteretic systems under random excitation. *Journal of Applied Mechanics, Transactions of the ASME*, 47, pages 150–154.

Wen, Y. (1985). Response and damage of hysteretic systems under random excitation. In *ICOSSAR'85, 4th International Conference on Structural Safety and Reliability*, 1, pages 291–300.

Appendix A

Random number generators

The basis for the Monte Carlo method is the statistical experiment done on the variety of the independent uniform random outcomes. Initially, manual methods were used to produce these, including such techniques as coin flipping, dice rolling, card shuffling, and roulette wheels. Certainly these methods are too slow for modern use, and, moreover, they possess another disadvantage. Namely, sequences generated by manual means are not reproducible. With the raise of digital computers other methods came to the stage, for instance, famous tables produced by the RAND Corporation in 1955. Hence, the random numbers became reproducible but still rather slow to process. There also existed the risk of exhausting the table. Electrical devices were also used such as noise diodes, Geiger counters to produce the "truly" random sequences. Nevertheless it was found that these generated numbers exhibit both bias and dependence. Considering these difficulties the arithmetic operations on the computers were suggested to be used for these purposes. John von Neumann was probably first with his mid-square method. The idea is the following: take the square of the preceding n-digit number and extract the n-middle digits. Hence these numbers actually are not random but just look like they are random. Though they possess all statistical properties of random numbers and in addition they are reproducible. These numbers are strictly referred as *pseudorandom* or *quasirandom* though it is conventional still to call them random. The methods which produce the random numbers are called *random number generators* or *RNG*. The RNG is considered as a high-quality generator if it is fast, takes minimum memory capacity, generated numbers are uniformly distributed, statistically independent, and have a long interval of aperiodicity. The method of Neumann does not have all these qualities and thus it is a rather poor generator. The most popular RNGs now are the congruential generators, introduced by Lehmer in 1951.

Congruential methods are based on a fundamental congruence relationship, which may be expressed as

$$X_{i+1} = (aX_i + c) \,(\mathrm{mod}\, m), \tag{A.0.1}$$

where the initial value, X_0, is called *seed*, the multiplier a and the divisor m are positive integers, the increment c is a nonnegative integer. The modulo operation means the remainder of the division of the integer numbers. In particular, if $c = 0$ the generator is called a multiplicative congruential generator (Rubenstein, 1981; Rubenstein and Melamed, 1998). Dividing by m gives the series of uniformly distributed numbers in the interval $(0, 1)$. Many diverse algorithms and variations of the congruential methods have been developed over the

years (Knuth, 1981; Maclaren, 1989). In this thesis the programming language C was used to program the algorithms. RNG from NAGC library was preferred to the standard RNG built in C language because of its quality. Though there is the manifold of different algorithms in the standard computer libraries as well as on the Internet.

Moreover, random numbers from other distributions may be obtained from the uniform random numbers by the use of transformations and rejection techniques, and for discrete distributions, by table based methods. For a continuous random variable X with a cumulative distribution function (cdf) $F(x)$ the inverse transformation is

$$x = F^{-1}(u), \tag{A.0.2}$$

where u is a uniform random number in the interval $(0, 1)$. This method is called the inverse-transform method. Illustration is given in Figure A.1. Though this method is only efficient when cdf is invertible.

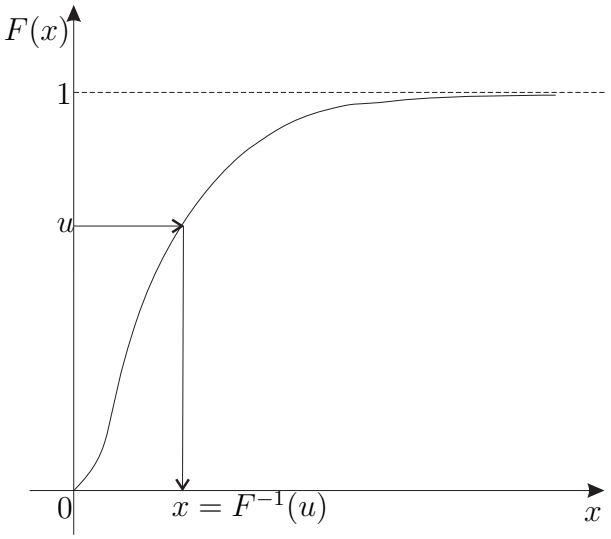

Figure A.1: The inverse-transform method.

The very popular algorithm for producing the random numbers from the normal Gaussian distribution is based on the polar representation of the 2D Euclidian space.

The other main class of transformation methods is called acceptance-rejection algorithms. The simplest method for generating numbers satisfying a non-uniform, arbitrary probability distribution $f(x)dx$ on (0,1) is proposed by von Neumann (Bauer, 1958). Choose an a which normalizes $f(x)$ such that $\max_{x\in(0,1)}[af(x)] = 1$. Numbers x_i and y_i are generated from a uniform distribution on (0,1) and x_i is accepted or rejected as a deviate depending on whether $y_i \leq af(x_i)$ or $y_i < af(x_i)$. The accepted x_i's have the required distribution.

Many other alternative procedures exist for generating pseudorandom numbers. They include shift register generators, generalized feedback shift register generators, and non-linear generators besides that mentioned above (Fishman, 1996).

Appendix B

Variance reduction techniques

The Monte Carlo simulation method is a robust and versatile tool for reliability estimation and probabilistic study of any general static and dynamic systems with arbitrary number degrees of freedom (Rubenstein, 1981; Ayyub and Haldar, 1985). However, this methodology is demanded as a last resort due to the slow convergency to the true solution. Although there exists diverse variance reduction procedures which allow to achieve a prescribed error bound with a smaller sample size. Those efficiency-improving methods usually take one of two forms (Fishman, 1996). The first alters the sample generating procedure and adjusts the parameter estimator of interest in a way that leads to smaller variance per observation. Importance sampling, stratified sampling and correlated sampling are examples of this approach. The second leaves the sample generating mechanism intact, but collects ancillary data that can be used to estimate already known parameters. By incorporating these additional data into the estimator of the unknown parameter of interest, one can reduce the variance for a given sample size. The control variate method is an example.

The importance sampling approach is of the main concern in this thesis, because it can lead to dramatic variance reduction, while all other procedures reduce the variance only by a constant factor.

B.1 Directional simulation

In directional simulation the reliability problem is reformulated in polar coordinates when it is possible and convenient. Thus the n-dimensional standardized normal vector U is written

$$U = RA \tag{B.1.1}$$

where the radial distance $R > 0$ is a stochastic variable such that R^2 is chi-square distributed with n degrees of freedom, and A is a unit vector of independent stochastic variables, indicating the direction in the u-space.

If R is independent on A then the probability of failure can be written as:

$$p_f = P(g(U) \leq 0) = \int_{\text{unit sphere}} P(g(RA) \leq 0 | A = a) f_A(a) da \tag{B.1.2}$$

where $f_A(a)$ is the constant density of A on the unit sphere.

The following assumption are made: the origin $u = \mathbf{0}$ is in the safe area, i.e. $g(\mathbf{0}) > 0$, and every half-line starting from $u = \mathbf{0}$ only crosses the failure surface once.

The probability $P(g(RA) \leq 0|A = a)$ in Eq. (B.1.2) can be calculated by

$$P(g(RA) \leq 0|A = a) = \int_{r(a)}^{\infty} f_R(s|A = a)ds = 1 - \chi_n^2\left(r(a)^2\right) \tag{B.1.3}$$

where $\chi_n^2()$ is the χ_n^2 distribution with n degrees of freedom. $r(a)$ is the distance from the origin $u = \mathbf{0}$ to the failure surface, i.e. $g(r(a)a) = 0$.

An unbiased estimator of p_f is

$$\hat{p}_f \approx E[\hat{p}_f] = \frac{1}{N}\sum_{j=1}^{N}\hat{p}_j = \frac{1}{N}\sum_{j=1}^{N}\left(1 - \chi_n^2\left(r(\hat{a}_j)^2\right)\right) \tag{B.1.4}$$

where N is the number of simulations and $\hat{a}_j$ is a simulated sample of A. Further evolution and generalization are possible, see Melchers (1999) and Ditlevsen and Madsen (2003).

B.2 Adaptive sampling

In adaptive sampling in order to develop the efficient importance sampling density and explore the failure domains the generated samples are chosen such that the regions, they belong to, have higher probability densities (Karamchandani and Cornell, 1991). Then the sampling density can be modified to generate sample points in these regions. The simplest approach is to locate the expected value point at the point in the region with the largest probability density function.

Another approach is to use a so-called multimodal sampling density which generates samples around a number of points in the failure domain, but emphasizes the region around a point in proportion to the probability density at the point.

Let $\hat{u}^{(i)}$ $(i = 1, \ldots, k)$ be the set of the points in the failure region which are used to construct the multimodal sampling density, which is given

$$h_U^k(u) = \sum_{j=1}^{k} w_j f_U^{(j)}(u) \tag{B.2.1}$$

where $f_U^{(j)}(u)$ is the density function of a normally distributed stochastic vector with uncorrelated variables, standard deviations 1 and expected value point equal to $\hat{u}^{(j)}$. The weights are determined by

$$w_j = \frac{f_U(\hat{u}^{(j)})}{\sum_{i=1}^{k} f_U(\hat{u}^{(i)})}. \tag{B.2.2}$$

An estimate of the probability of failure can now be obtained on the basis of N simulations where the importance sampling technique is used:

$$\hat{p}_f = \frac{1}{N}\sum_{j=1}^{N}\frac{f_U(\hat{u}^{(j)})}{h_U^j(\hat{u}^{(j)})}I[g(\hat{u}^{(j)})]. \tag{B.2.3}$$

B.3 Conditional Monte Carlo simulation

Let

$$E[f(X)] = \int f(x)dP(x) \tag{B.3.1}$$

be some expected performance measure. Suppose there exists a random variable, X, such that the conditional expectation $E[f(x)|X = x]$ can be analytically computed. Since

$$E[E[f(x)|X]] = E[f(X)] \tag{B.3.2}$$

it follows that $E[f(x)|X]$ is an unbiased estimator of $E[f(X)]$. Furthermore, it can be shown (Rubenstein and Melamed, 1998) that

$$Var[E[f(x)|X]] \leq Var[f(X)]. \tag{B.3.3}$$

B.4 Latin hypercube simulation

The basic Latin hypercube simulation method is based on the idea that the entire range of each variable is sampled (McKay et al., 1979). Thus, the range of each variable is divided into m intervals. In each interval the probability of an outcome should be equal.

For each variable, one point is generated from its marginal distribution for each of the intervals, i.e. $\hat{u}_{ij}$, $j = 1, \ldots, m$ represents the m points for variable i.

The first sample point $\hat{u}_1^k$ (k is the run number) in this bulk is generated by random combination of each of realizations $\hat{u}_{ij}$. Correspondingly the following $m-1$ samples contain the combinations of the remaining unused values. The probability of failure for this sample is estimated from

$$\hat{p}_f^k = \frac{1}{m}\sum_{j=1}^{m} I[g(\hat{u}_j^k)]. \tag{B.4.1}$$

This procedure is repeated N times and the final estimate of p_f is

$$\hat{p}_f = \frac{1}{Nm}\sum_{k=1}^{N}\sum_{j=1}^{m} I[g(\hat{u}_j^k)]. \tag{B.4.2}$$

where $\hat{\mathbf{u}}_j^k$ is realization number j in the k^{th} Latin hypercube sample.

The standard error is of magnitude $1/(Nm)$ times the standard error of the crude Monte Carlo simulation, though it can not be expressed in a simple way. The extensions and development of this method can be found in Olsson et al. (2003).

B.5 Stratified sampling

Stratified sampling is a commonly used technique in population survey. Mathematically, it can be viewed as a special importance sampling method with its trial density constructed as a piecewise constant function. In stratified sampling, the domain of integration D of an expectation

$$E[f(X)] = \int_D f(x)dP(x) \tag{B.5.1}$$

is partitioned into $m > 1$ disjoint subsets D_i, so that within each subregion, the function $f(x)$ is relatively "homogeneous" (e.g., close to being constant). Then, a fixed number of samples $X_{(i,1)}, \ldots, X_{(i,n_i)}$ is generated from each D_i, where D_i is referred as stratum i.

If we estimate the conditional expectation

$$E[f(X)|X \in D_i] \approx \frac{1}{n_i}\sum_{j=1}^{n_i} f(X_{(i,j)}), \tag{B.5.2}$$

then the weighted estimator

$$\sum_{i=1}^{m} P(D_i)\frac{1}{n_i}\sum_{j=1}^{n_i} f(X_{(i,j)}) \tag{B.5.3}$$

is unbiased for $E[f(X)]$.

If the n_i are chosen carefully, then the variance

$$Var = \sum_{i=1}^{m} \sigma_i^2 p_i^2/n_i, \tag{B.5.4}$$

$$\text{where} \quad \sigma_i^2 = \frac{1}{p_i}\int_{D_i} [f(x) - E[f(X)|X \in D_i]]^2 dP(x), \tag{B.5.5}$$

$$p_i = P(D_i) = \int_{D_i} dP(x), \tag{B.5.6}$$

$$p_1 + \ldots + p_m = 1, \tag{B.5.7}$$

of this estimator will be smaller than the variance $Var[f(X)]/n$ of the crude Monte Carlo estimator with the same number of samples $n = \sum_{i=1}^{m} n_i$ drawn randomly from D.

Although the exact values of the conditional variances $\sigma_i^2 = Var[f(X)|X \in D_i]$ are inaccessible in practice, one can estimate them using a small pilot sample of points from each D_i. Once this is done, one can collect a more intelligent, final stratified sample that puts the most points where $f(x)$ shows the most variation. Obviously, it is harder to give general advice about how to choose the strata D_i and compute their probabilities $P(D_i)$ in the first place (Lange, 1999).

B.6 Antithetic variates

In the method of antithetic variates, suppose U is the random number used in the production of a sample X that follows a distribution with cdf F, i.e. $X = F^{-1}(U)$. Then, $X' = F^{-1}(1-U)$ also follows distribution F. One look for unbiased estimators X and X' of an integral that are negatively correlated rather than independent. The average $(X + X')/2$ is also unbiased, and its variance

$$Var\left(\frac{X+X'}{2}\right) = \frac{1}{4}Var(X) + \frac{1}{4}Var(X') + \frac{1}{2}Cov(X, X') \tag{B.6.1}$$

is reduced compared to what it would be if X and X' were independent (Liu, 2001).

B.7 Control variates

In computing $E[f(X)]$, suppose that one can calculate exactly the expectation $E[g(X)]$ for a function $g(x)$ close to $f(x)$. Then it makes sense to write

$$E_\alpha[f(X)] = E[f(X) - \alpha g(X)] + \alpha E[g(X)] \tag{B.7.1}$$

and approximate $E[f(X) - \alpha g(X)]$ by a Monte Carlo estimate rather than $E[f(X)]$. This estimator has a variance

$$Var_\alpha[f(X)] = Var[f(X)] + \alpha^2 Var[g(X)] - 2\alpha Cov[f(X)g(X)]. \tag{B.7.2}$$

If the computation of $Cov[f(X)g(X)]$ and $Var[g(X)]$ is easy, then let

$$\alpha = Cov[f(X)g(X)]/Var[g(X)], \tag{B.7.3}$$

in which case

$$Var_\alpha[f(X)] = (1 - \rho^2(f(X), g(X)))Var[f(X)] < Var[f(X)]. \tag{B.7.4}$$

Extensions to more than one control variate are also useful in Monte Carlo computations (Rubenstein and Melamed, 1998).

Appendix C

Extreme value distributions

C.1 Generalized Extreme Value distribution (GEV)

The Generalized Extreme Value distribution (GEV) has the distribution function

$$F(y;k,c,\lambda)=\begin{cases}\exp\left[-\left(1-k\dfrac{y-c}{\lambda}\right)^{1/k}\right], & \text{if} \quad k\neq 0,\\ \exp\left[-\exp\left(-\dfrac{y-c}{\lambda}\right)\right], & \text{if} \quad k=0,\end{cases} \tag{C.1.1}$$

for $k(y-c)<\lambda$, $\lambda>0$, where k, c are arbitrary. Note: the Gumbel and Weibull distributions are the particular cases of GEV distribution for and $k=0$ and $k<0$, respectively. It can be shown that for a particular random process, the parameters in the GEV distribution and the parameters the corresponding Generalized Pareto Distribution (GPD, see below) have the following relation

$$\begin{aligned}k_{GEV}&=k_{GPD}\\ \lambda_{GEV}&=\lambda_{GPD}\bar{k}^{k_{GPD}}\\ c_{GEV}&=u+(\bar{k}^{k_{GPD}}-1)\frac{\lambda_{GPD}}{k_{GPD}}\\ \bar{k}&=E[n|X>u,T],\end{aligned} \tag{C.1.2}$$

where $\bar{k}$ is the mean number of peaks over threshold u during the time period T.

C.2 Generalized Pareto distribution (GPD)

The Generalized Pareto Distribution (GPD) has the distribution function

$$F(y;k,\lambda)=\begin{cases}1-\left(1-ky/\lambda\right)^{1/k}, & \text{if} \quad k\neq 0,\\ 1-\exp\left(-y/\lambda\right), & \text{if} \quad k=0,\end{cases} \tag{C.2.1}$$

for $0<y<\infty$ if $k\leq 0$ and for $0<y<\lambda/k$ if $k>0$. λ is a scale parameter and k is a shape parameter, or a tail index. In order to estimate parameters of GPD the Peaks

Over Threshold method (POT) (Naess, 1998; Wang and Moan, 2003) is frequently used. Otherwise the method of moments is most conventional

$$\hat{k} = \frac{1}{2}\left(1 - \frac{\mu^2}{\sigma^2}\right), \tag{C.2.2}$$

$$\hat{\lambda} = \frac{1}{2}\mu\left(1 + \frac{\mu^2}{\sigma^2}\right), \tag{C.2.3}$$

where μ and σ^2 are, respectively, the sample mean and the variance.

C.3 Gumbel distribution

Gumbel distribution is the limiting, asymptotic distribution of the largest of n random variables X_i as $n \to \infty$ (also has a name "double exponential"). In practice, the X_i of the underlying population need not to be completely independent nor completely identical. Also it may be difficult to determine the appropriate underlying distribution of the X_i, and convergence to the asymptotic distribution may be slow. Nevertheless extreme value distributions are useful for fitting to experimental data even where the underlying mechanisms are not fully understood. The cumulative distribution and probability density functions are given correspondingly

$$F_G(y;\alpha,b) = \exp\left[-\exp(-\alpha(y-b))\right], \quad -\infty < y < \infty, \tag{C.3.1}$$

$$f_G(y;\alpha,b) = \alpha \exp\left[-\alpha(y-b) - \exp(-\alpha(y-b))\right]. \tag{C.3.2}$$

The parameters are the mode b of the distribution (the location parameter) and α which is a measure of the dispersion of the distribution. α^{-1} is sometimes referred as the "slope" of the distribution (obtained when plotting the distribution on "Gumbel" paper). Both b and α may be obtained, via the moments, from curve fitting to observed data. The inverse of the Gumbel distribution is

$$y = b + \frac{1}{\alpha}[-\ln(-\ln(F))]. \tag{C.3.3}$$

The mean μ, the variance σ^2 and the skewness γ_1 of the Gumbel distribution are $\mu = b + \gamma/\alpha$, $\sigma^2 = \pi^2(1/\alpha)^2/6$ and $\gamma_1 = 1.13955$, where $\gamma = 0.57722$ is Euler's constant.

C.4 Three parameter Weibull distribution

Three parameter Weibull distribution is also the limiting, asymptotic distribution of the largest of n random variables X_i as $n \to \infty$, with limited in the tail of interest to some maximum (or minimum) value ε. The extreme values Y_j have cumulative distribution and

probability density

$$F_W(y;\varepsilon,u,k) = 1 - \exp\left(-\left[\frac{y-\varepsilon}{u-\varepsilon}\right]^k\right), \tag{C.4.1}$$

$$f_W(y;\varepsilon,u,k) = \frac{k(y-\varepsilon)^{k-1}}{(u-\varepsilon)^k}\exp\left(-\left[\frac{y-\varepsilon}{u-\varepsilon}\right]^k\right). \tag{C.4.2}$$

The parameters are the scale parameter $u > 0$ and the shape parameter $k > 0$. Estimation of all required parameters is not generally straightforward. If $\varepsilon = 0$ and $k = 2$ the distribution is also known as the Rayleigh distribution.

The inverse of three parameter Weibull distribution function is

$$y = \varepsilon + (u-\varepsilon)[-\ln(1-F)]^{1/k}. \tag{C.4.3}$$

DEPARTMENT OF STRUCTURAL ENGINEERING
NORWEGIAN UNIVERSITY OF SCIENCE AND TECHNOLOGY

N-7491 TRONDHEIM, NORWAY
Telephone: +47 73 59 47 00 Telefax:+47 73 59 47 01

"Reliability Analysis of Structural Systems using Nonlinear Finite Element Methods", C. A. Holm, 1990:23, ISBN 82-7119-178-0.

"Uniform Stratified Flow Interaction with a Submerged Horizontal Cylinder", Ø. Arntsen, 1990:32, ISBN 82-7119-188-8.

"Large Displacement Analysis of Flexible and Rigid Systems Considering Displacement-Dependent Loads and Nonlinear Constraints", K. M. Mathisen, 1990:33, ISBN 82-7119-189-6.

"Solid Mechanics and Material Models including Large Deformations", E. Levold, 1990:56, ISBN 82-7119-214-0, ISSN 0802-3271.

"Inelastic Deformation Capacity of Flexurally-Loaded Aluminium Alloy Structures", T. Welo, 1990:62, ISBN 82-7119-220-5, ISSN 0802-3271.

"Visualization of Results from Mechanical Engineering Analysis", K. Aamnes, 1990:63, ISBN 82-7119-221-3, ISSN 0802-3271.

"Object-Oriented Product Modeling for Structural Design", S. I. Dale, 1991:6, ISBN 82-7119-258-2, ISSN 0802-3271.

"Parallel Techniques for Solving Finite Element Problems on Transputer Networks", T. H. Hansen, 1991:19, ISBN 82-7119-273-6, ISSN 0802-3271.

"Statistical Description and Estimation of Ocean Drift Ice Environments", R. Korsnes, 1991:24, ISBN 82-7119-278-7, ISSN 0802-3271.

"Properties of concrete related to fatigue damage: with emphasis on high strength concrete", G. Petkovic, 1991:35, ISBN 82-7119-290-6, ISSN 0802-3271.

"Turbidity Current Modelling", B. Brørs, 1991:38, ISBN 82-7119-293-0, ISSN 0802-3271.

"Zero-Slump Concrete: Rheology, Degree of Compaction and Strength. Effects of Fillers as Part Cement-Replacement", C. Sørensen, 1992:8, ISBN 82-7119-357-0, ISSN 0802-3271.

"Nonlinear Analysis of Reinforced Concrete Structures Exposed to Transient Loading", K. V. Høiseth, 1992:15, ISBN 82-7119-364-3, ISSN 0802-3271.

"Finite Element Formulations and Solution Algorithms for Buckling and Collapse Analysis of Thin Shells", R. O. Bjærum, 1992:30, ISBN 82-7119-380-5, ISSN 0802-3271.

"Response Statistics of Nonlinear Dynamic Systems", J. M. Johnsen, 1992:42, ISBN 82-7119-393-7, ISSN 0802-3271.

"Digital Models in Engineering. A Study on why and how engineers build and operate digital models for decisison support", J. Høyte, 1992:75, ISBN 82-7119-429-1, ISSN 0802-3271.

"Sparse Solution of Finite Element Equations", A. C. Damhaug, 1992:76, ISBN 82-7119-430-5, ISSN 0802-3271.

"Some Aspects of Floating Ice Related to Sea Surface Operations in the Barents Sea", S. Løset, 1992:95, ISBN 82-7119-452-6, ISSN 0802-3271.

"Modelling of Cyclic Plasticity with Application to Steel and Aluminium Structures", O. S. Hopperstad, 1993:7, ISBN 82-7119-461-5, ISSN 0802-3271.

"The Free Formulation: Linear Theory and Extensions with Applications to Tetrahedral Elements with Rotational Freedoms", G. Skeie, 1993:17, ISBN 82-7119-472-0, ISSN 0802-3271.

"Høyfast betongs motstand mot piggdekkslitasje. Analyse av resultater fra prøving i Veisliter'n", T. Tveter, 1993:62, ISBN 82-7119-522-0, ISSN 0802-3271.

"A Nonlinear Finite Element Based on Free Formulation Theory for Analysis of Sandwich Structures", O. Aamlid, 1993:72, ISBN 82-7119-534-4, ISSN 0802-3271.

"The Effect of Curing Temperature and Silica Fume on Chloride Migration and Pore Structure of High Strength Concrete", C. J. Hauck, 1993:90, ISBN 82-7119-553-0, ISSN 0802-3271.

"Failure of Concrete under Compressive Strain Gradients", G. Markeset, 1993:110, ISBN 82-7119-575-1, ISSN 0802-3271.

"An experimental study of internal tidal amphidromes in Vestfjorden", J. H. Nilsen, 1994:39, ISBN 82-7119-640-5, ISSN 0802-3271.

"Structural analysis of oil wells with emphasis on conductor design", H. Larsen, 1994:46, ISBN 82-7119-648-0, ISSN 0802-3271.

"Adaptive methods for non-linear finite element analysis of shell structures", K. M. Okstad, 1994:66, ISBN 82-7119-670-7, ISSN 0802-3271.

"On constitutive modelling in nonlinear analysis of concrete structures", O. Fyrileiv, 1994:115, ISBN 82-7119-725-8, ISSN 0802-3271.

"Fluctuating wind load and response of a line-like engineering structure with emphasis on motion-induced wind forces", J. Bogunovic Jakobsen, 1995:62, ISBN 82-7119-809-2, ISSN 0802-3271.

"An experimental study of beam-columns subjected to combined torsion, bending and axial

actions", A. Aalberg, 1995:66, ISBN 82-7119-813-0, ISSN 0802-3271.

"Scaling and cracking in unsealed freeze/thaw testing of Portland cement and silica fume concretes", S. Jacobsen, 1995:101, ISBN 82-7119-851-3, ISSN 0802-3271.

"Damping of water waves by submerged vegetation. A case study of laminaria hyperborea", A. M. Dubi, 1995:108, ISBN 82-7119-859-9, ISSN 0802-3271.

"The dynamics of a slope current in the Barents Sea", Sheng Li, 1995:109, ISBN 82-7119-860-2, ISSN 0802-3271.

"Modellering av delmaterialenes betydning for betongens konsistens", Ernst Mørtsell, 1996:12, ISBN 82-7119-894-7, ISSN 0802-3271.

"Bending of thin-walled aluminium extrusions", Birgit Søvik Opheim, 1996:60, ISBN 82-7119-947-1, ISSN 0802-3271.

"Material modelling of aluminium for crashworthiness analysis", Torodd Berstad, 1996:89, ISBN 82-7119-980-3, ISSN 0802-3271.

"Estimation of structural parameters from response measurements on submerged floating tunnels", Rolf Magne Larssen, 1996:119, ISBN 82-471-0014-2, ISSN 0802-3271.

"Numerical modelling of plain and reinforced concrete by damage mechanics", Mario A. Polanco-Loria, 1997:20, ISBN 82-471-0049-5, ISSN 0802-3271.

"Nonlinear random vibrations - numerical analysis by path integration methods", Vibeke Moe, 1997:26, ISBN 82-471-0056-8, ISSN 0802-3271.

"Numerical prediction of vortex-induced vibration by the finite element method", Joar Martin Dalheim, 1997:63, ISBN 82-471-0096-7, ISSN 0802-3271.

"Time domain calculations of buffeting response for wind sensitive structures", Ketil Aas-Jakobsen, 1997:148, ISBN 82-471-0189-0, ISSN 0802-3271.

"A numerical study of flow about fixed and flexibly mounted circular cylinders", Trond Stokka Meling, 1998:48, ISBN 82-471-0244-7, ISSN 0802-3271.

"Estimation of chloride penetration into concrete bridges in coastal areas", Per Egil Steen, 1998:89, ISBN 82-471-0290-0, ISSN 0802-3271.

"Stress-resultant material models for reinforced concrete plates and shells", Jan Arve Øverli, 1998:95, ISBN 82-471-0297-8, ISSN 0802-3271.

"Chloride binding in concrete. Effect of surrounding environment and concrete composition", Claus Kenneth Larsen, 1998:101, ISBN 82-471-0337-0, ISSN 0802-3271.

"Rotational capacity of aluminium alloy beams", Lars A. Moen, 1999:1, ISBN 82-471-0365-6,

ISSN 0802-3271.

"Stretch Bending of Aluminium Extrusions", Arild H. Clausen, 1999:29, ISBN 82-471-0396-6, ISSN 0802-3271.

"Aluminium and Steel Beams under Concentrated Loading", Tore Tryland, 1999:30, ISBN 82-471-0397-4, ISSN 0802-3271.

"Engineering Models of Elastoplasticity and Fracture for Aluminium Alloys", Odd-Geir Lademo, 1999:39, ISBN 82-471-0406-7, ISSN 0802-3271.

"Kapasitet og duktilitet av dybelforbindelser i trekonstruksjoner", Jan Siem, 1999:46, ISBN 82-471-0414-8, ISSN 0802-3271.

"Etablering av distribuert ingeniørarbeid; Teknologiske og organisatoriske erfaringer fra en norsk ingeniørbedrift", Lars Line, 1999:52, ISBN 82-471-0420-2, ISSN 0802-3271.

"Estimation of Earthquake-Induced Response", Símon Ólafsson, 1999:73, ISBN 82-471-0443-1, ISSN 0802-3271.

"Coastal Concrete Bridges: Moisture State, Chloride Permeability and Aging Effects" Ragnhild Holen Relling, 1999:74, ISBN 82-471-0445-8, ISSN 0802-3271.

"Capacity Assessment of Titanium Pipes Subjected to Bending and External Pressure", Arve Bjørset, 1999:100, ISBN 82-471-0473-3, ISSN 0802-3271.

"Validation of Numerical Collapse Behaviour of Thin-Walled Corrugated Panels", Håvar Ilstad, 1999:101, ISBN 82-471-0474-1, ISSN 0802-3271.

"Strength and Ductility of Welded Structures in Aluminium Alloys", Miroslaw Matusiak, 1999:113, ISBN 82-471-0487-3, ISSN 0802-3271.

"Thermal Dilation and Autogenous Deformation as Driving Forces to Self-Induced Stresses in High Performance Concrete", Øyvind Bjøntegaard, 1999:121, ISBN 82-7984-002-8, ISSN 0802-3271.

"Some Aspects of Ski Base Sliding Friction and Ski Base Structure", Dag Anders Moldestad, 1999:137, ISBN 82-7984-019-2, ISSN 0802-3271.

"Electrode reactions and corrosion resistance for steel in mortar and concrete", Roy Antonsen, 2000:10, ISBN 82-7984-030-3, ISSN 0802-3271.

"Hydro-Physical Conditions in Kelp Forests and the Effect on Wave Damping and Dune Erosion. A case study on Laminaria Hyperborea", Stig Magnar Løvås, 2000:28, ISBN 82-7984-050-8, ISSN 0802-3271.

"Random Vibration and the Path Integral Method", Christian Skaug, 2000:39, ISBN 82-7984-061-3, ISSN 0802-3271.

"Buckling and geometrical nonlinear beam-type analyses of timber structures", Trond Even Eggen, 2000:56, ISBN 82-7984-081-8, ISSN 0802-3271.

"Structural Crashworthiness of Aluminium Foam-Based Components", Arve Grønsund Hanssen, 2000:76, ISBN 82-7984-102-4, ISSN 0809-103X.

"Measurements and simulations of the consolidation in first-year sea ice ridges, and some aspects of mechanical behaviour", Knut V. Høyland, 2000:94, ISBN 82-7984-121-0, ISSN 0809-103X.

"Kinematics in Regular and Irregular Waves based on a Lagrangian Formulation", Svein Helge Gjøsund, 2000-86, ISBN 82-7984-112-1, ISSN 0809-103X.

"Self-Induced Cracking Problems in Hardening Concrete Structures", Daniela Bosnjak, 2000-121, ISBN 82-7984-151-2, ISSN 0809-103X.

"Ballistic Penetration and Perforation of Steel Plates", Tore Børvik, 2000:124, ISBN 82-7984-154-7, ISSN 0809-103X.

"Freeze-Thaw resistance of Concrete. Effect of: Curing Conditions, Moisture Exchange and Materials", Terje Finnerup Rønning, 2001:14, ISBN 82-7984-165-2, ISSN 0809-103X.

"Structural behaviour of post tensioned concrete structures. Flat slab. Slabs on ground", Steinar Trygstad, 2001:52, ISBN 82-471-5314-9, ISSN 0809-103X.

"Slipforming of Vertical Concrete Structures. Friction between concrete and slipform panel", Kjell Tore Fosså, 2001:61, ISBN 82-471-5325-4, ISSN 0809-103X.

"Some numerical methods for the simulation of laminar and turbulent incompressible flows", Jens Holmen, 2002:6, ISBN 82-471-5396-3, ISSN 0809-103X.

"Improved Fatigue Performance of Threaded Drillstring Connections by Cold Rolling", Steinar Kristoffersen, 2002:11, ISBN: 82-421-5402-1, ISSN 0809-103X.

"Deformations in Concrete Cantilever Bridges: Observations and Theoretical Modelling", Peter F. Takâcs, 2002:23, ISBN 82-471-5415-3, ISSN 0809-103X.

"Stiffened aluminium plates subjected to impact loading", Hilde Giæver Hildrum, 2002:69, ISBN 82-471-5467-6, ISSN 0809-103X.

"Full- and model scale study of wind effects on a medium-rise building in a built up area", Jónas Thór Snæbjørnsson, 2002:95, ISBN82-471-5495-1, ISSN 0809-103X.

"Evaluation of Concepts for Loading of Hydrocarbons in Ice-infested water", Arnor Jensen, 2002:114, ISBN 82-417-5506-0, ISSN 0809-103X.

"Numerical and Physical Modelling of Oil Spreading in Broken Ice", Janne K. Økland Gjøsteen, 2002:130, ISBN 82-471-5523-0, ISSN 0809-103X.

"Diagnosis and protection of corroding steel in concrete", Franz Pruckner, 20002:140, ISBN 82-471-5555-4, ISSN 0809-103X.

"Tensile and Compressive Creep of Young Concrete: Testing and Modelling", Dawood Atrushi, 2003:17, ISBN 82-471-5565-6, ISSN 0809-103X.

"Rheology of Particle Suspensions. Fresh Concrete, Mortar and Cement Paste with Various Types of Lignosulfonates", Jon Elvar Wallevik, 2003:18, ISBN 82-471-5566-4, ISSN 0809-103X.

"Oblique Loading of Aluminium Crash Components", Aase Reyes, 2003:15, ISBN 82-471-5562-1, ISSN 0809-103X.

"Utilization of Ethiopian Natural Pozzolans", Surafel Ketema Desta, 2003:26, ISSN 82-471-5574-5, ISSN:0809-103X.

"Behaviour and strength prediction of reinforced concrete structures with discontinuity regions", Helge Brå, 2004:11, ISBN 82-471-6222-9, ISSN 1503-8181.

"High-strength steel plates subjected to projectile impact. An experimental and numerical study", Sumita Dey, 2004:38, ISBN 82-471-6281-4 (elektr. Utg.), ISBN 82-471-6282-2 (trykt utg.), ISSN 1503-8181.

"Alkali-reactive and inert fillers in concrete. Rheology of fresh mixtures and expansive reactions." Bård M. Pedersen, 2004:92, ISBN 82-471-6401-9 (trykt utg.), ISBN 82-471-6400-0 (elektr. utg.), ISSN 1503-8181.

"On the Shear Capacity of Steel Girders with Large Web Openings". Nils Christian Hagen, 2005:9 ISBN 82-471-6878-2 (trykt utg.), ISBN 82-471-6877-4 (elektr. utg.), ISSN 1503-8181.

"Behaviour of aluminium extrusions subjected to axial loading". Østen Jensen, 2005:7, ISBN 82-471-6872-3 (elektr. utg.) , ISBN 82-471-6873-1 (trykt utg.), ISSN 1503-8181.

"Thermal Aspects of corrosion of Steel in Concrete". Jan-Magnus Østvik, 2005:5, ISBN 82-471-6869-3 (trykt utg.) ISBN 82-471-6868 (elektr.utg), ISSN 1503-8181.

"Mechanical and adaptive behaviour of bone in relation to hip replacement." A study of bone remodelling and bone grafting. Sbastien Muller, 2005:34, ISBN 82-471-6933-9 (trykt utg.) (ISBN 82-471-6932-0 (elektr.utg), ISSN 1503-8181.

"Analysis of geometrical nonlinearities with applications to timber structures". Lars Wollebæk, 2005:74, ISBN 82-471-7050-5 (trykt utg.), ISBN 82-471-7019-1 (elektr. Utg.), ISSN 1503-8181.

"Pedestrian induced lateral vibrations of slender footbridges", Anders Rönnquist, 2005:102, ISBN 82-471-7082-5 (trykt utg.), ISBN 82-471-7081-7 (elektr.utg.), ISSN 1503-8181.

"Initial Strength Development of Fly Ash and Limestone Blended Cements at Various Tem-

peratures Predicted by Ultrasonic Pulse Velocity", Tom Ivar Fredvik, 2005:112, ISBN 82-471-7105-8 (trykt utg.), ISBN 82-471-7103-1 (elektr.utg.), ISSN 1503-8181.

"Behaviour and modelling of thin-walled cast components", Cato Dørum, 2005:128, ISBN 82-471-7140-6 (trykt utg.), ISBN 82-471-7139-2 (elektr. utg.), ISSN 1503-8181.

"Behaviour and modelling of selfpiercing riveted connections", Raffaele Porcaro, 2005:165, ISBN 82-471-7219-4 (trykt utg.), ISBN 82-471-7218-6 (elektr.utg.), ISSN 1503-8181.

"Behaviour and Modelling og Aluminium Plates subjected to Compressive Load", Lars Rønning, 2005:154, ISBN 82-471-7169-1 (trykt utg.), ISBN 82-471-7195-3 (elektr.utg.), ISSN 1503-8181.

"Bumper beam-longitudinal system subjected to offset impact loading", Satyanarayana Kokkula, 2005:193, ISBN 82-471-7280-1 (trykt utg.), ISBN 82-471-7279-8 (elektr.utg.), ISSN 1503-8181.

"Control of Chloride Penetration into Concrete Structures at Early Age", Guofei Liu, 2006:46, ISBN 82-471-7838-9 (trykt utg.), ISBN 82-471-7837-0 (elektr. utgave), ISSN 1503-8181.

"Modelling of Welded Thin-Walled Aluminium Structures", Ting Wang, 2006:78, ISBN 82-471-7907-5 (trykt utg.), ISBN 82-471-7906-7 (elektr.utg.), ISSN 1503-8181.